ELSEVIER

Coordination Chemistry Reviews
175 (1998) 271–322

COORDINATION CHEMISTRY REVIEWS

Annual survey of organometallic metal cluster chemistry for the year 1997

Michael G. Richmond *

Department of Chemistry, University of North Texas, Denton, TX 76203, USA

Received 22 May 1998; accepted 1 June 1998

Contents

Abstract

The synthetic, mechanistic and structural chemistry of organometallic metal cluster compounds is reviewed for the year 1997.

* Fax: + 1-940-5654318; e-mail: cobalt@unt.edu

0010-8545/98/$ - see front matter
PII S0010-8545(98)00175-1

Keywords: Organometallic metal cluster compound; Structural characterization; Reaction mechanisms

1. Dissertations

Details on the synthesis and structural characterization of trirhenium alkoxide and thiolate clusters have been published. The cluster compounds $Re_3(\mu\text{-}OCH_2CMe_3)_3[\mu\text{-}C(R)=CHR']$ $(OCH_2CMe_3)_5$ (where R and R′ = various groups) have been obtained from the reaction between alkynes and $Re_3(\mu\text{-}OCH_2CMe_3)_3(OCH_2CMe_3)_6$. The same starting material reacts with ethylene to yield the insertion product $Re_3(\mu\text{-}OCH_2CMe_3)_3(Et)(OCH_2CMe_3)_5$. Mechanisms related to these reactions are presented [1]. The reaction between $[C_3Cl_3][SbF_6]$ and carbonyl metalates affords the trimetal complexes $[M_3(\mu_3\text{-}C_3)][SbF_6]$ [where M = $Re(CO)_5$, $CpMo(CO)_3$, $CpW(CO)_3$, $CpFe(CO)_2$, $CpRu(CO)_2$]. Each of these new complexes has been fully characterized [2].

The alkylation reactivity of the chalcogen-bridged clusters $[EFe_3(CO)_9]^{2-}$ (where E = S, Se, Te) using methyl triflate and MeI has been examined. In the case of the sulfur cluster, methylation occurs at the capping atom to give $[Fe_3(CO)_9SMe]^-$, whereas the other two derivatives exhibit alkylation at the Fe_3 base. The catalytic activity of $[H_xM_3(CO)_9E]^{2-x}$ (where $x = 0, 1$; M = Fe, Ru; E = S, Se, Te) in methyl formate production from MeOH and CO was also investigated. The reaction of $NaAsO_2$ with $Mo(CO)_6$ in refluxing MeOH or EtOH gives the cluster complexes $[(OC)_5MoAsMo_3(CO)_9(\mu_3\text{-}OR)_3Mo(CO)_3]^{2-}$. Extended Hückel MO calculations on these electron-rich clusters reveal that the extra electron pair resides in an a_2 orbital which is delocalized over three $Mo(CO)_3$ units. Data from ^{205}Tl-NMR studies on several Tl-based cluster compounds are published. Evidence for cluster fragmentation in solution is presented [3]. The chemistry of osmium clusters containing germanium and tin atoms has been studied. Pyrolysis of $[(OC)_4OsSnMe_2]_2$ at 130°C yields the raft-like cluster $[(OC)_3OsSnMe_2]_3$, while reaction of the same diosmium complex with Me_3NO affords $[Os_2(CO)_7O(SnMe_2)_2]_2$, whose structure is based on a boat-like six-membered ring of $Os_2Sn_2O_2$ and Os_2SnO tetracycles. Treatment of $[Os(CO)_4]^{2-}$ with Ph_2SnCl_2 gives, in part, the cluster $[(OC)_4OsSnPh_2]_6$. X-ray analysis reveals an unprecedented planar 12-membered ring with alternating Os and Sn atoms. The fluxional behavior of the ancillary CO groups has been studied by VT ^{13}C-NMR spectroscopy. PMe_3 ligand substitution in $[(OC)_3OsGeMe_2]_2$ at high temperature gives $Os_3(CO)_{9-n}(GeMe_2)_3(PMe_3)_n$ (where $n = 1–3$) [4]. The reaction between $[E_8][SbF_6]_2$ (where E = S, Se) and $Fe(CO)_5$ in SO_2 yields the new isostructural clusters $[Fe_3(CO)_{10}(E)_2][SbF_6]_2$. The picnic-basket shape of these clusters was established by X-ray crystallography in the case of the selenium derivative. Use of $Fe_2(CO)_9$ in place of $Fe(CO)_5$ leads to a similar reaction. The sulfur analogue also gives the analogous picnic basket cluster, which subsequently reacts with its own gegenanion to furnish the new complex $[Fe_2(CO)_6Sb_2S_6]^{2+}$ [5]. The X-ray diffraction structures of $Ru_5C(CO)_{14}L$ [where L = PCy_3, $P(C_6H_4F\text{-}4)_3$, $P(C_6H_4OMe\text{-}4)_3$]

and $Ru_5C(CO)_{13}(etpb)_2$ have been determined and compared with related phosphine-substituted complexes based on $Ru_5C(CO)_{15}$. Ligand-induced perturbations within this genre of cluster are discussed [6]. The synthesis and characterization of $[(OC)_3MFe_3S_4(Smes)_3]^{3-}$ and related cubane clusters are reported. The reactivity of these clusters with CO and metal ions (Tl^+, Zn^{2+}, Cd^{2+}) has been explored. The redox properties of these products were also studied [7]. Iron carbonyl clusters containing dicarbide and tetracarbide ligands have been synthesized from suitable precursors bearing an ancillary ketenylidene ligand. The course of nucleophilic attack in $[Fe_3(CO)_9CCOC(O)Me]^-$ using $[Re(CO)_5]^-$ proceeds via cleavage of the acetate group, giving the dicarbide cluster $[Fe_3(CO)_9CCRe(CO)_5]^-$. The results of a fragment orbital analysis are presented within the context of bonding in four-metal ketenylidene clusters [8]. The reversible interconversions between $[HRu_3(CO)_{11}]^-$ and $[H_3Ru_4(CO)_{12}]^-$ on a hydroxylated magnesia surface in the presence of syn gas are documented. It is shown that the surface-bound species are mobile at room temperature, exhibiting facile rupture and formation of M–M bonds. Plausible reaction schemes are presented and discussed [9]. The synthesis and X-ray structure of $[Me_3NCH_2Cl]_3[Ru_3(\mu\text{-}InCl_3)(\mu\text{-}InCl_2)(\mu\text{-}CO)(CO)_9](MeCN)(CH_2Cl_2)$ have been reported. This cluster is reported to contain both the longest and shortest Ru–In bond lengths characterized structurally to date. The reaction of activated indium with $Fe_3(CO)_{12}$ in MeCN affords $[Fe(MeCN)_6]_2[Fe_7In_2(CO)_{40}](MeCN)_2$. The polyhedral shape of this Fe_7In_2 cluster has been determined by X-ray crystallography [10].

The trinuclear, phosphido-bridged clusters $Ir_3(\mu\text{-}PPh_2)_3(CO)_3L_2$ (where $L_2 =$ 2CO, $2PPh_3$, dppm) and $Ir_3(\mu\text{-}PPh_2)_3(CO)_4(^tBuNC)_3$ have been prepared from $Ir_2(cyclooctene)_4(\mu\text{-}Cl)_2$. The 46-electron dppm derivative possesses one formal 16-electron iridium center and two 18-electron iridium centers, as verified by X-ray crystallography. This cluster reversibly adds CO to produce the corresponding 48-electron cluster $Ir_3(\mu\text{-}PPh_2)_3(CO)_4(dppm)$. Structural comparisons between the 46- and 48-electron clusters are presented. Oxidative addition chemistry has been explored and mechanistic pathways discussed. Also included are the reactivity data of the mixed $RhIr_2$ and Rh_2Ir clusters. All new products have been characterized fully in solution and by X-ray diffraction analysis [11]. Treatment of $(TMS)_2S$ with $[Cp^*IrCl_2]_2$ yields the dicationic cluster $[Cp^*_3Ir_3S_2]^{2+}$, which has been purified by aqueous ion exchange chromatography. The trigonal bipyramidal Ir_3S_2 core present in this cluster was confirmed by X-ray analysis. Chemical reduction using Cp_2Co furnishes the corresponding neutral cluster $Cp^*_3Ir_3S_2$, which possesses a *nido* polyhedral core. ^{1}H-NMR measurements reveal the existence of dynamic Ir–Ir bond cleavage and formation at ambient temperature. The cuboidal cluster $[Cp^*_4Ir_4S_4]^{2+}$ has been synthesized also and its fluxional behavior investigated. The activation parameters for metal–metal bond fluxionality are reported. Other mixed-metal M_3S_4 clusters have been prepared and their reactivity studied [12]. The reaction of alkynes with $(CpCo)_3(CO)_2$ has been found to give $(CpCo)_3(CO)(\mu_3\text{-}\eta^2\text{-alkyne})$ and $(CpCo)_3(CO)[OCC(R)CH]$ depending upon the nature of the alkyne ligand employed. VT NMR data, electrochemical studies, and the X-ray diffraction structures are discussed. The pyrolysis chemistry of $(CpCo)_3(CO)$(alkyne) was investigated in

refluxing decalin, with linked bis-carbyne clusters being isolated as the major products [13]. The fluxional behavior of carbene, carbyne, and alkyne ligands in mixed-metal clusters has been studied by NMR spectroscopy. Conversion of a μ_2-carbene ligand into a μ_3-carbyne ligand was observed in $Cp^*Rh(CpCo)_2(\mu_2\text{-}CO)_2(\mu_2\text{-}CH_2)$. The related iridium analogue is shown to give an intermediate having a hydride and carbyne ligand at elevated temperatures. The reorientational dynamics of the aryl groups in $(CpCo)_3[\mu_3\text{-}C(aryl)]_2$ have been examined by ^{13}C-NMR relaxation methods. Steric interactions between the aryl and Cp groups are shown to control the rate of aryl group rotation in these clusters [14]. The indenyl-substituted clusters $Ir_3(\mu\text{-}CO)_3(\eta^5\text{-}ind)_3$ and $Ir_{3-x}Rh_x(\mu\text{-}CO)_3(\eta^5\text{-}ind)_3$ (where $x = 1–3$) have been synthesized and their reactivity with CO and PPh_3 studied. The interconversion between the various isomers of $Ir_3(CO)_3(\eta^5\text{-}ind)_3$ has been explored by using VT NMR spectroscopy. The relative energies of three of the four isomeric forms of this cluster are reported. Treatment of $Ir(CO)(\eta^2\text{-}C_8H_{14})(\eta^5\text{-}ind)$ with $Re_2(\mu\text{-}H)_2(CO)_8$ gives the mixed-metal cluster $IrRe_2(\mu\text{-}H)_2(CO)_9(\eta^5\text{-}ind)$, whose deprotonation chemistry and ligand substitution reactivity have been investigated [15]. The synthesis and characterization of cluster arrays based on $Co_3(CO)_9(\mu_3\text{-}CCO_2H)$ are presented [16].

New self-assembled, low-dimensional materials containing lanthanides and transition metals bridged by cyanate or cyanide groups have been prepared [17]. The spectroscopic and electrochemical properties of $[Ni_3(\mu_3\text{-}L)(\mu_3\text{-}I)(\mu_2\text{-}dppm)_3]^+$ (where L = CO, CNR), which have been obtained from $Ni_3(\mu_3\text{-}I)_2(\mu_2\text{-}dppm)_3$ and L, have been investigated [18]. The reaction of $[Ni_6(CO)_{12}]^{2-}$ with organoantimony halides or alkylbismuth halides yields the clusters $[Ni_{10}(ER)_2(CO)_{18}]^{2-}$. These clusters possess a common non-centered 1,12-$Ni_{10}E_2$ icosahedral cage, as verified by X-ray crystallography. ^{13}C-NMR data and the electrochemical properties are reported. $CuBr_2$ reacts with $[Ni_6(CO)_{12}]^{2-}$ to give low yields of a cluster tentatively identified as $[Cu_5Ni_{30}(CO)_9(\mu_2\text{-}CO)_{31}]^{5-}$ [19]. The high-nuclearity clusters $Pd_{28}(\mu_6\text{-}H)_{12}(PtMe_3)(PtPPh_3)_{12}(CO)_{27}$, $[Ni_{38}Pt_6(CO)_{48}]^{6-}$, and $[Pt_3CO_6]_n^{2-}$ (where $n = 5$, 6) have been characterized structurally. The polyhedral geometry and electron counts of the former two clusters are discussed [20].

2. Homometallic clusters

2.1. Group 4 clusters

Hydrolysis of $(C_5Me_4Ph)TiCl_3$ in the presence of Ag_2O leads to $[(C_5Me_4Ph)TiCl(\mu\text{-}O)]_3$. The NMR spectrum of this cluster indicates the existence of a nearly flat Ti_3O_3 ring, whose structure was confirmed by X-ray crystallography. The complex $[(C_5Me_4Ph)Ti]_4(\mu\text{-}O)_6$, obtained from the reaction between $(C_5Me_4Ph)TiCl_3$ and excess H_2O/Et_2NH, has also been isolated and structurally characterized [21]. The methylidyne-substituted cubane cluster $(Cp^*Ti)_4(\mu_3\text{-}CH)_4$ has been obtained from the thermolysis of Cp^*TiMe_3. NMR and X-ray data are presented, and a reaction mechanism involving methylene and carbyne intermedi-

ates is described [22]. The activation of the Ti–F bonds in $(Cp^*TiOF)_4$ and $[(C_5Me_4Et)TiOF]_4$ by added $AlMe_3$ has been reported [23].

2.2. Group 5 clusters

The synthesis and molecular structure of $[(MeCp)_2V(\mu\text{-}S)_2V(MeCp)_2]_2(\mu\text{-}O)$ have been published. Treating $(MeCp)_2VCl_2$ with the Na-reduced form of *cyclo*(MeAsS)$_{3,4}$ affords the oxo-bridged cluster. The diamagnetism exhibited by this complex has been explained by the presence of a V(IV)–V(IV) bond or the presence of mixed oxidation states involving V(III)–V(V) centers [24]. $VCl_3(THF)_3$ has been allowed to react with $C_5Me_5SnBu_3$ to furnish the cluster $[Cp^*V(\mu\text{-}Cl)_2]_3$. X-ray diffraction analysis reveals that the cluster core consists of an equilateral triangle of vanadium atoms. The reactivity of this cluster towards O_2 and NaN_3 has been examined, and the antiferromagnetic behavior verified [25]. The trivanadium complexes $Cp_3V_3(\mu\text{-}Cl)_6$ (where Cp = Cp*, C_5Me_4Et) have been synthesized from either $CpVCl_3$ or $VCl_3(THF)_3$ in the presence of $CpSnBu_3$. Included in this report are the X-ray structure of the C_5Me_4Et derivative and a discussion on the antiferromagnetic behavior exhibited by both complexes [26]. $Cp^*TaCl(S)(SCPh_3)$ reacts with $NaBH_4$ to give $Cp^*_3Ta_3(S)_3(S_3BH)$, whose X-ray structure accompanies this report (Fig. 1) [27].

2.3. Group 6 clusters

Thermolysis of $CpM(CO)_2(\eta^3\text{-}P_3)$ with $M'_2Cp_2(CO)_4$ (where M = M′ = Mo, W) produces the trimetallic complexes $Mo_nW_{3-n}Cp_3(CO)_6(\mu_3\text{-}P)$ (where $n = 0$–3). Air oxidation of these clusters affords complexes possessing a μ_3-PO ligand. Solution spectroscopic data and three X-ray structures are presented [28]. The anionic dimers $[Cp_2M_2(CO)_4(\mu\text{-}PH_2)]^-$ (where M = Mo, W) have been allowed to react with various organometallic halides to give $Cp_2M_2(CO)_4(\mu\text{-}H)(\mu\text{-}PHM')$ in low yield.

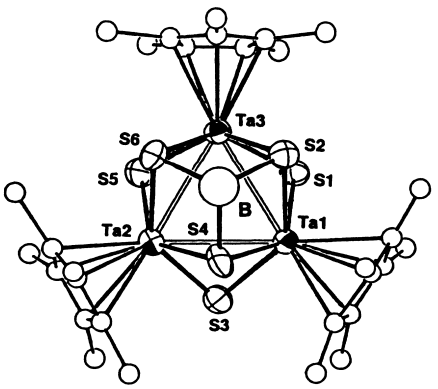

Fig. 1. X-ray structure of $Cp^*_3Ta_3(S)_3(S_3BH)$. Reprinted with permission from Organometallics. Copyright 1997 American Chemical Society.

Included in this report is the X-ray structure of $Cp_2W_2(CO)_4(\mu\text{-}H)[\mu\text{-}PH\{CpMo(CO)_3\}]$ [29]. The tetrahedrane clusters $Cp_3Mo_nW_{3-n}(CO)_6(\mu_3\text{-}P)$ (where $n = 0–3$) undergo oxidation by sulfur in CS_2 solution to afford the corresponding μ_3-PS capped clusters. The starting clusters are regenerated upon standing in solution at room temperature. The X-ray structure of $Cp_3W_3(CO)_6(\mu_3\text{-}PS)$ accompanies this report [30]. H_2 reacts with 1,2-$W_2(^i\text{Bu})_2(O^i\text{Pr})_4$ in hydrocarbon solvents to furnish the hexanuclear cluster $W_6H_5(C^i\text{Pr})(O^i\text{Pr})_{12}$ in moderate yields. The solid-state structure has been established by X-ray crystallography, and the hydrogenolysis and hydrogenation chemistry of this W_6 cluster has been investigated [31].

2.4. Group 7 clusters

The synthesis and NMR spectra (^{77}Se and ^{125}Te) of the mixed tellurium/selenium clusters $[Re_6(Te_{8-n}Se_n)(CN)_6]^{4-}$ (where $n = 0–8$) have been published. The hexarhenium clusters are obtained by treating Re_6Te_{15} with various amounts of added NaCN and Se at 600°C. Three X-ray structures are presented [32]. The syntheses and X-ray structures of $[E_2Mn_3(CO)_9]^-$ and $[E_2Mn_4(CO)_{12}]^{2-}$ (where E = S, Se) have been published [33]. The utility of hydro(solvo)thermal synthesis in the preparation of chalcogen-bridged manganese clusters has been presented. The X-ray structures of $[Mn_3(CO)_9(S_2)_2(SH)]^{2-}$ and $[Mn_4(CO)_{13}(Te_2)_3]^{2-}$ accompany this report [34].

Acetonitrile reacts with $[Re_3(\mu\text{-}H)_3(\mu\text{-}NC_5H_4)(CO)_{10}]^-$ in strong acid to give the *cis* and *trans* isomers of $Re_3(\mu\text{-}H)_3(py)(MeCN)(CO)_{10}$. Isotopic labeling studies reveal that the added proton is distributed among two of the three cluster hydridic sites and the *ortho* position of the pyridine ligand. The rate of MeCN displacement by added CO has been measured and the corresponding undecacarbonyl cluster isolated [35]. The cluster complex $[H_4Re_3(CO)_9][Re(CO)_3(DMF)_3]$ transforms to $[H_7Re_5(CO)_{15}][Re(CO)_3(DMF)_3]$ and $[H_5Re_4(CO)_{12}][Re(CO)_3(DMF)_3]$ in $CHCl_3$ solution. The former cluster was characterized by X-ray analysis, which revealed it to be a 74-electron square-pyramidal Re_5 cluster without a non-hydride interstitial atom. VT ^{1}H-NMR measurements confirm the fluxional nature of the ancillary hydride ligands about the cluster core. Mechanisms related to the formation of these clusters are presented, and the role of the solvent in determining the course of the reaction is discussed [36]. The anionic cluster $[Re_4H(\mu\text{-}H)_2(CO)_{17}]^-$ is readily obtained from the reaction between $[Re_2H(CO)_9]^-$ and $Re_2(\mu\text{-}H)_2(CO)_8$. The open chain metal skeleton in the Re_4 product has been established by X-ray crystallography. The hydride exchange behavior has been studied by NMR spectroscopy. Treatment with CO leads to clean cluster fragmentation and formation of $HRe(CO)_5$ and $[Re_3H(\mu\text{-}H)(CO)_{13}]^-$ [37]. The fluxional behavior of the CO ligands in $[Re_3(\mu\text{-}H)_3(\mu\text{-}\eta^2\text{-}NC_5H_4)(CO)_{10}]^-$ has been explored by VT ^{13}C-NMR spectroscopy, 1D SPT, and 2D EXSY measurements [38].

Treatment of the homoleptic neopentoxide cluster $Re_3(\mu\text{-}OCH_2^t\text{Bu})_3(OCH_2^t\text{Bu})_6$ with ethyne gives the ethyne addition adduct $Re_3(\mu\text{-}OCH_2^t\text{Bu})_2(OCH_2^t\text{Bu})_7(\mu\text{-}HCCH)$. This complex was fully characterized in solution and by X-ray crystallog-

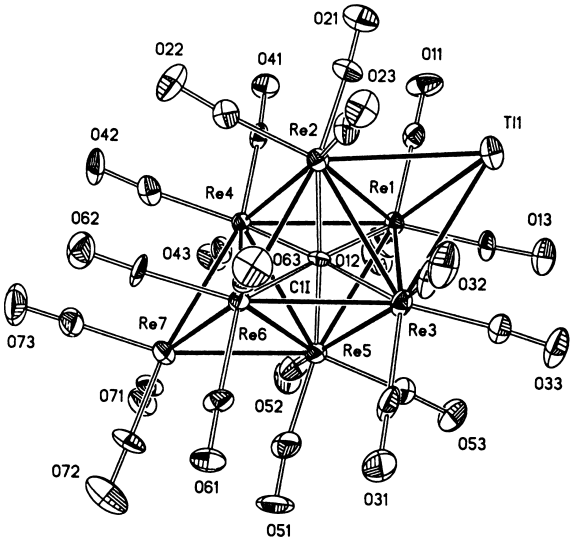

Fig. 2. X-ray structure of $[Re_7C(CO)_{21}Tl]^{2-}$. Reprinted with permission from Inorganic Chemistry. Copyright 1997 American Chemical Society.

raphy. Substituted alkynes undergo reaction to give alkenyl clusters and pivaldehyde [39]. The reactivity of $Re_3(\mu\text{-}O^iPr)_3(H)(O^iPr)_5$ with alkynes and alkenes has been studied. The insertion of ethylene and isobutylene into the Re–H bond yields the corresponding alkyl-substituted clusters, which undergo reversible β-hydrogen elimination of acetone and formation of $Re_3(\mu\text{-}O^iPr)_3(H)(R)(O^iPr)_4$. The X-ray structure of $Re_3(\mu\text{-}O^iPr)_3(\eta^1\text{-}CPhCH_2)(O^iPr)_5$ is presented [40]. The rhenium cluster $Re_3(\mu\text{-}OCH_2CMe_3)_3(OCH_2CMe_3)_6$ has been investigated for its reactivity with ethylene and alkynes. The results of isotopic labeling studies and one X-ray structure are presented [41].

$TlPF_6$ reacts with $[Re_7C(CO)_{21}]^{3-}$ to furnish the thallium-capped cluster $[Re_7C(CO)_{21}Tl]^{2-}$. The thallium dissociates from the cluster in coordinating solvents such as acetone and acetonitrile. The association constant (K_a) in acetone has been measured by using a modified Benisi–Hildebrand equation. The X-ray structure of $[Re_7C(CO)_{21}Tl]^{2-}$ (Fig. 2) shows that the thallium atom is nearly symmetrically bound to the octahedral face opposite the capping $Re(CO)_3$ moiety [42].

2.5. Group 8 clusters

A paper dealing with the mechanism of the low-energy fluxional process in $Fe_3(CO)_{12-n}L_n$ (where $n = 0$–2) has appeared. Application of the Bürgi–Dunitz approach reveals that the carbonyl exchange pathway (low energy) proceeds via a concerted bridge-opening bridge-closing mechanism and not by a C_2 libration sequence. The correctness of the ligand polyhedral model (LPM) is contrasted with the local bonding model (LBM) for assessment of CO fluxional behavior [43]. A

rebuttal to the previous article has also been published. The author's support of the LPM is thoroughly outlined, including examples from a diverse group of metal cluster complexes [44]. The old and new problems associated with the solution dynamics and fluxional behavior in many metal clusters are reviewed [45].

The use of $Ru_3(CO)_{12}$ as a catalyst precursor in the coupling of aryl C–H bonds in pyridylbenzenes to CO and alkenes is reported. The carbonylation proceeds at the *ortho* C–H bond of the phenyl ring exclusively and not at the *meta* or *para* C–H bonds, or the pyridyl ring. A working mechanism involving a mononuclear species is discussed [46]. The first example of a catalytic Pauson–Khand type reaction using a ruthenium catalyst has appeared. High to moderate yields of bicyclic cyclopentenones from 1,6-enynes are reported to be catalyzed by $Ru_3(CO)_{12}$. The reactions exhibit a high level of functional group compatibility [47]. The preparation of indenones from aryl imines has been published. The reaction employs $Ru_3(CO)_{12}$ as a catalyst precursor, and carbonylation at an *ortho* C–H bond, followed by ethylene insertion, ultimately gives the indenone ring system [48]. Selective hydroformylation of internal alkynes occurs using a cocatalyst system composed of $PdCl_2(PCy_3)_2$ and added $Fe_3(CO)_{12}$ or $Rh_4(CO)_{12}$ [49].

Treatment of $Ru_3(CO)_{12}$ with high area oxides of rare earth metals (La, Ce, Pr, Tb, Ho, Yb) affords the surface species $[(OC)_2Ru(OM)_2]_n$ for all of the oxides, along with the surface cluster $Ru_3(CO)_{10}(\mu\text{-H})(\mu\text{-OM})$ for metal loadings using Ce and Ho oxides. These reactions have been studied by using IR and X-ray photoelectron spectroscopy [50]. Reversible interconversions between $[HRu_3(CO)_{11}]^-$ and $[H_3Ru_4(CO)_{12}]^-$ on fully hydroxylated magnesia in the presence of H_2 or CO have been observed. Reaction pathways for these interconversions are discussed, along with the relevance of this chemistry to that of the anions in basic solution [51]. The synthesis of $Ru_3(CO)_{10}Cl_2$, $Ru_3(CO)_{12}$, $H_4Ru_4(CO)_{12}$, $[H_3Ru_4(CO)_{12}]^-$, $[HRu_6(CO)_{18}]^-$, and $[Ru_6C(CO)_{16}]^{2-}$ from the one-pot controlled reduction of $RuCl_3$ supported on silica in the presence of alkali carbonates has appeared. The variables controlling the selectivity are discussed, and a detailed reaction sequence showing the relationship between the clusters is presented [52]. $Os_3(CO)_{12}$ is activated by the surface silanol groups of silica to afford the clusters $H_4Os_4(CO)_{12}$ and $HOs_3(CO)_{10}L$ (where L = three-electron donors such as OH, OR, Cl, Br, I, O_2CR, SCN). These high-yield syntheses proceed via the silica-anchored species $HOs_3(CO)_{10}(OSi\equiv)$ as the reactive intermediate [53].

Cyclic voltammetric data for the C_{60}-mediated electron transfer to triosmium clusters have been published. The clusters studied include $Os_3(CO)_{11}(\eta^2\text{-}C_{60})$, $Os_3(CO)_{10}(PPh_3)(\eta^2\text{-}C_{60})$, and $Os_3(CO)_9(PPh_3)_2(\eta^2\text{-}C_{60})$ [54]. The fullerene compound C_{70} has been allowed to react with $Ru_3(CO)_{12}$ to give $[Ru_3(CO)_9]_n(\mu_3\text{-}\eta^2,\eta^2,\eta^2\text{-}C_{70})$ (where $n = 1, 2$). X-ray diffraction analysis has confirmed the identity of these products [55].

The reaction between $Ru_3(CO)_{12}$ and Na_2Te leads to $[Ru_4Te(CO)_{10}]^{2-}$ and $[Ru_5Te(CO)_{14}]^{2-}$. Both clusters have pseudo-octahedral cores composed of ruthenium and tellurium atoms. The ^{125}Te-NMR chemical shifts are also reported [56]. Benzo[b]tellurophene has been allowed to react with the trinuclear complexes $M_3(CO)_{12}$ (where M = Fe, Ru, Os) and $Os_3(CO)_{10}(MeCN)_2$. Many new cluster

compounds have been isolated and fully characterized. Included in this report are the X-ray structures of five products. The benzo[b]tellurophene ligand is shown to give complexes with the open-chain ligands $C_6H_4CHCHTe$ and/or the fragments Te and C_6H_6 as bridging ligands [57]. The use of heterocyclic tellurium/nitrogen compounds as precursors for the synthesis of organoiron compounds is reported. Benzoisotellurazole reacts with $Fe_3(CO)_{12}$ to give $(C_6H_4CHNTe)Fe_3(CO)_7$. The X-ray diffraction structure exhibits a non-linear chain of Fe_3 atoms, doubly bridged by the nitrogen and tellurium atoms. Treatment of 2-methylbenzotellurazole with $Fe_3(CO)_{12}$ gives the products $C_{18}H_7NFe_3O_{10}$ and $C_7H_7NFe_2O_6$. X-ray analysis confirms the detelluration associated with these two products [58].

Two isomeric clusters having the formula $Ru_4(CO)_9(C_{15}H_{20})$ have been isolated from the reaction of $Ru_3(CO)_{12}$ with 1,3,5-triisopropylbenzene. X-ray analysis of both products reveals that two hydrogen atoms have been transferred to a different carbon atom of the $C_{15}H_{18}$ ligand in each isomer. The polyhedral core of these clusters is based on a tetrahedral arrangement of ruthenium atoms [59]. Thermolysis of $Ru_3(CO)_{12}$ in octane containing cycloocta-1,3-diene furnishes the isomeric clusters $Ru_3H_2(CO)_9(C_8H_{10})$ and $Ru_3H(CO)_9(C_8H_{11})$. These clusters are structural isomers which differ only in the transfer of a hydrogen atom from the organic ligand to the metal core. The solid-state structures of both clusters have been determined, and the bonding of the organic ligands in these clusters has been examined by extended Hückel calculations [60]. Low yields of $Fe_3(CO)_9(\mu$-CO)[C=C=C(H)Ph] and $Fe_2(CO)_6$[Ph(H)CCCHC(OMe)O] have been obtained from the reaction between 1-phenylprop-2-yn-1-ol and methanol-stabilized $Fe_3(CO)_{12}$. The molecular structures of these complexes were crystallographically established [61]. Treatment of $Ru_3(CO)_{12}$ with $C_5H_5Me_2SiSiMe_2C_5H_5$ in boiling heptane gives $(Me_2SiSiMe_2)[(\eta^5$-$C_5H_5)Ru(CO)]_2(\mu$-$CO)_2$ [62]. The sandwich cluster $Ru_4(CO)_7(\mu$-$C_7H_7)_2$ has been isolated from the reaction between $Ru_3(CO)_{12}$ and cycloheptatriene. X-ray analysis reveals an unusual arrangement of two parallel edge-bridging organic rings [63]. *Nido*-7-$NMe_3CB_{10}H_{12}$ reacts with $Os_3(CO)_{12}$ in bromobenzene to afford $Os_3(CO)_8(\eta^5$-7-$NMe_3CB_{10}H_{10})$. This first example of a charge-compensated monocarbollide(octacarbonyl)triosmium complex was structurally characterized by X-ray crystallography [64]. $Fe_3(CO)_{12}$ undergoes fragmentation when treated with β-tetraethyl-tetracarba-*nido*-octaborane(8) to yield a 6,9-diferra-5,7,8,10-tetracarba-*nido*-decaborane(10) derivative. NMR data and the X-ray structure are presented [65]. CO replacement in $Ru_3(CO)_{12}$ by $HSi(OSiMe_3)_3$ and $HSiMe(OSiMe_3)_2$ leads to a series of siloxyl-substituted clusters. All of the new clusters have been fully characterized in solution by standard spectroscopic methods, and the reactivity exhibited by these clusters described [66]. The clusters $Ru_3(CO)_{12}$ and $Ru_3(CO)_{10}(MeCN)_2$ react with added phenylacetylene and *p*-tolylacetylene to give the clusters $Ru_3(CO)_9(\mu_2$-H)$(\mu_3$-η^2-C≡CAr) and $Ru_4(CO)_{12}(\mu_4$-η^2-HC≡CAr) (where Ar = Ph, C_6H_4Me-4). The X-ray structures of $Ru_4(CO)_{12}(\mu_4$-η^2-HC≡CPh) and $Ru_3(CO)_9(\mu_2$-H)$(\mu_3$-η^2-C≡CC_6H_4Me-4) exhibit *closo* polyhedral cores [67]. Thermolysis of $Os_3(CO)_{12}$ with ^{n}BuOCH=CHPEt_2 yields the triangular cluster $Os_3(\mu$-H)$(\mu_3$-^{n}BuOCH=CHPEt_2)$(CO)_9$ in moderate yield. The μ_3-^{n}BuOCH=CHPEt_2 ligand functions as a five-electron donor. The catalytic hydrosilation of terminal alkenes

with Et_3SiH using this cluster and the related clusters $Os_3(\mu\text{-H})(\mu\text{-CH=CHR})(CO)_{10}$ (where R = Cy, Ph) has been achieved at ambient temperature. A plausible hydrosilation mechanism involving intact, triangular metal clusters is presented [68]. The pentaruthenium cluster $Ru_5(\mu\text{-H})_2(CO)_{14}[\mu_4\text{-CC(Me)CO}_2\text{Et}]$ has been isolated from the reaction of $Ru_3(CO)_{12}$ with ethyl methacrylate. The product has been characterized by IR and NMR spectroscopy, and the molecular structure has been determined by X-ray analysis [69]. The reactivity of diacetylene ligands with $Ru_3(CO)_{12}$ has been explored. Treatment of hexa-2,4-diyne-1,6-diol and 1,4-diphenyl-1,3-butadiyne with $Ru_3(CO)_{12}$ gives $Ru_2(CO)_6[\mu_3,\eta^4\text{-C(Ph)C(C}_2\text{Ph)C(C}_2\text{Ph)C(Ph)}]$ and $Ru_3(CO)_{10}(\mu_3,\eta^2\text{-HOCH}_2\text{C}_2\text{C}_2\text{CH}_2\text{OH})$, respectively. The X-ray data and bonding in these complexes are discussed [70]. The endiones *trans*-ArCOCH=CHCOAr (where Ar = Ph, $p\text{-MeC}_6\text{H}_4$) have been allowed to react with $Ru_3(CO)_{12}$. The resulting products were isolated and fully characterized in solution and by X-ray diffraction analysis [71]. The synthesis and X-ray structure of the alkyne cluster $RuOs_3(\mu_4\text{-HC}_2\text{Me})(CO)_{12}$, which was obtained from the thermolysis reaction of $Ru_3(CO)_{12}$ with added $Os_3(CO)_9(\mu\text{-H})(\mu_3\text{-C}\equiv\text{CMe})$, have been published [72]. The dehydrohalogenation of iodoarenes to give ruthenium-bound μ_4-naphthyne and μ_4-phenanthryne ligands is described. Thermolysis of $Ru_3(CO)_{12}$ with 1-iodonaphthalene and 9-iodophenanthrene affords the aryne clusters $Ru_4(CO)_{12}(\mu_4,\eta^2\text{-L})$ (where L = 1,2-naphthyne, 9,10-phenanthryne). When the same reaction is carried out with iodobenzene and 4-iodotoluene, only the simple oxidative addition products $Ru_3(CO)_8(\mu\text{-I})(\mu_3,\eta^1\text{:}\eta^6\text{-C}_6\text{H}_4\text{R})$ (where R = H, Me) are observed. The reasons for the reactivity differences between these substrates are not known. The X-ray structures of two clusters accompany this report [73]. The alkyne cluster $Ru_3(CO)_{11}$(ethyne) is readily obtained from $Ru_3(CO)_{11}(\mu\text{-H})(H)$. NMR measurements ($^1H$ and ^{13}C) reveal that H_2 is lost and ethyne is coordinated rapidly at 183 K. These data suggest that the complex $Ru_3(CO)_{11}$(ethyne) serves as a reasonable intermediate to the known $Ru_3(CO)_9(\mu\text{-CO})(\mu_3\text{-}\eta^2\text{-alkyne})$ clusters [74]. The synthesis of a triosmium cluster containing a side-on-coordinated imine ligand has ben described. The X-ray structure of $Os_3(CO)_9(\mu_3\text{-}\eta^2\text{:}\eta^2\text{:}\eta^2\text{-NH=C}_6\text{H}_5\text{Ph})$ (Fig. 3) represents the first example of an η^2-coordinated imine complex with a N–H bond [75].

The solution structure and dynamics of several thallium-containing polynuclear complexes have been examined by ^{205}Tl spectroscopy. Some of the many complexes studied include $[Tl\{Fe(CO)_4\}_3]^{3-}$, $Tl[CpFe(CO)_2]_3$, $[Tl_2Fe_6(CO)_{24}]^{2-}$, and $[Tl_2Fe_4(CO)_{16}]^{2-}$. Generalizations concerning the ^{205}Tl chemical shift are discussed relative to the coordination number of the thallium atom(s) [76]. A paper dealing with the structural and bonding trends in osmium carbonyl clusters has appeared. Metal–metal bonding in $[Os_x(CO)_y]^{2-}$, $Os_x(CO)_y(H)_z$, and $[Os_x(CO)_y(H)_z]^{n-}$ is explored by examining the total metal–metal bond enthalpy of each compound [77]. The reaction of $Cp^*_3Ru_3(\mu\text{-H})_3(\mu_3\text{-H})_2$ with 1,3-cyclohexadiene leads to $Cp^*_3Ru_3(\mu\text{-H})_3(\mu_3\text{-}\eta^2\text{:}\eta^2\text{:}\eta^2\text{-C}_6\text{H}_6)$, whose solid-state structure confirms the coordination of the benzene ring. This benzene cluster undergoes two reversible one-electron oxidations to give the corresponding dicationic cluster. X-ray analysis of the oxidation product, $[Cp^*_3Ru_3(\mu\text{-H})_3(\mu_3\text{-}\eta^3\text{:}\eta^3\text{-C}_6\text{H}_6)]^{2+}$, confirms the hapticity

change of the benzene ring to the two allyl moieties in the dication. This represents the first example of an arene hapticity change induced by a redox process [78]. Treatment of $Ru_3(CO)_{12}$ with styrene, 4-methylstyrene, and 4-trifluorostyrene affords $Ru_3(CO)_8[\mu_3\text{-}\eta^6\text{:}\eta^2\text{:}\eta^1\text{-}HCC(H)C_6H_3R]$, $Ru_4(CO)_{12}(\mu_4\text{-}\eta^1\text{:}\eta^1\text{:}\eta^2\text{:}\eta^2\text{-}HCCC_6H_3R)$, and $Ru_6C(CO)_{14}(\eta^6\text{-}MeC_6C_6H_4R)$. The solution spectroscopic data for these clusters and the X-ray structures of three products are discussed [79]. Diphenylacetylene reacts with $Ru_3(\mu\text{-}H)(\mu_3\text{-}C_{12}H_{15})(CO)_9$ to give $Ru_3(\mu_3\text{-}C_2Ph_2C_{12}H_{16})(\mu\text{-}CO)_2(CO)_8$, whose solid-state structure was determined by X-ray crystallography. The presence of the metallabicyclo[10.3.0]pentadecatriene system in the product forms as a result of alkyne insertion into the C_{12} ring, coupled with hydride transfer to one of the ring carbons [80]. Kinetic measurements on the reaction of $Os_3(CO)_{10}(\mu\text{-}H)_2$ with CF_3CN, which gives the clusters $Os_3(CO)_{10}[\mu\text{-}\eta^1\text{-}CF_3C(H)\text{=}N](\mu\text{-}H)$ and $Os_3(CO)_{10}(\mu\text{-}\eta^2\text{-}CF_3C\text{=}NH)(\mu\text{-}H)$, have been carried out. The rate-limiting step in the reaction is the formation of $Os_3(CO)_{10}(CF_3CN)(\mu\text{-}H)(H)$, which cannot be directly observed. VT studies and kinetic parameters calculated for the overall reaction indicate that a major tunneling component is associated with the formation of $Os_3(CO)_{10}(\mu\text{-}\eta^2\text{-}CF_3C\text{=}NH)(\mu\text{-}H)$ but not $Os_3(CO)_{10}[\mu\text{-}\eta^1\text{-}CF_3C(H)\text{=}N](\mu\text{-}H)$ [81]. The kinetic site of protonation in $[Ru_3(CO)_{10}(\mu\text{-}NO)]^-$ using CF_3CO_2X and CF_3SO_3X (where X = H, D) has been investigated by using ^{13}C-NMR spectroscopy. The initial protonation occurs at the nitrosyl oxygen atom to give $Ru_3(CO)_9(\mu\text{-}CO)(\mu_3\text{-}NOX)$. These clusters transform

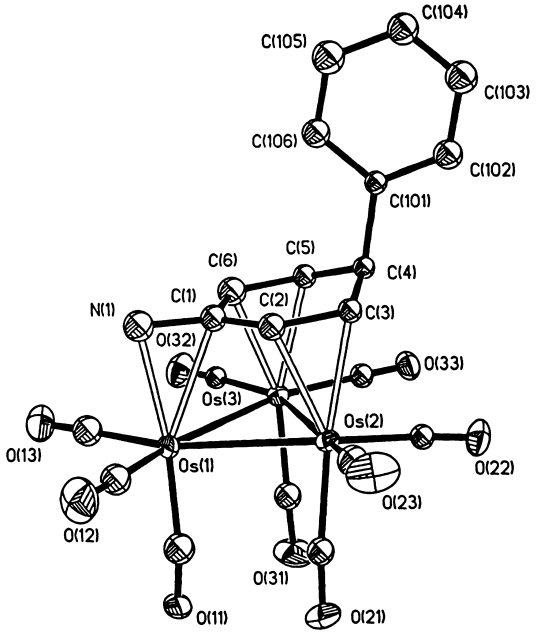

Fig. 3. X-ray structure of $Os_3(CO)_9(\mu_3\text{-}\eta^2\text{:}\eta^2\text{:}\eta^2\text{-}NH\text{=}C_6H_5Ph)$. Reprinted with permission from Organometallics. Copyright 1997 American Chemical Society.

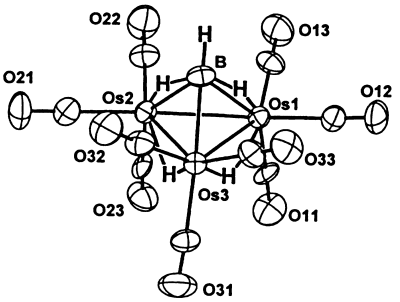

Fig. 4. X-ray structure of $(\mu\text{-H})_2Os_3(CO)_9(\mu\text{-H})_2BH$. Reprinted with permission from Inorganic Chemistry. Copyright 1997 American Chemical Society.

into $Ru_3(CO)_{10}(\mu\text{-NO})(\mu\text{-X})$ at comparable rates. These data are contrasted with proton data in related M_3 clusters, and the differences in the kinetic deuterium isotope effects are discussed with respect to the mechanism for proton transfer [82].

The reaction of $Os_3(CO)_{10}(CNPr)(MeCN)$ with methyl propiolate affords $Os_3(CO)_6[\mu\text{-}\eta^2\text{:}\eta^3\text{-C(OH)C(CO}_2\text{Me)=CHCNHPr}]$ (major product) and $Os_2(CO)_6[\mu\text{-}\eta^2\text{:}\eta^3\text{-C(OH)CH=C(CO}_2\text{Me)CNHPr}]$ (minor product). The regioselectivity associated with these C–C bond-forming reactions and the X-ray structures of the products are discussed [83]. Rearrangement of the uncoordinated allyl moiety in $Os_3(CO)_{10}(\mu\text{-H})(\mu\text{-OCNHCH}_2\text{CH=CH}_2)$ leads to the clusters $Os_3(CO)_{10}(\mu\text{-H})(\mu\text{-OCNHCH=CHMe})$ (four isomers) [84]. The borylidyne cluster $(\mu\text{-H})_2Os_3(CO)_9(\mu\text{-H})_2BH$, a methylidyne cluster analogue, has been isolated from the reaction between $(\mu\text{-H})_2Os_3(CO)_{10}$ and BH_3SMe_2 at room temperature. Carrying the same reaction out at 65°C yields $(\mu\text{-H})_3Os_3(CO)_9(\mu_3\text{-BCO})$. The new borylidyne cluster was fully characterized in solution, and its molecular structure was determined by X-ray analysis (Fig. 4) [85].

The kinetics for CO dissociation in $(\mu_2\text{-H})(H)Os_3(CO)_{10}L$ (where L = various phosphines and phosphites) to give $(\mu_2\text{-H})_2Os_3(CO)_9L$ have been studied. Rate comparisons to analogous $Os_3(CO)_{11}L$ clusters are made, and rate correlations with respect to the steric and donor properties of the P ligand are discussed [86]. The X-ray structures of $Ru_3(CO)_{12-n}(PMe_3)_n$ ($n = 1, 2$) have been solved. The X-ray data from these two clusters are compared with the known cluster $Ru_3(CO)_9(PMe_3)_3$ [87]. The clusters $Fe_3(CO)_{10}LL'$ [where L, L′ = CO, $P(OMe)_3$, $P(OCH_2)_3CMe$] react with CN^tBu in the presence of Me_3NO to give tetra-substituted derivatives. These highly substituted triiron clusters were characterized in solution by IR and NMR spectroscopy, and by mass spectrometry [88]. Diphenylvinylphosphine has been allowed to react with $M_3(CO)_{12}$ (where M = Ru, Os) in refluxing octane or toluene to give the simple substitution products $M_3(CO)_{11}(Ph_2PCH=CH_2)$, $M_3(CO)_{10}(Ph_2PCH=CH_2)$, and $M_3(CO)_{10}(Ph_2PCH=CH_2)_2$. The reaction with divinylphenylphosphine proceeds in a similar fashion. In the case of $Ru_3(CO)_{10}(Ph_2PCH=CH_2)$, oxidative addition of the vinylic C–H bond occurs to give $(\mu\text{-H})Ru_3(CO)_8(Ph_2PCH=CH_2)[\mu_3\text{-}Ph_2P(CH=CH)]$, with $(\mu\text{-H})$

$Ru_3(CO)_8[PhP(CH{=}CH_2)_2][\mu_3\text{-}PhP(CH{=}CH_2)(CH{=}CH)]$ being isolated from the corresponding divinylphenylphosphine-substituted cluster. The X-ray structure of the former oxidative addition product accompanies this report [89]. The activated clusters $Os_3(CO)_{12-n}(MeCN)_n$ (where $n = 1, 2$) react with $Ph_2PCH{=}CH_2$ to give the corresponding P-substituted clusters in good yield. $Os_3(\mu\text{-}H)(H)(CO)_{10}(Ph_2PCH{=}CH_2)$ was isolated from the reaction between $Os_3(\mu\text{-}H)_2(CO)_{10}$ and $Ph_2PCH{=}CH_2$. Analogous ruthenium clusters have been prepared by using electron transfer catalysis. The thermal and photochemical reactivity of these and related clusters have been investigated, and all new products have been characterized in solution by IR and NMR spectroscopy. The X-ray structures of two clusters are reported [90]. 1,2,3-Triphenylphosphirene undergoes C–P bond cleavage during thermolysis with $H_2Os_3(CO)_{10}$. The molecular structure of the resulting product, $Os_3(CO)_9(Ph_3C_2PO)$, was confirmed by X-ray analysis. The five-membered Os–C–C–P–O ring present represents the first such metallacycle ring system in a transition metal complex [91]. The inversion isomers of $Os_3(CO)_{10}(PPh)_5$ have been obtained from the reaction between pentaphenylcyclopentaphosphane and $Os_3(CO)_{10}(MeCN)_2$. The mixed-metal cluster complex $(OC)_{11}Os_3[(PPh)_5]Ru_3(CO)_{11}$ has been isolated from the reaction between $Os_3(CO)_{11}(PPh)_5$ and $Ru_3(CO)_{11}(MeCN)$. The thermolysis chemistry of these clusters and the results of the fluxional behavior of the inversion isomers are presented. Two-dimensional ^{31}P-NMR measurements have allowed for correlations between the various $(PPh)_5$-substituted clusters to be established [92].

The two clusters $Os_3(CO)_{10}[Ph_2P(SH)NP(S)Ph_2\text{–}S,S]$ and $Os_3H(CO)_9[Ph_2P(S)NP(S)Ph_2\text{–}S,S]$ are the main products from the reaction between $Os_3(CO)_{11}(MeCN)$ and bis(diphenylthiophosphinyl)amine. The molecular structures of both clusters were determined by X-ray crystallography [93]. The reaction of the chalcogenides $[R_2P(E)]_2NH$ (where R = Ph, ^{i}Pr; E = S, Se) with $Ru_3(CO)_{12}$ has been explored. Several new tri- and tetranuclear capped chalcogen clusters have been isolated and characterized in solution. Included in this report are the X-ray structures of $Ru_4(\mu_4\text{-}Se)_2(\mu\text{-}CO)(CO)_8[(Ph_2P)_2NH\text{–}P,P']$, $Ru_4(\mu_4\text{-}S)_2(\mu\text{-}CO)(CO)_8[(^iPr_2P)_2NH\text{–}P,P']$, and $Ru_3(\mu_3\text{-}S)_2(CO)_7[(Ph_2P)_2NH\text{–}P,P']$ [94]. The X-ray structure of the phosphido-bridged cluster $Os_3(\mu\text{-}H)(CO)_{10}(\mu\text{-}PPh_2)$ has been solved. The Os–Os edge bridged by the phosphido moiety and the hydride group is slightly longer than the other two Os–Os bonds due to steric interactions between the phenyl groups and the carbonyl ligands. The bonding in this cluster and the related clusters $M_3(\mu\text{-}H)(CO)_{10}(\mu\text{-}PhPH)$ (where M = Ru, Os) has been examined by Fenske–Hall MO calculations. The importance of electronic versus steric effects on the bond angles and bond lengths is discussed [95]. The formation of two *tert*-butyl ketenyl phosphinidene ligands in a triruthenium cluster has been established. Excess ^{t}BuC≡P reacts with $Ru_3(CO)_{10}(\mu\text{-dppm})$ in refluxing THF to give $Ru_3(CO)_7(\mu\text{-dppm})[\mu_3\text{-}P(C{=}C{=}O)^tBu]_2$. X-ray diffraction analysis confirms the presence of the two bridging phosphinidene ligands [96]. The reaction between $Ru_3(CO)_{12}$ and $R_2PCH_2PR_2$ (where R = Me, Ph, Cy) under high CO pressure (ca. 1300 psi) has been studied. In all cases cluster fragmentation to bi- and mononuclear species was observed [97]. The reactivity of the diphosphine diselenide ligands

$dppmSe_2$, $dppeSe_2$, and $dppfSe_2$ with $Fe_3(CO)_{12}$ has been examined in order to study the progressive deformation of the Fe_3Se_2 core in the *nido* clusters $Fe_3Se_2(CO)_7[\mu\text{-}(Ph_2P)_2R]$ by widening the bite of the bridging ligand. Five X-ray structures are presented [98]. Treatment of $Ru_3(CO)_{12}$ with $[CuCl(^tBu_2PH)]_4$ in refluxing toluene gives $Ru_3(CO)_6(\mu\text{-}P^tBu_2)(\mu\text{-}Cl)(^tBu_2PH)$, $Ru_3(CO)_7(\mu\text{-}H)(\mu\text{-}P^tBu_2)_2(\mu\text{-}Cl)$, and $Ru_3(CO)_8(\mu\text{-}H)_2(\mu_3\text{-}P^tBu)(^tBu_2PH)$. The copper complex functions simply as a phosphine and chloride transfer reagent. The X-ray structures of the latter two clusters were determined crystallographically [99]. Thermolysis of $Ru_3(CO)_{12}$ with the redox-active ligand bma affords $Ru_3(CO)_{10}$(bma), $Ru_2(CO)_6$(bma), and $Ru_2(CO)_6[\mu\text{-}C{=}C(PPh_2)C(O)OC(O)](\mu_2\text{-}PPh_2)$. The X-ray structure of $Ru_3(CO)_{10}$(bma) reveals that the bma ligand bridges adjacent ruthenium centers, residing in the plane defined by the ruthenium atoms. The geometrical deviation associated with the bma ligand is discussed, and independent thermolysis experiments revealed that this cluster does not serve as a precursor to the binuclear ruthenium products [100]. Me_3NO activation of $Ru_3(CO)_{12}$ in the presence of added (R)-BINAP does not give the expected cluster $Ru_3(CO)_{10}$[(R)-BINAP], but rather the dihydroxy-bridged cluster $Ru_3(CO)_8(\mu\text{-}OH)_2[\mu\text{-}$(R)-BINAP]. This represents the first example of a μ-BINAP complex. VT NMR studies using isotopically enriched (^{13}CO) samples indicate that the fluxionality is not cluster-centered. COSY spectra reveal that two of the four P–Ph groups rotate freely in solution. Thermolysis of $Ru_3(CO)_{12}$ with (R)-BINAP gives $Ru_3(\mu\text{-}H)[\mu\text{-}$(R)-BINAP–H](CO)$_9$, as a result of orthometalation of one of the phenyl groups. The X-ray structure of $Ru_3(CO)_8(\mu\text{-}OH)_2[\mu\text{-}$(R)-BINAP] is shown in Fig. 5 [101].

$Ru_3(CO)_{12}$ has been allowed to react with excess 2-(chloromethyl)pyridine in refluxing toluene to yield $[RuCl(C_5H_4N\text{-}2\text{-}CH_2CO)(CO)_2]_2$ [102]. The coupling of two alkyne units has been observed in the reaction between $Ru_3(\mu\text{-}H)(CO)_9[\mu_3\text{-}NS(O)MePh]$ and *para*-nitrotolane. The trinuclear clusters $Ru_3(CO)_9[\mu_3\text{-}\eta^3\text{-}PhCC\text{-}CC(H)Ph][\mu_2\text{-}NS(O)MePh]$ and $Ru_3(\mu_2\text{-}CO)(CO)_7[\mu_3\text{-}\eta^3\text{-}PhCCCC(H)Ph][\mu_3\text{-}NS(O)MePh]$ were isolated and characterized in solution and by X-ray crystallography [103]. The electron-deficient cluster $Os_3(CO)_9(\mu\text{-}H)[\mu_3\text{-}\eta^2\text{-}C_9H_5(Me)N]$ reacts with RSH (where R = Et, Ph) to give the hydrido clusters $Os_3(CO)_9(\mu\text{-}H)(H)[\mu\text{-}\eta^2\text{-}C_9H_5(Me)N](\mu\text{-}SR)$. H_2S reacts with the same cluster to afford the known sulfido-capped cluster $Os_3(CO)_9(\mu\text{-}H)_2(\mu_3\text{-}S)$. The reactivity of the thiol clusters with CCl_4 and the dynamic ^{1}H-NMR behavior are reported, along with the X-ray structure of the μ-SEt derivative [104]. Different coordination modes of 3-hydroxy-1,2,3-benzotrianzin-4(3H)-one have been demonstrated at ruthenium and osmium clusters. $Os_3(CO)_{10}(MeCN)_2$ reacts with this ligand to furnish $Os_3(CO)_{10}(\mu\text{-}H)[\mu_2\text{-}(2,3\text{-}\eta^2)\text{-}(O)NNNC_7H_4O]$, while reaction with $Ru_3(CO)_{10}(MeCN)_2$ produces $Ru_3(CO)_{10}(\mu\text{-}H)[\mu_2\text{-}(1,2\text{-}\eta^2)\text{-}NNN(O)C_7H_4O]$. X-ray crystallography has confirmed the molecular structure of each cluster [105]. Treatment of the acyl-substituted cluster $Os_3(CO)_{10}H(\mu\text{-}COC_4H_4N)$ with Me_3NO gives the novel cluster $Os_3(CO)_9H(NMe_3)(\mu\text{-}COC_4H_4N)$ and not the expected pyrrole-linked cluster. X-ray analysis reveals that the NMe_3 ligand adopts an equatorial site on the osmium triangle [106]. The photochemistry of $M_3(CO)_{12}$ (where M = Ru,Os) with nitrogen heterocycles has

been investigated. The ligands employed in this study include pyridine, 2-Mepyridine, 2,6-Me_2pyridine, 2,2′-bpy, and pyridazine. The X-ray structure of $Os_3(CO)_{10}$(bpy) accompanies this report [107]. The reaction of 7-azaindole with $Os_3(CO)_{10}(MeCN)_2$ produces $Os_3(CO)_{10}(\mu\text{-H})(\mu\text{-L})$, which exists as two structural isomers. X-ray diffraction studies have established that the 7-azaindole ligand bridges one edge of each triosmium triangle by both nitrogen atoms in one isomer and by one nitrogen atom and an orthometalated C–H bond in the second isomer [108]. NMR relaxation data have revealed the role played by Os–H···H–N interactions in directing the stereochemistry of carbonyl hydride cluster complexes. The unconventional hydrogen-bond interactions in $H_2Os_3(CO)_{10}L$ (where $L = NH_2Et$, $NHEt_2$) are important in directing the stereochemical disposition of the ancillary ligands about the cluster polyhedron and controlling intramolecular ligand exchange processes [109]. A paper dealing with the comparative reactivity of Ru_3 and Os_3 clusters bearing μ_3-η^2-imidoyl ligands has appeared. The ligand substitution chemistry and ligand dynamics of $Ru_3(CO)_9(\mu_3\text{-}\eta^2\text{-RC=NR}')(\mu\text{-H})$ (where R, R′ = various alkyl groups) are fully discussed. The hemilabible nature of the μ_3-imidoyl ligand is outlined, and the X-ray structures of $Ru_3(CO)_8[\mu_3\text{-}\eta^2\text{-C}\equiv\text{N(CH}_2)_3](\mu\text{-H})(PPh_3)$ and $Ru_3(CO)_8(\mu_3\text{-}\eta^2\text{-MeC=NEt})(\mu\text{-H})(CNMe)$ are also presented [110]. The reactivity of RC≡CR (where R = Me, Ph, CO_2Me) with the imidoyl clusters $Ru_3(CO)_9(\mu_3\text{-}\eta^2\text{-MeC=NEt})(\mu\text{-H})$ and $M_3(CO)_9[\mu_3\text{-}\eta^2\text{-C}\equiv\text{N(CH}_2)_3](\mu\text{-H})$ (where M = Ru, Os) has been explored. The initial alkyne insertion products and their subsequent thermolysis chemistry are thoroughly discussed. Four X-ray structures

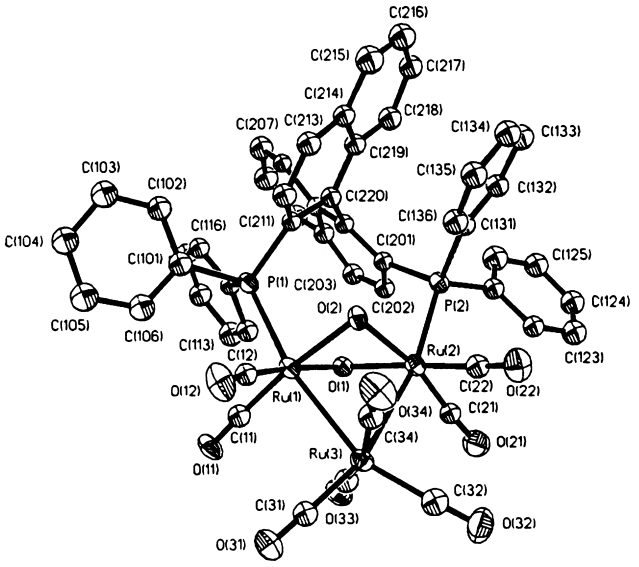

Fig. 5. X-ray structure of $Ru_3(CO)_8(\mu\text{-OH})_2[\mu\text{-(R)-BINAP}]$. Reprinted with permission from Organometallics. Copyright 1997 American Chemical Society.

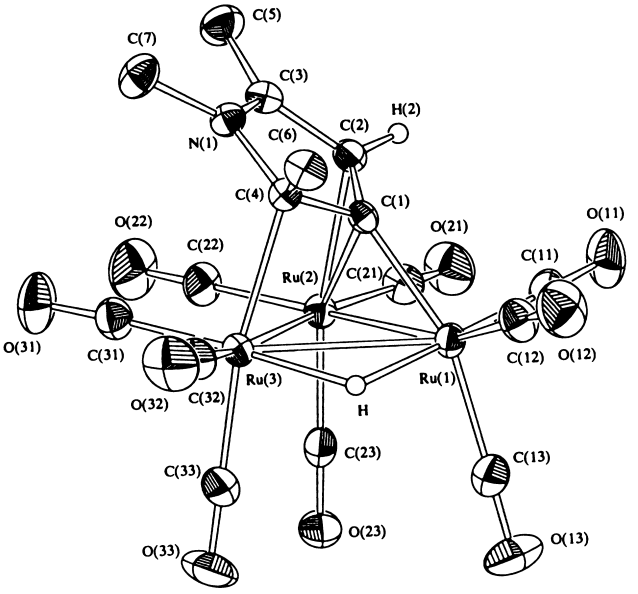

Fig. 6. X-ray structure of $Ru_3(CO)_9(\mu\text{-}H)(\mu_3\text{-}\eta^3\text{-}C_4HMe_2NMe)$. Reprinted with permission from Organometallics. Copyright 1997 American Chemical Society.

are presented, and the results of a comparative electrochemical study on $Ru_3(CO)_9(\mu_3\text{-}\eta^2\text{-}MeC{=}NEt)(\mu\text{-}H)$ and $Ru_3(CO)_7(\mu\text{-}\eta_2{:}\eta^4\text{-}C_4Me_4)(\mu\text{-}\eta^2\text{-}MeC{=}NEt)[\eta^1\text{-}COC(Me)C(H)Me]$ are described [111]. Metalation at the 3-position of 1-methylpyrrole occurs when $Ru_3(CO)_{12}$ is thermolyzed with 1-methylpyrrole. The resulting product, $Ru_3(CO)_9(\mu\text{-}H)(\mu_3\text{-}\eta^3\text{-}C_4H_4NMe)$, exists as two, interconverting isomers in solution, as determined by VT NMR spectroscopy. The clusters $Ru_3(CO)_9(\mu\text{-}H)(\mu_3\text{-}\eta^3\text{-}C_4HMe_2NMe)$ (Fig. 6) and $Ru_3(CO)_9(\mu\text{-}H)(\mu_3\text{-}\eta^3\text{-}C_4HMe_2NH)$ have been obtained from the thermolysis of $Ru_3(CO)_{12}$ with 1,2,5-Me_3pyrrole and 2,5-Me_2pyrrole, respectively, in refluxing THF. Treatment of $Ru_3(CO)_{12}$ with 2,5-Me_2pyrrole in refluxing toluene leads to both N–H and C–H bond cleavage, to give $Ru_3(CO)_9(\mu\text{-}H)[\mu_3\text{-}\eta^3\text{-}CH{=}C_4H_2(Me)N]$ and $Ru_3(CO)_9(\mu\text{-}CO)(\mu\text{-}H)[\mu_3\text{-}\eta^2\text{-}CHC_4H_2(Me)N]$ [112].

Diphenylacetylene inserts into the Ru–N bond in $Ru_3(CO)_9(\mu_2\text{-}H)(\mu_2\text{-}NPh_2)$ to give $Ru_2(CO)_4(\mu\text{-}CO)[\mu\text{-}PhC{=}CPhCPh{=}CPhNPh(C_6H_4)]$. The molecular structure of the product was solved by X-ray crystallography [113]. P–C bond activation of the coordinated PPh_3 in $[Ru_3(CO)_8(PPh_3)_2(\mu_3\text{-ampy})]^+$ occurs during thermolysis to yield the phenyl-bridged cluster $[Ru_3(CO)_7(PPh_3)(\mu\text{-}Ph)(\mu_2\text{-}PPh_2)(\mu_3\text{-ampy})]^+$. This cluster regenerates the bisphosphine cluster upon treatment with CO, via the 50-electron intermediate $[Ru_3(CO)_8(PPh_3)(\mu\text{-}Ph)(\mu_2\text{-}PPh_2)(\mu_3\text{-ampy})]^+$. These reactions provide the first documented example for reversible P–C bond activation in a metal cluster. The reaction of the heptacarbonyl cluster $[Ru_3(CO)_7(PPh_3)(\mu\text{-}Ph)(\mu_2\text{-}PPh_2)(\mu_3\text{-ampy})]^+$ with [PPN][Cl] affords the neutral cluster $Ru_3(CO)_5(PPh_3)(\mu\text{-PhCO})(\mu_2\text{-}PPh_2)(\mu\text{-Cl})(\mu_3\text{-ampy})$, whose molecular structure was deter-

mined by X-ray crystallography [114]. The cationic clusters $[Ru_3(CO)_9(\mu\text{-}X)(\mu_3\text{-}ampy)]^+$ (where X = Cl, I, AcO) have been obtained from the reaction of $[Ru_3(CO)_{10}(\mu_3\text{-}ampy)]^+$ with $[X]^-$. Use of [PPN][BH_4] gives the neutral cluster $Ru_3(CO)_9(\mu\text{-}H)(\mu_3\text{-}ampy)$. The reaction of $[Ru_3(CO)_{10}(\mu_3\text{-}ampy)]^+$ with $[Ru_3(CO)_9(\mu_3\text{-}S)]^{2-}$ gives the hexaruthenium cluster $Ru_6(CO)_{17}(\mu\text{-}H)(\mu_4\text{-}S)(\mu_3\text{-}ampy)$, whose structure consists of two closed triruthenium units joined by two Ru–Ru bonds [115]. New neutral and cationic triruthenium clusters with a bridging 1-azavinylidene ligand have been synthesized. $Ru_3(CO)_{10}(\mu\text{-}H)(\mu\text{-}N{=}CPh_2)$ reacts with Ph_2PH to afford $Ru_3(CO)_9(Ph_2PH)(\mu\text{-}H)(\mu\text{-}N{=}CPh_2)$, which upon thermolysis gives $Ru_3(CO)_8(\mu\text{-}PPh_2)(\mu\text{-}H)_2(\mu\text{-}N{=}CPh_2)$. This latter cluster loses H_2 upon exposure to CO to yield the corresponding nonacarbonyl cluster [116]. The ureato-bridged cluster $Ru_3(CO)_9(\mu\text{-}H)(\mu_3\text{-}HNCONMe_2)$ reacts with PPh_3 or Ph_2PH (1.0 equivalents) to give $Ru_3(CO)_8(L)(\mu\text{-}H)(\mu_3\text{-}HNCONMe_2)$. X-ray crystallography in the case of the PPh_3 derivative reveals that the PPh_3 group occupies an equatorial position *cis* to the bridging NH moiety. When the same reaction is carried out in the presence of excess PPh_3, the phenyl-bridged cluster $Ru_3(CO)_6(\mu\text{-}\eta^1\text{-}Ph)(\mu\text{-}PPh_2)_2(\mu_3\text{-}HNCONMe_2)$ may be isolated as the major product. The X-ray structure of this cluster (Fig. 7) is presented. The carbonyl substitution chemistry exhibited by $Ru_3(CO)_9(\mu\text{-}H)(\mu_3\text{-}HNCONMe_2)$ is contrasted with related clusters containing N- and/or P-donor ligands. It is concluded that the hard donor ligands render the cluster more reactive in CO substitution reactions [117].

The vinyl cluster $Ru_3(CO)_6(\mu_2\text{-}CO)_2[\mu_3\text{-}NS(O)MePh)](\mu_2\text{-}\eta^1,\eta^2\text{-}PhCH_2C{=}CH_2)$ has been isolated from the reaction between $Ru_3(CO)_9(\mu_2\text{-}H)[\mu_3\text{-}NS(O)MePh)]$ and $PhCH_2C{\equiv}CH$. Internal alkynes react in a similar fashion to give the new clusters $Ru_3(CO)_7(\mu_2\text{-}CO)[\mu_3\text{-}NS(O)MePh)](\mu_3\text{-}\eta^1,\eta^2\text{-}RC{=}CHR')$. Here vinyl group coordi-

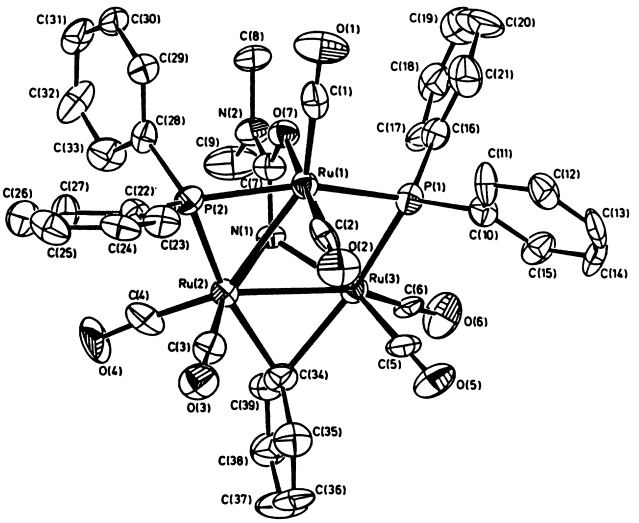

Fig. 7. X-ray structure of $Ru_3(CO)_6(\mu\text{-}\eta^1\text{-}Ph)(\mu\text{-}PPh_2)_2(\mu_3\text{-}HNCONMe_2)$. Reprinted with permission from Organometallics. Copyright 1997 American Chemical Society.

nation leads to an opening of the Ru_3 framework [118]. Treatment of [(μ-^{t}BuS)(μ-CO)$Fe_2(CO)_6$][Et_3NH] with $Zn(OAc)_2 \cdot H_2O$ has furnished the triiron cluster $Fe_3(CO)_9(\mu$-SH)(μ_3-S^{t}Bu). The molecular structure of this *nido* cluster was determined by X-ray crystallography [119]. Thionylaniline reacts with $Os_3(CO)_{12}$ in refluxing methylcyclohexane to give $Os_3(CO)_9(\mu_3$-NPh)(μ_3-S) in good yield. Use of the activated cluster $Os_3(CO)_{10}(MeCN)_2$ gives both $Os_3(CO)_9(\mu_3$-NPh)(μ_3-S) and $Os_3(CO)_9[\mu_3$-η^2-$(PhN)_2SO](\mu_3$-S). Both clusters were characterized fully in solution and by X-ray diffraction analysis [120].

The synthesis and X-ray structure of $[Cp_3^*(Ph_2C_2S_2)Fe_4S_5][BF_4] \cdot$(acetone) has been reported. The Fe_4S_5 core is flexible in solution [121]. The X-ray structure of $[Fe(CO)_3]_3[\mu_3$-CC{$CpFe(CO)_2$}$C(CF_3)$] has been determined, and the IR and NMR data briefly discussed with respect to the molecular structure [122]. The phosphaalkyne-bridged cluster $Fe_4Se_2(CO)_{11}(\mu$-$Se_2PC^tBu)$ has been obtained from $Fe_2(CO)_6(\mu$-$Se)_2$ and P≡C^{t}Bu. The results of full solution characterization are discussed, and the molecular structure, which was determined by X-ray crystallography, exhibits a bow-tie Fe_3Se_2 moiety. One face of this cluster is capped by an unusual $FeSe_2P$ unit [123]. New iron–sulfur clusters containing dimethylsilyl-bridged Cp groups have been prepared. Thermolysis of $[Me_2Si(\eta^5$-$C_5H_4)_2]Fe_2(CO)_4$ with S_8 affords the cubane cluster $[Me_2Si(\eta^5$-$C_5H_4)_2]_2Fe_4S_6$ and $[Me_2Si(\eta^5$-$C_5H_4)_2]_2Fe_5S_{12}$, whereas photolysis gives the related cluster $[Me_2Si(\eta^5$-$C_5H_4)_2]_2Fe_4S_6(CO)$. The electrochemical properties, as studied by cyclic voltammetry, and the Mössbauer data for these clusters are presented [124].

Hydrogenation of $Ru_5(\mu_5$-CN^{t}Bu)$(CO)_{14}$(CN^{t}Bu) gives both $Ru_4(\mu$-H)$_4(CO)_{10}$(CN^{t}Bu)$_2$ and $Ru_4(\mu$-H)$_4(CO)_{11}$(CN^{t}Bu); the crystal and molecular structures of the latter cluster are reported [125]. The X-ray structures of $Os_4(\mu$-Cl)(μ-H)$_3(CO)_{12}$ and $Os_5(\mu$-Cl)(μ-H)$_3(CO)_{14}$ have been published [126]. Thermolysis of $Fe_2(CO)_6(\mu_2$-η^2-C≡CPh)(μ-$PPh_2)$ in toluene leads to the linking of two acetylide units by a plane of four iron atoms. The product, $Fe_4(\mu_4$-$PPh_2)_2(\mu_4$-η^2-C≡CPh)$_2(CO)_8$, has been characterized in solution and by X-ray crystallography [127]. Treatment of $Fe_4(CO)_{12}$[C=C(Me)(OMe)] with Super-Hydride, followed by $CF_3SO_3SiMe_3$, gives the μ_4-vinylidene cluster $Fe_4(CO)_{12}(\mu_4$-η^2-C=CHMe). The cluster possesses an open butterfly arrangement of iron atoms, with the prop-1-ene-1,1-diyl ligand bound to all four iron centers. The molecular structure has been determined by X-ray analysis. The bonding in this cluster has been studied by carrying out Fenske–Hall calculations [128]. The rectangular cluster $Fe_4(CO)_8(\mu$-$PPh_2)_2(\mu_4$-η^1,η^1,η^2,η^2-$C_2Ph_2)_2$ has been isolated from the thermolysis of $Fe_2(CO)_4(\mu$-$PPh_2)(\mu$-η^1,η^2-$C_2Ph_2)$. The Fe_4 cluster reacts with CO to yield $Fe_3(CO)_8[\mu$-$Ph_2PC(CPh)$=C(CPh)$PPh_2]$, as a result of C–C and C–P bond formation. The solid-state structures of both products were determined by X-ray methods [129]. The tetranuclear clusters $RuM_3H(C{\equiv}CFc)(CO)_{12}$ (where M = Ru, Os) have been obtained from the acetylide clusters $M_3H(C{\equiv}CFc)(CO)_9$ and $Ru_3(CO)_{12}$ in refluxing hexane. VT ^{1}H- and ^{13}C-NMR studies reveal that the μ_4-acetylide ligand undergoes a σ/π bond exchange between adjacent metal centers. Two X-ray structures accompany this report [130]. Photolysis of $HRu_4(CO)_{12}(BH_2)$ with $HPPh_2$ leads to the formation of mono-, di-, and trisubstituted products. The identity of these new clusters was established by IR and NMR measurements, and

by X-ray diffraction analysis in the case of $HRu_4(CO)_{10}(HPPh_2)_2(BH_2)$. Thermolysis of the bisphosphine cluster yields the phosphido-bridged cluster $H_2Ru_4(CO)_9(HPPh_2)(\mu\text{-}PPh_2)(BH_2)$ [131]. Triazaligands have been allowed to react with $H_4Ru_4(CO)_{12}$ to give the anionic clusters $[LH][H_3Ru_4(CO)_{12}]$. This single-step route to $[H_3Ru_4(CO)_{12}]^-$ proceeds without complications and in high yield. The reactivity of these clusters in the water–gas shift reaction and the carbonylation of methanol is discussed [132]. Pyrolysis of $[Bi_4Fe_4(CO)_{12}]^{2-}$ in MeCN gives the square–pyramidal cluster $[Fe_3(CO)_9Bi_2]^{2-}$. X-ray diffraction analysis confirms that this cluster belongs to the square–pyramidal class of 50-electron M_3E_2 clusters. The bonding in the Fe_3Bi_2 cluster has been investigated by extended Hückel MO calculations [133]. The reaction between $[Bi_4Fe_4(CO)_{13}]^{2-}$ and $MePCl_2$ in MeCN affords a mixture of products, depending upon the stoichiometry of the reagents employed. The new clusters $[(\mu\text{-}H)Fe_2(CO)_6Bi\{Fe(CO)_4\}]^-$ and $[Bi_3Cl_4(\mu\text{-}Cl)_4\{Fe(CO)_3\}]^{3-}$ have been synthesized when a cluster to $MePCl_2$ ratio of 1:1.33 was used. The X-ray diffraction data and the results from extended Hückel MO calculations are discussed [134]. A report on the synthesis and characterization of the first metal cluster containing a diphosphorus monoxide ligand has appeared. Starting with either $Ru_4(CO)_{13}(\mu_3\text{-}PN^iPr_2)$ or $Ru_4(CO)_{13}(\mu_3\text{-}POH)$, small amounts of $(OC)_{13}Ru_4(\mu_6,\eta^2\text{-}P_2O)Ru_4(CO)_{12}$ have been isolated. The identity of this Ru_8 cluster was established by X-ray diffraction analysis. A working mechanism accounting for the formation of this novel cluster is discussed [135]. The synthesis of unsymmetrically capped bisphosphinidene clusters has been described. Treatment of the 62-electron cluster $Ru_4(CO)_{13}(\mu_3\text{-}PPh)$ with the phosphalkynes RC≡P (where $R = {}^tBu$, 2,4,6-$^tBu_3C_6H_2$) leads to $Ru_4(CO)_{12}(\mu_3\text{-}PPh)[\mu_3\text{-}PC(CO)R]$, which loses CO to give the *closo* clusters $Ru_4(CO)_{10}(\mu\text{-}CO)(\mu_4\text{-}PPh)[\mu_3\text{-}PC(CO)R]$. The X-ray structure of $Ru_4(CO)_{12}(\mu_3\text{-}PPh)[\mu_3\text{-}PC(CO)^tBu]$ (Fig. 8) and the other three product clusters are presented [136].

The reactivity of $[SFe_3(CO)_9]^{2-}$ with some transition metal complexes and organic halides has been studied. Treatment of the dianion with $Ru_3(CO)_{12}$ in acetone affords the pentanuclear cluster $[SeFe_2Ru_3(CO)_{14}]^{2-}$, whose molecular structure was unequivocally established by X-ray crystallography. Use of HgI_2 leads to the mixed-metal cluster $[SeFe_3(CO)_9(\mu\text{-}HgI)]^-$ [137]. The substitution chemistry of $Ru_5C(CO)_{14}L$ [where $L = P(OPh)_3$, PCy_3] with added P ligands has been examined. These reactions proceed by an associative pathway, and the effects of the electronic and steric properties of the P ligands have been analyzed [138]. The bonding in several organometallic clusters containing exposed dicarbon moieties has been explored by MO calculations. It is shown that the bonding of the C_2 moiety with the metallic host follows the Dewar–Chatt–Duncanson bonding model [139]. Facile Ru–Ru bond cleavage and cluster structural changes are observed when $Ru_5C(CO)_{15}$ is allowed to react with 1,10-phen and 2,2′-bpy. The butterfly clusters $Ru_5C(CO)_{14}$(1,10-phen) and $Ru_5C(CO)_{14}$(2,2′-bpy) have been isolated as the major products when the substitution reaction is carried out with Me_3NO. Also isolated from these reactions are minor amounts of the orthometalated clusters $Ru_5(\mu\text{-}H)C(CO)_{13}(C_{12}H_7N_2)$ and $Ru_5(\mu\text{-}H)C(CO)_{13}(C_{10}H_7N_2)$. The X-ray structures of three clusters are presented [140]. The reactivity of $Ru_5(\mu_5\text{-}C_2PPh_2)(\mu\text{-}$

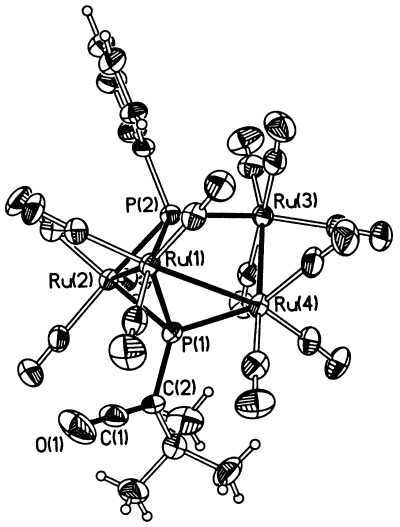

Fig. 8. X-ray structure of $Ru_4(CO)_{12}(\mu_3\text{-}PPh)[\mu_3\text{-}PC(CO)^tBu]$. Reprinted with permission from Organometallics. Copyright 1997 American Chemical Society.

$PPh_2)(CO)_{13}$ with Me_2S has been studied [141]. The use of $[Ru_5C(CO)_{14}]^{2-}$ as a cluster building block is described. The reaction of the dianion with $[CpRu(MeCN)_3]^+$ gives the hexanuclear cluster $[Ru_6C(CO)_{14}Cp]^-$ and the heptanuclear cluster $Ru_7C(CO)_{14}Cp_2$. A similar build-up scheme using $[Ru_6C(CO)_{16}]^{2-}$ is also discussed. The X-ray data and the solution spectroscopic data are fully discussed [142]. The mononuclear complex $Ru(CO)_4(\eta^1\text{-diphosphine})$ has been used as a capping ligand in reactions with $Ru_5C(CO)_{15}$ and $Ru_3(CO)_{12}$ [143]. The ionic coupling of $[Os_4H_4(CO)_{12}]^{2-}$ with $[(\eta^6\text{-}C_6H_6)Ru(MeCN)_3]^{2+}$ furnishes the $RuOs_4$ cluster $Os_4Ru(\mu\text{-}H)_2(CO)_{12}(\eta^6\text{-}C_6H_6)$. $P(OMe)_3$ reacts with this cluster to give $Os_4Ru(\mu\text{-}H)_2(CO)_{12}(\eta^6\text{-}C_6H_6)[P(OMe)_3]$; this cluster rearranges in solution to yield the ruthenium-spiked cluster $Os_4Ru(\mu\text{-}H)_3(CO)_{12}(\mu_3\text{-}\eta^6\text{-}C_6H_5)[P(OMe)_3]$. The solid-state structure of this latter cluster was solved by X-ray diffraction analysis [144]. Treatment of C_{60} with $Ru_5C(CO)_{15}$ and $Ru_6C(CO)_{17}$ in refluxing chlorobenzene, followed by reaction with a tertiary phosphine ligand, gives the face-bonded clusters $Ru_5C(CO)_{11}(PPh_3)(\mu_3\text{-}\eta^2\text{:}\eta^2\text{:}\eta^2\text{-}C_{60})$ (Fig. 9) and $Ru_6C(CO)_{12}(dppm)(\mu_3\text{-}\eta^2\text{:}\eta^2\text{:}\eta^2\text{-}C_{60})$. The X-ray structure of each product is presented and discussed [145].

The results of a single-crystal neutron diffraction study on $H_2Os_6(CO)_{18}$ have been published. Both hydrides occupy edge-bridging positions [146]. Acetylenic diphosphine ligands have been used to link two triruthenium cluster units together. Treatment of $Ru_3(CO)_9(\mu\text{-}H)(\mu_3\text{-}C_2^tBu)$ with P–P (where P–P = dppa, $Bu_2PC{\equiv}CPBu_2$) gives the phosphine-bridged clusters $[Ru_3(CO)_8(\mu\text{-}H)(\mu_3\text{-}C_2^tBu)]_2(\mu\text{-}P\text{–}P)$ in moderate yields. The solution NMR data and the X-ray structure of the dppa derivative are presented [147]. The thermolysis of $Ru_3(CO)_{12}$ with either cyclohexene or 1,3-COD produces a variety of cluster complexes, including one

cluster which possesses a C_6 ligand which has undergone a ring contraction. The new clusters $Ru_6(\mu_3\text{-H})(\mu_4\text{-}\eta^2\text{-CO})_2(CO)_{13}(\eta^5\text{-}C_5H_4Me)$ and $Ru_6(\mu_3\text{-H})(\mu_4\text{-}\eta^2\text{-CO})_2(CO)_{13}(\eta^5\text{-}C_8H_9)$ have been structurally characterized by X-ray crystallography [148]. Partial hydrogenation of the acetylide moiety in $[Ru_3(CO)_8(\mu\text{-H})(\mu_3\text{-}C_2^t Bu)]_2(\mu\text{-dppa})$ affords the hexanuclear clusters $Ru_6(\mu_5\text{-}^t BuCH{=}CHC_2PPh_2)(\mu_4\text{-}C_2^t Bu)(\mu\text{-}PPh_2)(CO)_{13}$ and $Ru_6(\mu_6\text{-}C_2CH{=}CH^t Bu)(\mu_3\text{-}C_2^t Bu)(\mu\text{-}PPh_2)(\mu\text{-CO})(CO)_{12}$. The identity of these clusters was established by ^{1}H-NMR spectroscopy and X-ray diffraction analysis [149]. Pyridine reacts with $Os_6(CO)_{16}(MeCN)_2$ in CH_2Cl_2 at room temperature to give the new clusters $Os_6(CO)_{15}(\mu_4\text{-}\eta^2\text{-CO})(C_5H_5N)_3$, $Os_6(CO)_{15}(\mu\text{-H})(\mu\text{-CO})(\mu_3\text{-O})(C_5H_5N)(\mu\text{-}\eta^2\text{-}NC_5H_4)$, and $Os_6(CO)_{14}(\mu\text{-H})(\mu\text{-CO})(MeCN)(C_5H_5N)(\mu\text{-}\eta^2\text{-}NC_5H_4)$. The molecular structure of the oxo-capped cluster was determined by X-ray methods [150].

The synthesis and characterization of the arene–alkyne clusters $Ru_6C(CO)_{12}(\eta^6\text{-}C_6H_6)(\mu_3\text{-}C_2Me_2)$, $Ru_6C(CO)_{12}(\eta^6\text{-}C_6H_5Me)(\mu_3\text{-}C_2Me_2)$, $Ru_6C(CO)_{12}(\eta^6\text{-}C_6H_4Me_2\text{-}1,3)(\mu_3\text{-}C_2Me_2)$, $Ru_6C(CO)_{12}(\eta^6\text{-}C_6H_3Me_3\text{-}1,3,5)(\mu_3\text{-}C_2Me_2)$, and $Ru_6C(CO)_{12}(\mu_3\text{-}C_{16}H_{16})(\mu_3\text{-}C_2Me_2)$ have been published. The X-ray structures and crystallographic packing motifs of four clusters are discussed [151]. New hexaruthenium carbide clusters containing arenes derived from biphenyls have been synthesized from $Ru_3(CO)_{12}$ and the requisite arene. The solid-state supramolecular architecture of some of the products has been examined relative to the construction of organometal networks [152]. $Ru_6C(CO)_{17}$ reacts with $Ph_2P(CH_2)_nPPh_2$ (where $n = 1-3$) to afford the phosphine-bridged clusters $Ru_6C(CO)_{15}[\mu\text{-}Ph_2P(CH_2)_nPPh_2]$ in good yield. In the case of the ligand dppb, both $Ru_6C(CO)_{15}(\mu\text{-dppb})$ and $Ru_6C(CO)_{16}$(dppb–P)

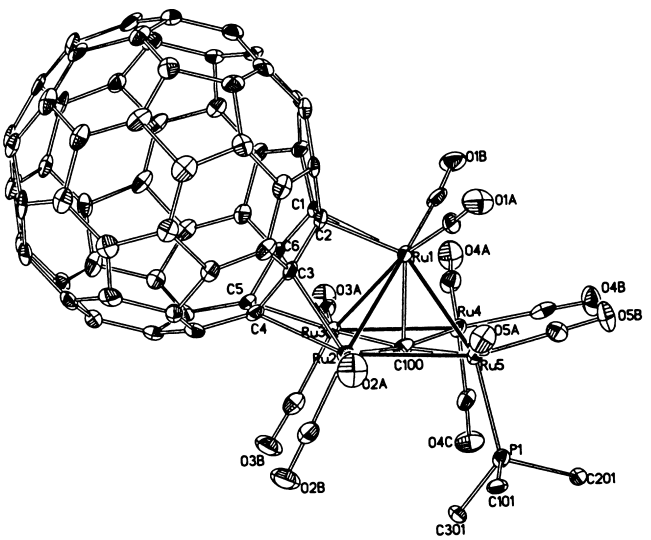

Fig. 9. X-ray structure of $Ru_5C(CO)_{11}(PPh_3)(\mu_3\text{-}\eta^2{:}\eta^2{:}\eta^2\text{-}C_{60})$. Reprinted with permission from Organometallics. Copyright 1997 American Chemical Society.

have been isolated. All new clusters were fully characterized in solution, and the X-ray structures of the dppm, dppe, and dppp derivatives were determined [153]. The fluxional behavior of the ancillary ligands in $[Ru_6C(CO)_{14}(SO_2)(\mu\text{-}\eta^3\text{-}C_3H_5)]^-$, $Ru_6C(CO)_{14}(NO)(\mu\text{-}\eta^3\text{-}C_3H_5)$, and $Ru_6C(CO)_{14}(NO)(\mu\text{-}\eta^3\text{-}C_3H_4CO_2Me)$ has been examined by VT ^{1}H- and ^{13}C-NMR spectroscopy. Plausible exchange mechanisms, activation parameters, and the X-ray structure of the latter cluster are presented [154]. $Ru_6C(CO)_{17}$ reacts with phenylacetylene in the presence of Me_3NO to initially give the alkyne cluster $Ru_6C(CO)_{15}(PhC_2CH)$. This cluster reacts with excess phenylacetylene to afford the isomeric clusters $Ru_6C(CO)_{14}$[C(Ph)CHC(Ph)CH] and $Ru_6C(CO)_{14}$[C(Ph)CHCHC(Ph)]. Treatment of the head-to-tail alkyne coupling product with additional phenylacetylene leads to the carbyne cluster $Ru_6C(CO)_{13}(\eta^5\text{-}C_5H_3Ph_2)(\mu_3\text{-}CPh)$ [155]. The isomeric cluster complexes $Ru_6C(CO)_{14}[\eta^6\text{-}C_6H_4(CO_2Me)_2\text{-}1,4]$ and $Ru_6C(CO)_{14}[\mu_3\text{-}\eta^2\text{:}\eta^2\text{-}C_6H_4(CO_2Me)_2\text{-}1,4]$ have been obtained from the thermolysis reaction of $Ru_6C(CO)_{17}$ with $C_6H_4(CO_2Me)_2$-1,4. The solid-state structures and molecular architectures of these new clusters were determined by X-ray crystallography. The utility of the bifunctionalized arene ligand in copolymerization reactions is discussed [156]. Reversible phenyl coordination of a PPh_3-coordinated ligand was reported for $Ru_6C(CO)_{16}(PPh_3)$. CO loss and aryl-group coordination is observed in refluxing chlorobenzene to give $Ru_6C(CO)_{13}[Ph_2P(\mu\text{-}\eta^6\text{-}C_6H_5)]$. This reaction is readily reversed upon reaction with added CO. The X-ray structure of the latter cluster confirms the reaction sequence [157]. Chemical activation of $Ru_6C(CO)_{17}$ in the presence of 2-butyne has allowed for the synthesis of $Ru_6C(CO)_{15}(\mu_3\text{-}\eta^1\text{:}\eta^2\text{:}\eta^1\text{-}C_2Me_2)$, $Ru_6C(CO)_{14}(\mu\text{-}\eta^2\text{:}\eta^2\text{-}C_2Me_2)(\mu_3\text{-}\eta^1\text{:}\eta^2\text{:}\eta^1\text{-}C_2Me_2)$, $Ru_6C(CO)_{13}(\mu_3\text{-}\eta^1\text{:}\eta^2\text{:}\eta^1\text{-}C_2Me_2)_2$, and $Ru_6C(CO)_{12}(\mu_3\text{-}\eta^1\text{:}\eta^2\text{:}\eta^1\text{-}C_2Me_2)_3$. Coordination of two alkyne ligands promotes a geometrical change in the metallic core from octahedral to a monocapped square-pyramid [158]. CO substitution in $Ru_6C(CO)_{17}$ by SO_2 yields $Ru_6C(CO)_{16}(SO_2)$ (Fig. 10), whose molecular structure was solved by X-ray diffraction analysis. This reaction is reversible under added CO. The dianionic cluster $[Ru_6C(CO)_{16}]^{2-}$ reacts with SO_2 in the presence of Me_3NO to afford $[Ru_6C(CO)_{15}(SO_2)]^{2-}$ and $[Ru_6C(CO)_{14}(SO_2)_2]^{2-}$. The reactivity of these latter clusters with NO and $MeOSO_2CF_3$ has been explored [159].

Oxidation of $[Ru_{10}C_2(CO)_{24}]^{2-}$ by $[Cp_2Fe][BF_4]$ in the presence of disubstituted alkynes gives the neutral clusters $Ru_{10}C_2(CO)_{23}(C_2RR')$. Reduction by methanolic hydroxide yields the known clusters $[Ru_{10}C_2(CO)_{22}(C_2RR')]^{2-}$. The solution NMR data and the X-ray structure of $Ru_{10}C_2(CO)_{23}(C_2Ph_2)$ are discussed [160]. Cyclic voltammetric and spectroelectrochemical studies on $[Ru_{10}(\mu\text{-}H)(\mu_6\text{-}C)(CO)_{24}]^-$ and $[Ru_{10}(\mu_6\text{-}C)(CO)_{24}]^{2-}$ have been carried out. The effect of the hydride ligand on the redox properties of these clusters is discussed [161]. The electronic spectra of high nuclearity ruthenium clusters are discussed with respect to the nature of the HOMO and LUMO levels. Local density functional (LDF) calculations support the optical spectral assignments. The results from EPR and magnetic susceptibility studies are also discussed [162].

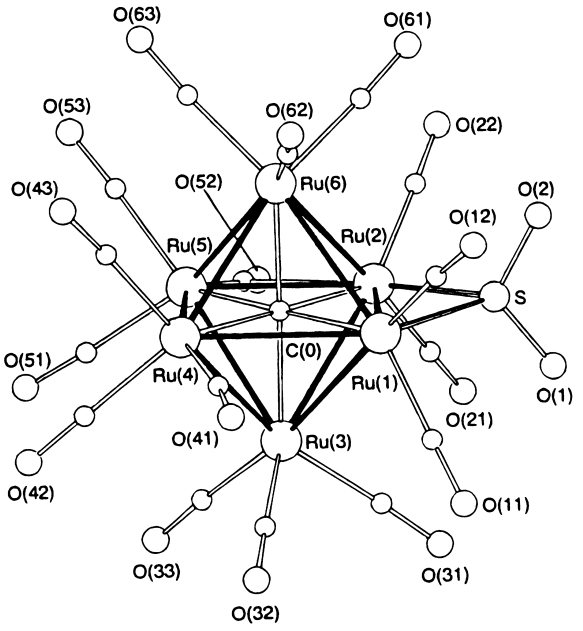

Fig. 10. X-ray structure of $Ru_6C(CO)_{16}(SO_2)$. Reprinted with permission from Inorganic Chemistry. Copyright 1997 American Chemical Society.

2.6. Group 9 clusters

A database study which explored the relationship between the molecular and crystal structures of organometallic clusters possessing methylidyne and methylene ligands has been published. These ligands are shown to participate in intermolecular hydrogen-bonding networks (C–H···O) with the CO groups as the oxygen acceptors. The methylidyne ligand in $(\mu_3\text{-CH})Co_3(CO)_9$ participates in a trifurcated interaction with two neighboring cluster molecules [163]. The X-ray structure of $[PhCCo_3(CO)_8]_2(Ph_2PC_6H_4PPh_2)$ has been solved and published. Included in this report are the IR and ^{31}P-NMR data for this cluster and the methyl-capped derivative [164]. New face-capped thioether derivatives of $PhCCo_3(CO)_9$ have been synthesized. Treatment of $PhCCo_3(CO)_9$ with tridentate sulfur donor ligands leads to the clusters $PhCCo_3(CO)_6(S_3)$ [where $S_3 = 1,3,5$-trithiacyclohexane, tris(thiomethyl)methane]. Use of Me_2S allows for the isolation of $PhCCo_3(CO)_{9-n}(Me_2S)_n$ (where $n = 1–3$). The X-ray structures of the clusters with the tridentate sulfur ligands are discussed [165]. Reaction of the carboxylic acid group in $(\mu_3\text{-}CCO_2H)Co_3(CO)_9$ with $Cd(OAc)_2$ in the presence of tetraethylene glycol dimethyl ether (TGM) gives $Cd_2[(OC)_9Co_3(\mu_3\text{-}CCO_2)]_4$(TGM). The X-ray structure of this cluster is presented [166]. Ph_2PH reacts with $RCCo_3(CO)_9$ (where R = Me, CO_2Me) to give $RCCo_3(CO)_{9-n}(Ph_2PH)_n$ (where $n = 1$, 2), along with $MeCCo_3(CO)_6(Ph_2PH)(\mu\text{-}Ph_2POPPh_2)$. Thermolysis of $MeCCo_3(CO)_8(Ph_2PH)$ in

heptane solution leads to the activation of the phosphine ligand and formation of $MeCCo_3(CO)_7(\mu\text{-}H)(\mu\text{-}PPh_2)$. A plausible mechanism which accounts for the formation of $MeCCo_3(CO)_7(\mu\text{-}Ph_2POPPh_2)$ from the intermediate cluster $MeCCo_3(CO)_7(\mu\text{-}Ph_2PPPh_2)$ is discussed. All new clusters have been fully characterized in solution and by X-ray crystallography in the case of $MeCCo_3(CO)_6(Ph_2PH)(\mu\text{-}Ph_2POPPh_2)$ and $MeCCo_3(CO)_7(\mu\text{-}H)(\mu\text{-}PPh_2)$ [167]. The syntheses and magnetic properties of the low-valent clusters $[X\{Co(\mu\text{-}CO)(PMe_3)_2\}_3]$ (where X = none, H, H_3) have been published. The molecular structures of X = none and $X = H_3$ exhibit a central Co_3 unit which is a perfect equilateral triangle. The temperature-dependent magnetic moment of each cluster has been examined, with the magnetic behavior discussed relative to the Curie–Weiss law [168].

C–H bond activation of simple alkenes is reported to take place at CpCo fragments. Treatment of cycloalkanes with $CpCo(ethylene)_2$ leads to the trinuclear clusters $Cp_3Co_3(\mu\text{-}H)_2[\mu_3\text{-}C_2(CH_2)_{n-2}]$. Use of the more active reagent $[Cp_2Co][K]$ allows for the isolation of the same tricobalt clusters and small amounts of $Cp_4Co_4[\mu_4\text{-}C_2(CH_2)_{n-2}]$. The molecular structures of four clusters are presented, and the dynamic behavior of the alkyne and hydride ligands, as studied by NMR spectroscopy, is discussed [169]. The reactivity of C_{3v} $(\eta^5\text{-ind})_3Ir_3(\mu\text{-}CO)_3$ with metal electrophiles has been studied. The resulting tetranuclear clusters have been fully characterized [170]. An NMR study on the ligand fluxionality in $Cp^*Rh(CpCo)_2(\mu\text{-}CO)_2(\mu\text{-}CH_2)$ has provided data on the existence of a $\mu_3\text{-}CH_2$ intermediate. NOESY spectra and the ^{13}C isotopic enrichment studies unequivocally establish the exchange pathways which equilibrate the $\mu_2\text{-}CH_2$ moiety between the two M–M edges in this cluster [171]. The rate of isomerization between the different isomers of $Cp^*Ir(CpCo)_2(CO)_3$ has been measured as a function of the cluster's oxidation state. The relative rate of cluster isomerization increases in the order $48e^- \ll 49e^- \ll 47e^-$, and the rate enhancements are discussed relative to the orbital occupancies of the $IrCo_2$ frame [172]. A family of bis(carbyne)Cp_3Co_3 clusters has been studied by ^{13}C-NMR spectroscopy. The data from T_1 measurements have been used to assess the reorientational dynamics of each cluster system [173]. New tricobalt clusters possessing a furyne ligand have been prepared and characterized. Pyrolysis of the butynediol clusters $(CpCo)_3(CO)(HOCH_2C{\equiv}CCH_2OH)$ and $(CpCo)_2Cp^*Co(CO)(HOCH_2C{\equiv}CCH_2OH)$ affords the furyne complexes $(CpCo)_3(CO)(\mu_3\text{-}\eta^2\text{-}\overline{CH_2C{\equiv}CCH_2O})$ and $(CpCo)_2Cp^*Co(CO)(\mu_3\text{-}\eta^2\text{-}\overline{CH_2C{\equiv}CCH_2O})$, respectively. Fig. 11 shows the ORTEP diagrams of these two clusters. The electrochemical properties and the fluxional behavior of the furyne ligand are reported [174].

The anionic clusters $[Ir_4(CO)_{11}X]^-$ (where X = Br, I) undergo reaction with ^{13}CO to give isotopically enriched $Ir_4(CO)_{12}$. The extent of ^{13}CO enrichment amounts to one ^{13}CO per $Ir_4(CO)_{12}$. Repeating the exchange cycle with added $[X]^-$ and ^{13}CO allows for higher ^{13}CO enrichment levels of $Ir_4(CO)_{12}$ [175]. The surface chemistry and catalysis of SiO_2-supported $RhCo_3(CO)_{12}$ have been published. The catalyst system shows high activity and stability in the hydroformylation of ethylene to propanal and *n*-propanol. IR studies on the stability of the surface-supported

clusters under a variety of conditions are described [176]. The dinuclear complexes $Cp^*MCl(\mu_2\text{-}SH)_2MCp^*Cl$ (where M = Ir, Rh) may be used to prepare tri- and tetranuclear sulfido-capped clusters. Treatment of these complexes with Et_3N gives the cuboidal clusters $(Cp^*M)_4(\mu_3\text{-}S)_4$, while the reaction with $[RhCl(1,5\text{-}COD)]_2$ or $Pd(PPh_3)_4$ yields the triangular clusters $(Cp^*M)_2Rh(\mu_3\text{-}S)_2(1,5\text{-}COD)$ and $[(Cp^*Ir)_2Pd(\mu_3\text{-}S)_2Cl(PPh_3)]^{2+}$ [177]. *N*-(2-pyridinyl)piperazines undergo carbonylation in the presence of ethylene and CO using the catalyst precursor $Rh_4(CO)_{12}$. The carbonylation reaction occurs regioselectively at a C–H bond which is α to the nitrogen atom bound to the pyridine ring [178]. Selective P–C bond cleavage in the $Ph_2PCHCPh$ ligand bound to the cluster $Ir_4(CO)_9(\mu_3\text{-}\eta^3\text{-}Ph_2PCHCPh)(\mu\text{-}PPh_2)$ occurs at 70°C, giving the η^1-phenyl substituted cluster $Ir_4(CO)_8(\eta^1\text{-}Ph)(\mu_4\text{-}\eta^3\text{-}Ph\text{-}PCHCPh)(\mu\text{-}PPh_2)$ in moderate yield. Spectroscopic data (^{31}P-, ^{13}C-, and ^1H-NMR) indicate that this cluster exists as an isomeric mixture in solution. The minor isomer was structurally characterized by X-ray diffraction analysis, which revealed a flat butterfly array of iridium atoms. The structure of the major isomer was assigned by using the NMR data. VT ^{31}P-NMR spectroscopy did not show any interconversion of these isomers over the temperature range 25–90°C. A scheme showing the possible steps involved in the P–C bond cleavage reaction is described [179]. The rhodium-catalyzed hydroformylation of vinylpyridines has been studied as a function of temperature. Using the catalyst precursor $Rh_4(CO)_{12}$, it has been found that the branched aldehyde was the major product. The greater importance of β-hydride elimination in the branched alkyl–rhodium intermediate compared to the linear alkyl–rhodium species was demonstrated by studying the deuterioformylation reaction using ^1H-NMR spectroscopy [180].

The site preference of ligand substitution in trigonal–bipyramidal clusters containing 72 or 76 CVEs has been explored by using Allen's atomic energy index (EI). The EIs have been computed by using extended Hückel methodology [181]. The reaction between $[Co(CO)_4]^-$ and 2-mercaptopyridine yields the pentacobalt cluster $Co_5(CO)_2(\mu_3\text{-}S)_3(SC_5H_4N)_7$. The molecular structure, as determined by X-ray crys-

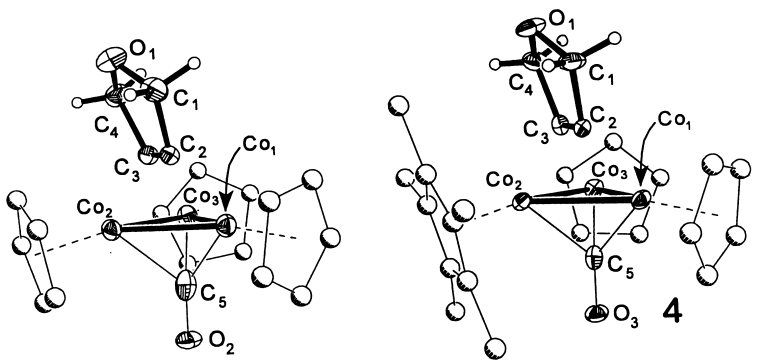

Fig. 11. X-ray structures of $(CpCo)_3(CO)(\mu_3\text{-}\eta_2\text{-}\overline{CH_2C{\equiv}CCH_2O})$ and $(CpCo)_2Cp^*Co(CO)(\mu_3\text{-}\eta^2\text{-}\overline{CH_2C{\equiv}CCH_2O})$. Reprinted with permission from Organometallics. Copyright 1997 American Chemical Society.

tallography, consists of a skeleton with three incomplete cubane-like units. The cyclic voltammetric properties of this cluster are reported [182].

Spherical tensor harmonic models for the spectral intensities of IR and Raman bands of $M_6(CO)_{16}$ (where M = Rh, Ir) and other large, spherical clusters have been used to study the spectral simplicity of metal carbonyl clusters [183].

The hydroformylation of 2,4,4-trimethyl-1-pentene using $[Rh_{12}(CO)_{30}]^{2-}$ has been studied. The reaction exhibits high chemioselectivity, producing 3,5,5-trimethylhexanal in quantitative yield. IR studies have revealed that the catalyst precursor degrades to the lower nuclearity species $[Rh_6(RCO)(CO)_{15}]^-$ and $[Rh_5(CO)_{15}]^-$ during the reaction. Details on the turnover numbers, CO and catalyst concentrations, and IR data are discussed [184]. The synthesis and structural characterization of the largest rhodium cluster known have been published. Pyrolysis of $[Rh_6N(CO)_{15}]^-$ at 140–150°C gives the dianion $[Rh_{14}N_2(CO)_{25}]^{2-}$, which upon protonation affords $[Rh_{28}N_4(CO)_{41}H_x]^{4-}$. Elemental analysis and ^{1}H-NMR data indicate that this cluster may be reasonably formulated as $[Rh_{28}N_4(CO)_{41}H_x]^{5-}$ [185].

2.7. Group 10 clusters

The cyclopentadienylnickel clusters $(CpNi)_3CMe$, $(CpNi)_3CCH_2Ph$, and $(CpNi)_4(\mu\text{-}C_5H_6)$ have been obtained from the reaction between $(CpNi)_2$ and THF. Labeling studies using d_8-THF confirm the role played by the solvent [186]. The dinuclear complex $[CpNi(PEt_3)]_2$ reacts with InCl and TlCl to give $[CpNi(PEt_3)_2ECl]_2$. The thallium complex is unstable and disproportionates in solution to give $[CpNi(PEt_3)]_3Tl$. The gallium analogue of this last derivative may be obtained from the conproportionation reaction of $[CpNi(PEt_3)]_2$ with gallium metal [187]. Treatment of *cis*-$Pt(C_6F_5)_2(THF)_2$ with the *tert*-butylalkynyl complexes *cis*-$Pt(C{\equiv}C'Bu)_2L_2$ (where $L = Ph_2PC{\equiv}CPh$, $Ph_2PC{\equiv}C'Bu$) furnishes the trinuclear complexes $Pt(\mu\text{-}\kappa(P):\eta^2\text{-}L)_2(\mu\text{-}\eta^1:\eta^2\text{-}C{\equiv}C'Bu)_2[Pt(C_6F_5)_2]_2$. Details related to the syntheses and spectral data of these complexes are discussed [188]. Carbon monoxide reacts with $[\{Pt(C_6F_5)_2(\mu\text{-}PPh_2)_2Pt(\mu\text{-}Cl)\}_2]^{2-}$ to produce $[Pt(C_6F_5)_2(\mu\text{-}PPh_2)_2PtCl(CO)]^{2-}$, which upon treatment with $AgClO_4$ yields the tetraplatinum cluster $Pt_4(\mu\text{-}PPh_2)_4(C_6F_5)_4(CO)_2$. The related cluster $Pt_2Pd_2(\mu\text{-}PPh_2)_3(C_6F_5)_3(Ph_2PC_6F_5)$ reacts with added CO to give $Pt_2Pd_2(\mu\text{-}PPh_2)_2[\mu_3\text{-}PPh(1,2\text{-}\eta^2\text{-}Ph)\text{-}\kappa^3P](C_6F_5)_3(CO)(Ph_2PC_6F_5)$. The X-ray structures of two tetranuclear clusters are presented [189].

The synthesis and characterization of the linear, dpmp-bridged trimer $[Pd_3(\mu\text{-}dpmp)_2(RNC)_2]^{2+}$ (where R = 2,6-xyl, 2,4,6-mes) are described. The molecular structure of the xyl derivative was solved by X-ray crystallography, and the reactivity of this particular complex towards I_2 was investigated [190]. The electrochemical reduction of $[Pd_3(dppm)_3(CO)]^{2+}$ has been examined by cyclic and rotating disk voltammetry and bulk electrolytic methods. Two-electron reduction affords the neutral cluster $Pd_3(dppm)_3(CO)$, which is stable for short periods of

time at room temperature. The results of geometry optimization using density functional theory are discussed relative to the structural features found in the model complexes $[Pd_3(PH_3)_6(CO)]^n$ (where $n = 0, +1, +2$) [191]. The one-pot syntheses of $[M_3(\mu_3\text{-}CO)(Cl)(\mu\text{-}dppm)_3]^+$ (where M = Pd, Pt) from CO, dppm, $NaBH_4$, and the metal salt are reported. The reported X-ray structures exhibit a triangular array of metal atoms. The syntheses of other Pt(dppm) and Pt(dppm)(CO) complexes are also described [192]. The fluxional clusters $[Pd_3(\mu_2\text{-}CO)_3(\mu\text{-}dppm)_2]_n$ (where $n = 1, 2$) have been prepared from $Pd(OAc)_2$. The attempted growth of crystals for X-ray diffraction analysis yielded a second crystal modification of $Pd_6(\mu_2\text{-}CO)_3(\mu\text{-}dppm)_3$, whose structure is fully discussed [193]. Bicluster oxidative addition as a route to bicapped hexaplatinum clusters has been demonstrated. Treatment of the 84-electron cluster $Pt_6(\mu\text{-}CO)_6(\mu\text{-}dppm)_3$ or the 82-electron cluster $[Pt_6(CO)_6(\mu\text{-}dppm)_3]^{2+}$ with $[SnX_3]^-$ (where X = F, Cl, Br) or HgX_2 (where X = Cl, Br, I) affords the bicapped trigonal prismatic 86-electron clusters $Pt_6(\mu_3\text{-}SnX_3)_2(\mu\text{-}CO)_6(\mu\text{-}dppm)_3$ and $Pt_6(\mu_3\text{-}HgX_2)_2(\mu\text{-}CO)_6(\mu\text{-}dppm)_3$, respectively. Two X-ray structures are presented, and the structural data are discussed with respect to extended Hückel MO calculations [194]. Ligand addition of $P(OCH_2)_3CMe$ to $Pt_6(\mu_2\text{-}CO)_6(\mu_2\text{-}dppm)_3$ affords the 86-electron cluster $Pt_6(\mu_2\text{-}CO)_6(\mu_2\text{-}dppm)_3[P(OCH_2)_3CMe]$. The phosphite ligand exhibits fluxional behavior, as judged by VT NMR measurements. Below -70°C, the ligand is terminally bound to one platinum center, but migrates around one triangular face of the cluster at higher temperatures. The addition of only one ligand to the 84-electron parent cluster, coupled with extended Hückel MO data, provides evidence for long-range electronic effects across the Pt_6 cluster [195].

New nickel–antimony clusters have been synthesized from the reaction of $[Ni_6(CO)_{12}]^{2-}$ with R_2SbBr (where R = Me, Et, ^{i}Pr) or R_2SbCl (where R = ^{t}Bu, p-FC_6H_4). The clusters $[Ni_{10}(SbR)_2(CO)_{18}]^{2-}$ were isolated as the major product in all cases. These dianions possess a common non-centered 1,12-$Ni_{10}Sb_2$ icosahedral cage which is surrounded by a 20-vertex ligand polyhedron. The redox properties, magnetic data, and the X-ray structures of six complexes are fully discussed [196]. The reaction of $[Ni_6(CO)_{12}]^{2-}$ with $MeBiCl_2$ affords the cluster $[Ni_{10}(BiMe)_2(CO)_{18}]^{2-}$ in moderate yield. The results of a geometrical analysis of the clusters $[Ni_{10}(EMe)_2(CO)_{18}]^{2-}$ (where E = P, As, Sb) with the new bismuth derivative are presented. The X-ray structure of $[Ni_{10}(BiMe)_2(CO)_{18}]^{2-}$ (Fig. 12) exhibits a non-centered 1,12-$Ni_{10}Bi_2$ icosahedral cage and is isolobal with the regular icosahedral $[B_{12}H_{12}]^{2-}$ complexes. VT ^{13}C-NMR studies indicate that the CO groups migrate rapidly about the cluster polyhedron via terminal-to-bridge CO exchange [197].

The high nuclearity cluster $H_{12}Pd_{28}(PtPMe_3)(PtPPh_3)_{12}(CO)_{27}$ has been prepared in low yield from the reaction of $PtCl_2(PMe_3)_2$ and $PdCl_2(PPh_3)_2$ with $[Ni_6(CO)_{12}]^{2-}$. The X-ray structure of this 41-atom cluster exhibits pseudo-C_3-3 symmetry, along with a four-layer hcp $Pd_{28}Pt$ core which contains four tetrahedrally linked interior Pd atoms which have a localized hcp environment. The ability of this cluster to serve as a hydrogen-storage system is discussed [198].

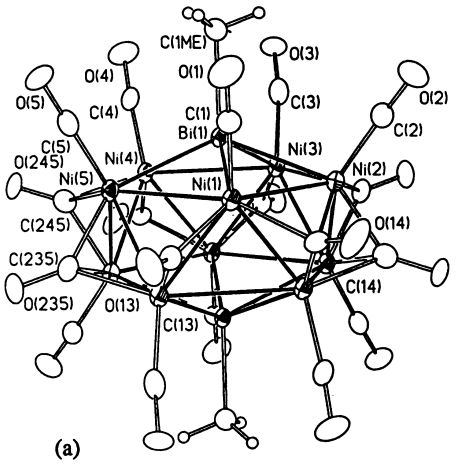

Fig. 12. X-ray structure of $[Ni_{10}(BiMe)_2(CO)_{18}]^{2-}$. Reprinted with permission from Organometallics. Copyright 1997 American Chemical Society.

2.8. Group 11 clusters

The synthesis and photophysics of the luminescent clusters $[M_3(\mu\text{-dppm})_3(\mu_3\text{-}\eta^1\text{-}C{\equiv}CC_6H_4C{\equiv}C\text{-p})M_3(\mu\text{-dppm})_3]^{4+}$ (where M = Cu, Ag) are reported. These complexes are obtained from $[M_2(\mu\text{-dppm})_2(MeCN)_2]^{2+}$ and 1,4-diethynylbenzene. The molecular structures of both clusters were determined by X-ray analysis [199]. Polymeric solids have been obtained from the reaction of the trigold(I) triacetylide complex $[C_6H_3(C{\equiv}CAu)_3\text{-}1,3,5]$ with monodentate ligands. The isolated solids exhibit intermolecular Au···Au bonding. Use of bidentate ligands affords covalently linked network polymers of the form $[C_6H_3(C{\equiv}CAu)_3\text{-}1,3,5]_2(\mu\text{-L–L})_3$ [200]. Restricted rotation about the P–C bond in metalated gold(phosphonium) salts has been observed by VT ^{1}H-NMR spectroscopy. The two polynuclear complexes studied include $(AuPPh_3)_2[\mu_2\text{-}\{C(PTol_3)(py\text{-}2)\}][Ag(\eta^2\text{-}O_2NO)(OClO_3)]$ and $[(AuPPh_3)_2\{\mu_2\text{-}\{C(PTol_3)(py\text{-}2)\}\}(AuPPh_3)]^{2+}$ [201]. The first (hydrosulfido)- and anionic sulfidoorganogold(I) complexes have been prepared and characterized. The reaction between $[Me_4N][Au(C_6F_5)Cl]$ and H_2S yields the bridged cluster $[Me_4N]_2[\{Au(C_6F_5)\}_3(\mu_3\text{-S})]$, whereas the $[Et_4N]^+$ derivative gives $[Et_4N]_2[\{Au(C_6F_5)\}_3(\mu_3\text{-S})]$ or $[Et_4N][Au(C_6F_5)SH]$, depending on the work-up procedure employed. The X-ray structure of $[Et_4N]_2[\{Au(C_6F_5)\}_3(\mu_3\text{-S})]$ exhibits short Au···Au contacts and narrow Au–S–Au angles. The aurophilic interactions displayed by this cluster are contrasted with those found in related homologues [202]. New trinuclear copper(I) complexes having the general formula $[Cu_3(\mu\text{-PNP})_3(\mu_3\text{-}\eta^1\text{-}C{\equiv}CR)_2]^+$ [where $PNP = (Ph_2P)_2NR'$; R and R′ = various groups] have been synthesized and their excited state properties investigated. The redox chemistry and excited state reducing abilities using pyridinium acceptor salts are reported. The spectroscopic data provide evidence for electron transfer quenching from the

phosphorescent state of the cluster and the pyridinium acceptor [203]. The mono- and bicapped acetylide complexes $[Ag_3(L–L)_3(\mu_3\text{-}\eta^1\text{-}C{\equiv}CC_6H_4R)]^{2+}$ and $[Ag_3(L–L)_3(\mu_3\text{-}\eta^1\text{-}C{\equiv}CC_6H_4{-}NO_2\text{-}p)_2]^+$, [where L–L = dppm, $(Ph_2P)_2N^nPr$] have been synthesized and their luminescent behavior examined. The X-ray structures of $[Ag_3(\mu\text{-dppm})_3(\mu_3\text{-}\eta^1\text{-}C{\equiv}CC_6H_4{-}NO_2\text{-}p)]^{2+}$ (Fig. 13) and $[Ag_3(\mu\text{-dppm})_3(\mu_3\text{-}\eta^1\text{-}C{\equiv}CC_6H_4{-}NO_2\text{-}p)_2]^+$ are reported [204].

Treatment of Au(mes)(dppm) with $[Au(THF)_2]^+$ or $AgClO_4$ in a molar ratio of 2:1 gives the trinuclear complexes $[M(\mu\text{-dppm})_2\{Au(mes)\}_2]^+$. The X-ray structure of the $AgAu_2$ derivative has been solved, and short Au–Ag distances have been found [205]. The cycloaurated cation $[Au_5(C_6H_4PPh_2)_4]^+$ has been synthesized and structurally characterized by X-ray diffraction analysis. The solid-state structure exhibits a butterfly arrangement of four gold atoms [206].

3. Heteronuclear clusters

3.1. Trinuclear clusters

$Cp_2Ti(CO)_2$ reacts with $Cp^*MoCl(O)_2$ to furnish the heterometallic cluster $[(CpTi)_2(Cp^*MoCl)](\mu_2\text{-O})_3(\mu_3\text{-O})$. The structure was established by IR and NMR

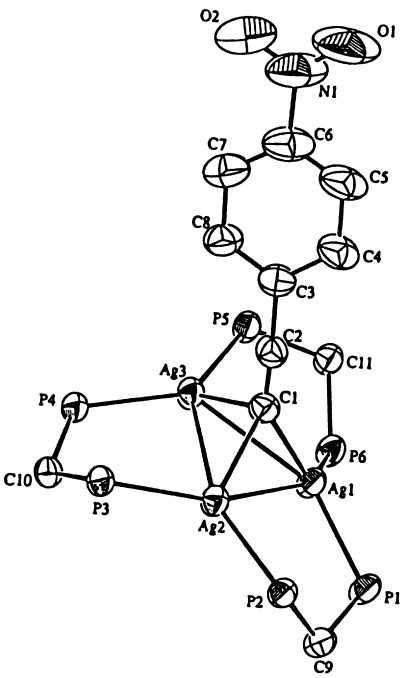

Fig. 13. X-ray structure of $[Ag_3(\mu\text{-dppm})_3(\mu_3\text{-}\eta^1\text{-}C{\equiv}CC_6H_4{-}NO_2\text{-}p)]^{2+}$. Reprinted with permission from Organometallics. Copyright 1997 American Chemical Society.

spectroscopy and high resolution mass spectrometry. The two cluster electrons of this diamagnetic complex are localized in an antibonding orbital involving both titanium centers [207].

Site-selective substitution of CO by Ph_2PMe occurs at the ruthenium atom in the cluster $Mo_2Ru(\mu_3\text{-}C{=}CHR)(CO)_7Cp_2$ (where R = H, Me, Ph, CO_2Me). The site of ligand attack has been verified by X-ray crystallography in the case of $Mo_2Ru(\mu_3\text{-}C{=}CHMe)(CO)_6(Ph_2PMe)Cp_2$. Use of Ph_2PH leads to a more complicated reaction, with the following clusters $Mo_2Ru(\mu_3\text{-}C{=}CH_2)(CO)_6(Ph_2PH)Cp_2$, $Mo_2Ru(\mu_3\text{-}CCH_2R)(\mu\text{-}PPh_2)(CO)_5Cp_2$, and $Mo_2Ru(\mu_3\text{-}C{=}CHR)(\mu\text{-}PPh_2)_2(CO)_4Cp_2$ being isolated. Independent experiments prove that these products are formed sequentially, starting with the transformation of the initial vinylidene ligand into an alkylidyne ligand and then back to a vinylidene ligand. All of the new complexes were fully characterized in solution by IR and NMR spectroscopy [208]. The reaction of $Fe_2(CO)_6(\mu\text{-}E)_2$ (where E = S, Se) with $Cr(CO)_5(THF)$ at room temperature gives the clusters $CrFe_2(CO)_{10}E_4$. The molecular structure of $CrFe_2(CO)_{10}Se_4$, as determined by X-ray analysis, exhibits a quadricyclane-like core having a base of two iron and two selenium atoms [209]. The complexes $Fe_2(CO)_6[\mu_4\text{-}EC(Ph){=}C(E'){C(OEt){=}M(CO)_5}]$ (where E and E′ = S, Se, Te; M = Cr, W) react with Bu_3SnH to give the enol ether derivatives $(OC)_6Fe_2[\mu\text{-}EC(Ph)(H)\text{–}C(E'){=}C(H)(OEt)]$ [210]. The reaction of the single-tetrahedral clusters $(Cp)(RCp)MoNiFeS(CO)_5$ (where R = H, MeCO, MeO_2C) with $Fe_2(CO)_9$ affords the addition products $(Cp)(RCp)MoNiFe_2S(CO)_{10}$. The double-tetrahedral cluster $[CpMoNiFeS(CO)_5]_2[\eta^5\text{-}C_5H_4C(O)CH_2]_2$ reacts with $Fe_2(CO)_9$ in a similar fashion to give $[CpMoNiFe_2S(CO)_{10}]_2[\eta^5\text{-}C_5H_4C(O)CH_2]_2$ [211]. The synthesis and characterization of the new chiral clusters $FeCoM(\mu_3\text{-}S)(CO)_8(RCp)$ [where M = Mo, W; R = PhC(O), $MeOC(O)C_6H_4C(O)$] from $FeCo_2(\mu_3\text{-}S)(CO)_9$ are presented [212]. The reaction of $[RCpMo(CO)_2]_2$ (where R = MeO_2C, EtO_2C) with $Fe_2(CO)_6(\mu\text{-}SEt)_2$ in boiling xylene gives the trinuclear clusters $(RCp)_2Mo_2Fe(CO)_7(\mu_3\text{-}S)$ and the tetranuclear clusters $(RCp)_4Mo_4(CO)_4(\mu_3\text{-}S)_2$. Photolysis of $[(EtO_2CCp)Mo(CO)_2]_2$ with $Fe_2(CO)_6(\mu\text{-}SEt)_2$ and $[CpMo(CO)_2]_2$ with $Fe_2(CO)_6(\mu\text{-}SPh)_2$ gives the aforementioned trinuclear $Mo_2Fe(\mu_3\text{-}S)$ clusters. The spectroscopic data and the X-ray structures of two clusters are presented [213]. The heterometallic clusters $SRuCoMo(CO)_8(RCp)$ [where R = HC(O), MeC(O), PhC(O), $MeOCH_2C(O)C_6H_4C(O)$] have been synthesized from the thermolysis reaction between $RuCo_2(CO)_9(\mu_3\text{-}S)$ and $[(RCp)Mo(CO)_3]^-$. This report includes the X-ray data on the $MeOCH_2C(O)C_6H_4C(O)$ derivative [214]. Treatment of $RuCo_2(CO)_9(\mu_3\text{-}S)$ with $[M(CO)_3CpC(O)]_2C_6H_4$ (where M = Mo, W) leads to the new clusters $[(\mu_3\text{-}S)RuCoM(CO)_8CpC(O)]_2C_6H_4$ by an addition–elimination sequence. The X-ray structure of the tungsten analogue has been established by X-ray crystallography [215]. The substitution of one or two $HFe(CO)_3$ groups in $Fe_3(CO)_9(\mu_3\text{-}Te)(\mu\text{-}H)_2$ by the isolobal $CpM(CO)_2$ fragments (where M = Mo, W) gives the clusters $Fe_2M(CO)_8Cp(\mu_3\text{-}Te)(\mu\text{-}H)$ and $FeM_2(CO)_7Cp_2(\mu_3\text{-}Te)$, respectively. The new clusters were characterized in solution by IR and NMR (^1H and ^{125}Te) spectroscopy, and the solid-state structure of $FeMoW(CO)_7Cp_2(\mu_3\text{-}Te)$ was determined by X-ray analysis [216]. The sequential substitution of $HFe(CO)_3$ in $Fe_3(CO)_9(\mu_3\text{-}Se)(\mu\text{-}H)_2$

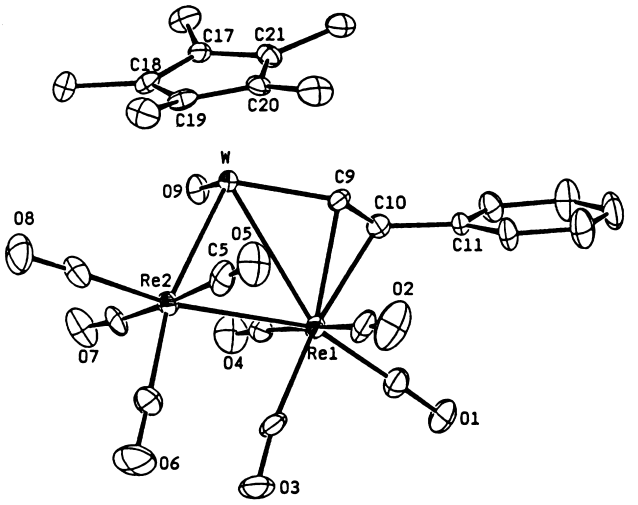

Fig. 14. X-ray structure of $Cp^*W(O)Re_2(CHCHPh)(CO)_8$. Reprinted with permission from Organometallics. Copyright 1997 American Chemical Society.

by $CpW(CO)_2$ (first stage) and $CpMo(CO)_2$ (second stage) is reported. The resulting chiral cluster $FeMoW(CO)_7Cp_2(\mu_3\text{-Se})$ has been characterized in solution and by X-ray crystallography [217]. PhHgCl has been allowed to react with $[\{\eta^5\text{-}C_5(PhCH_2)_5\}M(CO)_3]^-$ (where M = Cr, Mo, W) to yield the trimetallic clusters $[\{\eta^5\text{-}C_5(PhCH_2)_5\}M(CO)_3]_2Hg$. The corresponding $\eta^5\text{-}HO_2CC_5H_4$ ligand containing M_2Hg systems has also been prepared via hydrolysis of the requisite ester precursors [218].

Dioxygen reacts with $Cp^*WRe_2(CCR)(CO)_9$ [where R = Ph, C(Me)=CH_2] to give the oxo clusters $Cp^*W(O)Re_2(CCR)(CO)_8$. These clusters react with CO at 110°C to afford the corresponding nonacarbonyl clusters $Cp^*W(O)Re_2(CCR)(CO)_9$. These latter clusters possess an open triangular skeletal arrangement and a terminal oxo moiety attached to the W atom. The phenylacetylide cluster $Cp^*W(O)Re_2(CCPh)(CO)_8$ reacts with H_2 to produce $Cp^*WRe_2(\mu\text{-}O)(\mu\text{-}H)_2(CCPh)(CO)_6$, the alkenyl cluster $Cp^*W(O)Re_2(CHCHPh)(CO)_8$, whose X-ray structure is shown in Fig. 14, and the alkylidene cluster $Cp^*W(O)Re_2(\mu\text{-}H)(CHCH_2Ph)(CO)_8$. The reactivity of the oxo-vinylacetylide cluster with H_2 is also discussed. Solution data and mechanistic studies on the transformation of the acetylide moiety to alkenyl and alkylidene groups are discussed in detail [219].

The cluster compounds $CpMCo_2(CO)_8(\mu_3\text{-}CCO_2H)$ (where M = Mo, W) were synthesized in good yield from the protected clusters $Co_3(CO)_9(\mu_3\text{-}CCO_2R)$ via metal fragment exchange, followed by acid hydrolysis. These clusters were next used in the construction of new Ti and Zr alkoxy- and oxoalkoxycarboxylate derivatives [220]. Metal fragment exchange in $PhCCo_3(CO)_9$ using $[\{RC(O)Cp\}M(CO)_3]^-$ (where M = Mo, W; R = various groups) has been employed in the synthesis of six μ_3-benzylidyne Co_2M clusters [221]. The use of PS

ligands as building blocks for the synthesis of chiral dimetallatetrahedranes is described. Treatment of $Cp'_2Ni_2(\mu_3\text{-}P)_2[W(CO)_4]$ (where $Cp' = \eta_5\text{-}C_5H^iPr_4$) with sulfur gives the tetragonal–pyramidal cluster $Cp'_2Ni_2W(CO)_4(\mu_3\text{-}PS)_2$, which upon thermolysis at 100°C affords the cluster $Cp'Ni(\mu_2\text{-}PS)W(CO)_2NiCp'(\mu_2\text{-}PS)$. This latter cluster consists of two tetrahedra joined by a common vertex, as verified by X-ray analysis [222]. $CpMoH(CO)_2L$ (where $L = PMe_3$, PPh_3) reacts with $[AuPPh_3]^+$ at -40°C to produce the $MoAu_2$ clusters $[CpMo(CO)_2L(AuPPh_3)_2]^+$. The X-ray structure of $[CpMo(CO)_2(PMe_3)(AuPPh_3)_2]^+$ reveals a four-legged piano stool geometry at the Mo center, where the PMe_3 and the $\eta^2\text{-}(AuPPh_3)_2$ ligands occupy *trans* positions [223].

The dianion $[Re_2(\mu\text{-}H)(\mu\text{-}PCy_2)\{PhC(O)\}(CO)_7]^{2-}$ reacts with $XAuPPh_3$ (two equivalents; X = Cl, Br, I), coupled with reductive elimination of benzaldehyde, to give the clusters $Re_2(AuPPh_3)_2(\mu\text{-}PCy_2)(CO)_7X$. The anionic clusters $[Re_2(AuPPh_3)(\mu\text{-}PCy_2)(CO)_7X]^-$ have been isolated from the reaction between $Re_2(\mu\text{-}H)(\mu\text{-}PCy_2)(CO)_8$ and $XAuPPh_3$ (one equivalents) [224]. The thermally unstable complex $(OC)_4Mn(\mu\text{-}SePh)_2Co(CO)(\mu\text{-}SePh)_3Mn(CO)_3$ has been synthesized from $Co(ClO_4)_2$ and *cis*-$[Mn(CO)_4(SePh)_2]^-$. This complex reacts with added $[SePh]^-$ to give $[(OC)_3Mn(\mu\text{-}SePh)_3Co(\mu\text{-}SePh)_3Mn(CO)_3]^-$. The linear geometry adopted by this anionic complex was confirmed by X-ray crystallography. Starting with *cis*-$[Mn(CO)_4(SeMe)_2]^-$ leads to the stable compound $(OC)_4Mn(\mu\text{-}SeMe)_2Co(CO)(\mu\text{-}SeMe)_3Mn(CO)_3$. The electronic effects between the SeMe and SePh moieties in stabilizing the neutral Mn(I)–Co(III)–Mn(I)–selenolate complexes are discussed [225]. Addition of $Re_2(\mu\text{-}H)_2(CO)_8$ to $Ir(CO)(\eta^2\text{-}C_8H_{14})(\eta^5\text{-ind})$ in refluxing hexane affords $IrRe_2(\mu\text{-}H)_2(CO)_9(\eta^5\text{-ind})$. The X-ray structure (Fig. 15) confirms the presence of a central $IrRe_2$ triangle, and the different Ir–Re distances suggest that the hydrides bridge an Ir–Re edge and a Re–Re edge in this cluster.

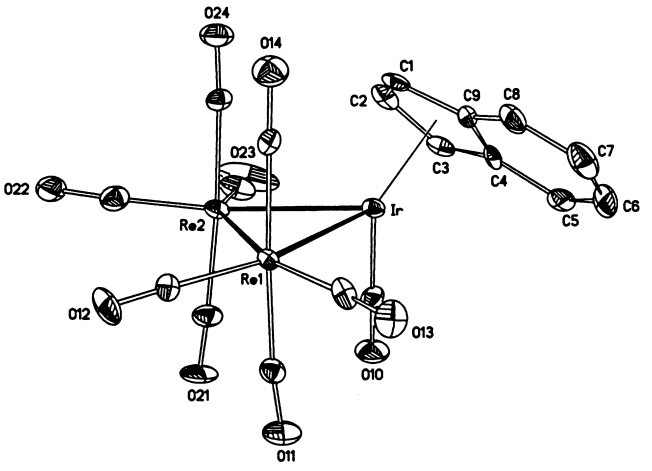

Fig. 15. X-ray structure of $IrRe_2(\mu\text{-}H)_2(CO)_9(\eta^5\text{-ind})$. Reprinted with permission from Organometallics. Copyright 1997 American Chemical Society.

VT ^{1}H- and ^{13}C-NMR data indicate that the hydrides and CO ligands are scrambled about the cluster polyhedron at elevated temperatures. Reaction of this cluster with PPh_3 leads to $IrRe_2(\mu\text{-}H)_2(CO)_8(PPh_3)(\eta^5\text{-ind})$ and some cluster fragmentation [226].

New mixed-metal spiked-triangular clusters have been synthesized from either $Re_2Pt(\mu\text{-}H)_2(CO)_8$(1,5-COD) or $Re_2Pt(\mu\text{-}H)_2(CO)_9[Re(CO)_5]$. A scale of thermodynamic nucleophilicity has been developed for the addition of carbonyl metalates to the platinum center. The solid-state structure of $Re_2Pt(\mu\text{-}H)_2(CO)_9[Re(CO)_4(PPh_3)]$ and solution IR and NMR data are discussed [227]. The catalytic activity of $Re_2Pt(CO)_{12}$ supported on $\gamma\text{-}Al_2O_3$ has been investigated by using EXAFS spectroscopy. The supported catalyst was observed to be more resistant to deactivation during the dehydrogenation of methylcyclohexane than the catalyst prepared from Re and Pt salts. It is suggested that the resistance to deactivation may be due to the role of the Re in stabilizing the dispersion of the Pt [228].

Sulfido–persulfido equilibria have been observed in the clusters $[Cp^*_3MRu_2S_4(MeCN)]^{2+}$ (where M = Rh, Ir). These clusters may be synthesized from $[Cp^*M(MeCN)_3]^{2+}$ and $Cp^*_2Ru_2S_4$. The X-ray structure of the rhodium derivative consists of an asymmetric $RhRu_2S_4$ core having an isosceles triangle of metal atoms. The three metals are tethered by two $\mu_3\text{-}\eta^1\text{:}\eta^2\text{:}\eta^1\text{-}S_2$ moieties, with each persulfide bonding to the rhodium atom in a monodentate fashion. The fluxional properties have been studied by VT NMR spectroscopy, and a racemization mechanism involving a 'base-free' intermediate containing a cleaved S–S bond is discussed [229]. Treatment of the butadiynyl complexes $Ru_2(CO)_6(\mu\text{-}PPh_2)(\mu\text{-}\eta^1,\eta^2_{\alpha,\beta}\text{-}C{\equiv}C{-}C{\equiv}CR)$ (where R = ^{t}Bu, Ph) with the labile complexes $Ni(CO)_4$, $Pt(PPh_3)_2$(ethylene), Pt(dppb)(ethylene), or Ni(1,5-COD)$_2$, affords the clusters $Ru_2Pt(CO)_7(PPh_3)(\mu_3\text{-}\eta^1,\eta^1,\eta^1\text{-}C{\equiv}C{-}C{\equiv}CR)(\mu\text{-}PPh_2)$, $Ru_2Pt(CO)_6$(dppb)$(\mu_3\text{-}\eta^1,\eta^1,\eta^1\text{-}C{\equiv}C{-}C{\equiv}CR)(\mu\text{-}PPh_2)$, and $Ru_4Pt(CO)_{12}(\mu\text{-}PPh_2)(\mu_4\text{-}\eta^1,\eta^1,\eta^2,\eta^4\text{-}^t$BuC≡C–C≡C^{t}Bu) [230]. $CpCoFe_2(S)(Se)(CO)_6$ has been found to exhibit large optical non-linearity, with limiting characteristics greater than that of C_{60} [231]. The adducts $[\{Cp^*RuH_3(PCy_3)\}_2M]^+$ (where M = Ag, Au) have been isolated from the reaction between $Cp^*RuH_3(PCy_3)$ and the appropriate metal salt. The exchange coupling and hydride dynamics have been studied by VT NMR spectroscopy [232]. $CpCoFe_2(CO)_6(\mu_3\text{-}Se)_2$ reacts with dppm and dppe to give $CpCoFe_2(CO)_5(P{-}P)(\mu_3\text{-}Se)_2$. The X-ray structure of the dppm derivative reveals that the dppm ligand bridges the Co and one of the Fe atoms [233].

The neutral acetylide clusters $Pt(\mu\text{-}C{\equiv}CR)_4[Rh(1,5\text{-}COD)]_2$ (where R = ^{t}Bu, $SiMe_3$) have been synthesized from $[Rh(1,5\text{-}COD)(acetone)_2]^+$ and $[Pt(\mu\text{-}C{\equiv}CR)_4]^{2-}$. The reaction of $[Rh(\mu\text{-}X)(1,5\text{-}COD)]_2$ (where X = Cl, OH) with $Pt(\mu\text{-}C{\equiv}C^tBu)_4[Rh(1,5\text{-}COD)]_2$ leads to the unusual pentanuclear complexes $[Pt(\mu\text{-}C{\equiv}CR)_4\{Rh_2(\mu\text{-}X)(1,5\text{-}COD)_2\}_2]$. The molecular structures of both pentanuclear complexes have been determined by X-ray crystallography [234]. The synthesis and characterization of $[Pt(\mu\text{-}C{\equiv}CR)_4\{CoCl_2\}_2]^{2-}$ (where R = ^{t}Bu, $SiMe_3$) are reported [235]. $Pt_2(PPh_3)_4(\mu\text{-}S)_2$ has been allowed to react with $AgCl(PPh_3)$ and CuCl under CO to give $Pt_2(CO)(PPh_3)_3(\mu_3\text{-}S)MCl$, by way of the intermediate clusters $[Pt_2(PPh_3)_4(\mu_3\text{-}S)_2Ag(PPh_3)][Cl]$ and $Pt_2(PPh_3)_5(\mu_3\text{-}S)_2MCl$. The unprece-

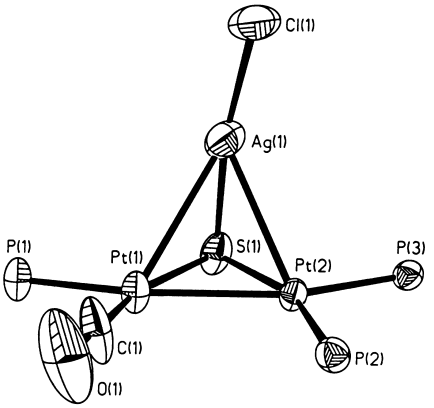

Fig. 16. X-ray structure of $Pt_2(CO)(PPh_3)_3(\mu_3\text{-}S)AgCl$. Reprinted with permission from Journal of American Chemical Society. Copyright 1997 American Chemical Society.

dented heterometalation, carbonylation, reductive elimination, and M–M bond formation are discussed. All clusters have been characterized fully in solution, and the X-ray structures of $Pt_2(CO)(PPh_3)_3(\mu_3\text{-}S)AgCl$ (Fig. 16) and two other clusters are presented. The elimination of COS in these aggregates-to-cluster conversions is discussed, along with a working mechanism [236].

3.2. Tetranuclear clusters

$Fe_2(CO)_6(\mu\text{-}EE')$ (where $EE' = SeTe$, STe, SSe, S_2, Se_2) reacts with $Mo(CO)_5(THF)$ at room temperature to give the tetrametal clusters $Fe_3Mo(CO)_{11}(\mu_3\text{-}E)(\mu_3\text{-}E')$ and the 'hour-glass' clusters $Fe_4Mo(CO)_{14}(\mu_3\text{-}E)_2(\mu_3\text{-}E')_2$. The crystal structures of four clusters are presented [237]. The synthesis and reactivity studies of the cubane-type clusters $[(OC)_3MFe_3S_4(SR)_3]^{3-}$ (where M = Mo, W; R = Et, mes) are reported. The redox chemistry and Mössbauer spectra have been examined, and the redox assignments in $[(OC)_3MoFe_3S_4(SEt)_3]^{3-}$ have been reinterpreted. The CO stretching frequencies are sensitive to the oxidation state of the cluster and provide evidence for the long-range coupling between the $M(CO)_3$ site and the Fe_3S_4 fragment [238]. The synthesis and structural characterization of $(C_6Cl_4O_2)MoFe_3S_3(PEt_3)_2(CO)_6$ and $(C_6Cl_4O_2)Mo(O)Fe_3S_3(PEt_3)_2(CO)_5$ have appeared. These new $MoFe_3S_3$ cuboidal clusters serve as model compounds for the Fe/Mo cofactor of nitrogenase [239]. The reaction between $(\mu\text{-}H)_2Fe_3(CO)_9(\mu_3\text{-}Se)$ and $[CpW(CO)_3]_2$ has been investigated. Besides the expected tetrahedrane cluster products, the minor cluster product $Fe_2W_2(\mu_3\text{-}Se)_2(\mu_3\text{-}CO)(\mu\text{-}CO)(CO)_5Cp_2$ has been isolated and structurally characterized by X-ray analysis [240]. The clusters $(RCp)_2(\mu_3\text{-}CO)_2M_2Fe_2(\mu_3\text{-}S)_2(CO)_6$ (where M = Mo, W; R = MeCO, MeO_2C, EtO_2C) have been prepared and characterized fully. The reduction chemistry of the keto moiety of the functionalized Cp rings has been studied also [241]. Reaction of the dinuclear compound $Cp_2Mo_2(CO)_6$ with $(OC)_6Fe_2[\mu\text{-}$

SeC(H)=C(C≡CR)Se] (where R = Me, Bu) yields the addition adducts $(OC)_6Fe_2[\mu$-HC=C(C≡CR)$Cp_2Mo_2(CO)_4]$. Similar products were obtained when the activated clusters $Ru_3(CO)_{10}(MeCN)_2$ and $Os_3(CO)_{10}(MeCN)_2$ were employed [242]. The acetylide clusters $Cp^*WOs_3(CO)_{11}(CCR)$ (where R = Ph, Bu, CH_2OMe, CH_2OPh) are synthesized from $Os_3(CO)_{10}(MeCN)_2$ and $Cp^*W(CO)_3(CCR)$. These clusters exist as a mixture of two isomers, which exhibit an interconversion of the $Cp^*W(CO)_2$ fragment between the hinge and wingtip positions at elevated temperatures. Thermolysis of the phenyl derivative gives the carbido-alkylidyne cluster $Cp^*WOs_3(CO)_{10}(\mu_4$-C)(μ-CPh) by reversible scission of the C–C bond. Treatment of this cluster with CO restores the starting cluster. A reactivity comparison between the different R-substituted clusters is presented, and mechanistic schemes describing the various transformations exhibited by these clusters are discussed. Solution NMR data and the X-ray data for seven clusters are discussed fully [243]. The oxo-bridged cluster $Cp^*W(\mu$-$O)_2Os_3(CO)_9(\mu$-CCPh) has been prepared and examined for its reactivity with H_2 and CO. The X-ray structures of $Cp^*W(\mu$-$O)_2Os_3(CO)_9(\mu$-CCPh) (Fig. 17) and $Cp^*W(O)(\mu$-$O)Os_3(CO)_{11}(\mu$-CCPh) have been determined [244].

Mechanistic aspects relevant to hydrosulfurization catalysis have been studied by using $Cp'_2Mo_2Co_2S_3(CO)_4$. When this cluster is allowed to react with RSH, the cluster $Cp'_2Mo_2Co_2S_4(CO)_2$, R–H, and CO are observed. The kinetics for the desulfurization process have been measured. Intermediates involving clusters with η^1-SR and μ_2,η^1-SR moieties have been spectroscopically observed by NMR spectroscopy. A plausible C–S bond cleavage mechanism is discussed and contrasted with data obtained from heterogeneous Co/Mo/S catalysts [245]. The

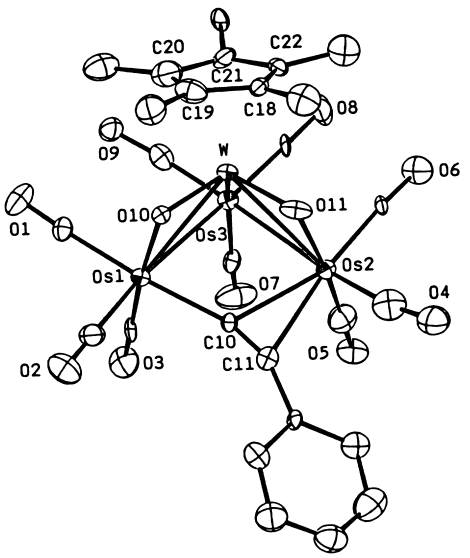

Fig. 17. X-ray structure of $Cp^*W(\mu$-$O)_2Os_3(CO)_9(\mu$-CCPh). Reprinted with permission from Organometallics. Copyright 1997 American Chemical Society.

nitrosyl clusters $Cp_2M_2M'_2S_4(NO)_2$ (where $Cp = C_5Me_2EtH_2$, Cp*, Cp; M = Mo, W; M′ = Fe, Co) have been prepared and structurally characterized by X-ray crystallography. The synthesis of the carbonyl clusters $Cp^*_2W_2Co_2S_4(CO)_2$ and $Cp^{Et}_2W_2Co_2S_3(CO)_5$ is described also, and the X-ray structure of the latter cluster is presented. The redox properties of these clusters have been investigated by cyclic voltammetry. A discussion on the electronic structure relative to the redox state of these clusters is presented [246]. The paramagnetic clusters $[Cp'_2Mo_2Co_2S_4(CO)_2]^-$ and $[Cp^*_2Mo_2Co_2S_4(CO)_2]^-$ have been synthesized from the reaction of $Cp'_2Mo_2Co_2S_3(CO)_3$ with $[Stol]^-$ or by Na amalgam reduction of $Cp^*_2Mo_2Co_2S_4(CO)_2$, respectively. Structural changes in the cluster core as a function of electron addition or removal are discussed [247]. Oxidation of $Cp^{Et}_2Mo_2Co_2S_4(CO)_4$ (where $Cp^{Et} = C_5Me_4Et$) by halogens and PhSSPh yields the 58-VSE clusters $Cp^{Et}_2Mo_2Co_2S_4(X)_2$ (where X = Cl, Br, I, SPh). The magnetic behavior of the halide clusters reveals complex spin equilibria, while the thiolate-substituted cluster exhibits simple paramagnetism. Treatment of $Cp^{Et}_2Mo_2Co_2S_4(CO)_4$ with benzene thiol under CO (1000 psi) yields PhS(CO)Ph and PhSSPh [248]. Dppm and dppe have been allowed to react with $Cp'_2Mo_2Co_2S_3(CO)_4$ to give the clusters $Cp'_2Mo_2Co_2S_3(CO)_2$(P-–P) Using the diphosphine ligand dmpe gives $Cp'_2Mo_2Co_2S_3(\mu_3\text{-}CO)(\eta^2\text{-dmpe})_2$. This latter cluster reacts with CH_2Cl_2 to furnish the μ_3-methylidyne cluster $[Cp'_2Mo_2Co_2S_3(\mu_3\text{-}CH)(\eta^2\text{-dmpe})_2]^+$. An isotopic labeling study using $^{13}CH_2Cl_2$ and CD_2Cl_2 confirms that the source of the μ_3-CH(D) ligand is from the solvent and not the μ_3-CO moiety [249].

Two routes have been used to prepare the cluster $Cp_2Mo_2Ir_2(CO)_{10}$. Treatment of $CpMo(CO)_3H$ and $IrCl(CO)_2$(*p*-toluidine) with CO in the presence of Zn gives the title cluster, as does the reaction between $[CpMo(CO)_3]^-$ and $IrCl(CO)_2$(*p*-toluidine). The tetrahedral metal core, which possesses a μ_3-CO and five μ-CO groups, was confirmed by X-ray diffraction analysis [250]. The reactivity of $Cp_2Mo_2Ir_2(CO)_{10}$ with phosphines and alkynes has been investigated. The X-ray structures of $Cp_2Mo_2Ir_2(\mu\text{-}CO)_3(CO)_3(PMe_3)$ and $Cp_2Mo_2Ir_2(\mu_4\text{-}\eta^2\text{-}HC_2Ph)(\mu\text{-}CO)_4(CO)_4$ are presented. The alkynes are shown to insert into the Mo–Mo bond of the parent cluster [251].

The synthesis and X-ray structure of $[CpCr(\mu\text{-}SCMe_3)]_2(\mu_4\text{-}S)[PtMe_3(\mu\text{-}I)]_2$ are reported. The antiferromagnetic behavior exhibited by this cluster arises from the interaction of two paramagnetic Cr(III) centers [252].

The anionic complex $Cp^*Re(NO)(PPh_3)(C{\equiv}C^-)$ reacts with $Os_3(CO)_{12}$ to give the heterometallic complex $Cp^*Re(NO)(PPh_3)[C{\equiv}CC(COMe)]Os_3(CO)_{11}$ after methylation. Solution IR and NMR data and the X-ray structure reveal substantial contributions by $^+Re{=}C{=}C{=}C(OMe){-}M^-$ resonance forms [253]. Sulfidation of Pt_3Re clusters has been studied as a model for Pt–Re bimetallic catalysts. $[Pt_3\{Re(CO)_3\}(\mu\text{-dppm})_3]^+$ undergoes sulfidation with propylene sulfide to give the clusters $[Pt_3\{Re(CO)_3S\}(\mu\text{-dppm})_3]^+$ and $[Pt_3\{Re(CO)_3\}(\mu_3\text{-}O)(\mu_3\text{-}S)(\mu\text{-dppm})_3]^+$. Analogous sulfidation occurs with the oxo clusters $[Pt_3(ReO_3)(\mu\text{-dppm})_3]^+$, $[Pt_3\{Re(CO)_3\}(\mu_3\text{-}O)_2(\mu\text{-dppm})_3]^+$, and $[Pt_3\{Re(CO)_3\}(\mu_3\text{-}O)(\mu\text{-dppm})_3]^+$. The addition of each μ_3-O or μ_3-S moiety leads to a decrease in metal–metal bonding in these clusters. Three X-ray structures accompany this report [254].

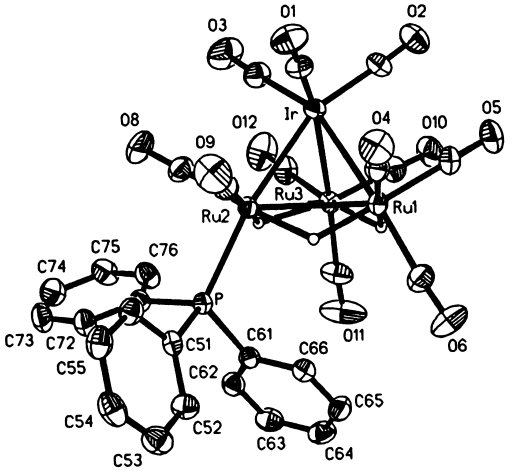

Fig. 18. X-ray structure of $Ru_3IrH_3(CO)_{11}(PPh_3)$. Reprinted with permission from Organometallics. Copyright 1997 American Chemical Society.

The CO hydrogenation activity of several tetranuclear Co/Ru clusters supported on SiO_2 has been investigated. The activity and observed selectivity of these catalysts are different from catalyst systems obtained by impregnation techniques [255]. The synthesis and X-ray structure of $[Ru_3Ir(CO)_{11}(\mu\text{-}CO)_2]^-$ have been published. Two isomers, $[Ru_3Ir(CO)_{11}(\mu\text{-}CO)_2]^-$ and $[Ru_3Ir(CO)_9(\mu\text{-}CO)_4]^-$, were observed in the solid state. VT ^{13}C-NMR spectroscopy confirms the existence of fluxional groups and the interconversion of both isomers in solution. The protonation chemistry and reactivity with H_2 are discussed [256]. The reaction of $Ir(CO)Cl(PPh_3)_2$ with $[HRu_3(CO)_{11}]^-$ gives the new Ru/Ir clusters $Ru_3IrH_3(CO)_{11}(PPh_3)$ (two isomers), $Ru_3IrH(CO)_{12}(PPh_3)$, and $Ru_{4-x}Ir_xH_{4-x}(CO)_{10}(PPh_3)_2$ (where $x = 1, 2$). These clusters were characterized by IR and NMR (^{1}H and ^{31}P) spectroscopy, and by X-ray crystallography in the case of $Ru_3IrH_3(CO)_{11}(PPh_3)$, whose ORTEP diagram is shown in Fig. 18 [257].

Gold(I)–gold(III) interactions in polynuclear sulfur-centered complexes have been observed in the mixed-valence complexes $[S(Au_2dppf)\{Au(C_6F_5)\}]$ and $[\{S(Au_2dppf)\}_2\{Au(C_6F_5)\}]^+$. DFT calculations show that when a sulfur center bridges three gold atoms it adopts a pyramidal geometry and promotes weak Au(I)–Au(III) interactions [258]. The patterns of hydrogen bonding in $(\mu_3\text{-}H)Co_3Fe(CO)_9[P(OMe)_3]_3$, $(\mu_3\text{-}H)_3Os_3Ni(CO)_9Cp_2$, and other organometallic crystals have been reviewed. The importance of packing motifs and hydrogen bonds in determining the construction of crystalline materials based on cocrystallization of organic and organometallic molecules is discussed [259]. The clusters $Ru_3IrH(CO)_{12}(PPh_3)$, $Ru_4H_4(CO)_{11}(PPh_3)$, and $Ru_4H_2(CO)_{12}(PPh_3)$ have been synthesized from $Ir(CO)Cl(PPh_3)_2$ and $[HRu_3(CO)_{11}]^-$. The spectroscopic data and X-ray structures of the first two clusters are presented [260]. The reaction of $IrCl^tBu_2PH)_3$ with $M_3(CO)_{12}$ (where M = Fe, Ru) in refluxing toluene has been

studied. In the case of $Ru_3(CO)_{12}$, the two clusters $Ru_3(CO)_8(\mu\text{-}H)_2(\mu_3\text{-}P^tBu)(^tBu_2PH)$ and $Ru_3Ir(CO)_7(\mu\text{-}H)_2(\mu\text{-}P^tBu_2)_2(^tBu_2PH)(\mu_3\text{-}Cl)$ were isolated. Using $Fe_3(CO)_{12}$ gives a mononuclear iron complex and a dinuclear Fe/Ir complex [261]. The reaction of $RhCl(^tBu_2PH)_3$ and $[RhCl(^tBu_2PH)_2]_2$ with $M_3(CO)_{12}$ has been studied. Cluster fragmentation occurs with $Fe_3(CO)_{12}$; however, $Ru_3(CO)_{12}$ yields the cluster compounds $Ru_3Rh(CO)_7(\mu_3\text{-}H)(\mu\text{-}P^tBu_2)_2(^tBu_2PH)(\mu\text{-}Cl)_2$, $Ru_3Rh(CO)_8(\mu_3\text{-}H)(\mu\text{-}H)_2(\mu_3\text{-}P^tBu)(\mu\text{-}P^tBu_2)_2$, and $Ru_3(CO)_8(\mu\text{-}H)_2(\mu_3\text{-}P^tBu)(^tBu_2PH)$. The X-ray structures of both Ru_3Rh clusters display butterfly geometries [262].

The Pd/Co clusters $CoPd_3(\mu_3\text{-}X)(\mu\text{-}CO)_3(\mu_3\text{-}CO)(CO)(P^tBu_3)_3$ (where X = Cl, Br, I) have been obtained from the reaction between $Co_2(CO)_8$ and $Pd_4(\mu_3\text{-}CH)(\mu\text{-}Cl)_3(P^tBu_3)_3$ and $Pd_2(\mu\text{-}X)_2(P^tBu_3)_2$. The chloro cluster exhibits a core geometry which is intermediate between a tetrahedron and a butterfly [263]. $AgClO_4$ adds to *trans*-$Pd(C{\equiv}CR)_2(PMe_2Ph)_2$ (where R = ^{t}Bu, H) to give 1:1 adducts having the formula *trans*-$[PtAg(ClO_4)(C{\equiv}CR)_2(PMe_2Ph)_2]_2$. The X-ray structure of the ^{t}Bu derivative displays a square Pt_2Ag_2 polyhedral shape [264].

3.3. Pentanuclear clusters

Thermolysis of $Cp_2Mo_2(O)(\mu\text{-}C_4Ph_4)$ with $Ru_3(CO)_{12}$ gives the pentanuclear cluster $Cp_2Mo_2Ru_3(\mu_3\text{-}O)_2(\mu_3\text{-}CPh)(\mu\text{-}C_3Ph_3)(CO)_8$. X-ray diffraction analysis reveals a distorted bow-tie structure formed by two virtually perpendicular metal triangles [265]. The cluster compounds $Fe_3(CO)_9(\mu_3\text{-}EM)_2$ [where E = P, As, Sb; M = $CpMn(CO)_2$, $Cr(CO)_5$] have been examined by cyclic voltammetry and Fenske–Hall MO calculations in order to evaluate the effect of the μ_3-EM groups on the structures, bonding, spectroscopic, and redox properties of these clusters. The X-ray structures of six clusters are discussed [266]. The reaction of $Ru_4(CO)_{13}(\mu_3\text{-}PPh)$ with $Cp^*W(O)_2(CCPh)$ in refluxing toluene yields the clusters $Cp^*W(O)_2Ru_4(CO)_{10}(\mu_4\text{-}PPh)(CCPh)$, $Cp^*W(O)_2Ru_4(CO)_7(C_7H_8)(\mu_4\text{-}PPh)(CCPh)$, and $Cp^*W(O)_2Ru_5(CO)_{12}(\mu_4\text{-}PPh)(CCPh)$. The molecular structures of these three compounds, as determined by X-ray crystallography, reveal that the high oxidation state tungsten and low oxidation state ruthenium carbonyl fragments can coexist together [267]. Competitive acetylide C–C bond cleavage versus the formation of a μ_4-CO ligand has been observed in the reaction between $Cp^*WRu_2(CCPh)(CO)_8$ and excess $Cp^*W(CO)_3H$. The isolated products include the carbido-alkylidyne cluster $Cp^*_3W_3Ru_2(\mu_4\text{-}C)(\mu_3\text{-}CPh)(CO)_9$, $Cp^*WRu_3(\mu\text{-}H)_3(CO)_{11}$, $Cp^*_2W_2Ru_2(CCHPh)(CO)_9$, and $Cp^*_2W(O)Ru_3(\mu_5\text{-}C)(CO)_{11}$. Use of the *tert*-butyl acetylide complex yields $Cp^*_3W_3Ru_2(\mu_3\text{-}CC^tBu)(CO)_9$ as the major condensation product. The X-ray structure of this latter cluster (Fig. 19) exhibits a butterfly crater with a μ_4-bridged CO group. A mechanism showing the course of these reactions is presented [268].

Addition of M′L fragments to $[Fe_3MC(CO)_{12}]^-$ leads to the new pentanuclear clusters $Fe_3MC(CO)_{12}M'L$ (where M = Co, Rh; M′ = Au, Pd; L = various ligands). The presented X-ray data and solution spectroscopic data are discussed [269]. The X-ray structure of $Ru_3(\mu_3\text{-}CEtCMeCPhCPh)(CO)_7[Au_2(PPh_3)_2]$ has been published.

An unusual geometry consisting of a Au_2 unit interacting with a C_4Ru_3 pentagonal bipyramid was observed [270]. Treatment of $Ir_4(CO)_{12}$ with dppf yields $H_4Ir_4(CO)_4[Fe(C_5H_3PPh_2)\{C_5H_4P(Ph)C_6H_4\}]_2$. The X-ray structure confirms the orthometalation of the Cp and phenyl ligands [271]. The oxo-capped cluster $[Fe_3(CO)_9(\mu_3\text{-}O)]^{2-}$ reacts with $Au(PPh_3)X$ (where X = Cl, NO_3) and $[Rh(CO)_2Cl]_2$ to give the trigonal–bipyramidal cluster $Fe_3Au_2(CO)_{12}(PPh_3)_2(\mu_3\text{-}O)$ and the octahedral cluster $[Fe_3Rh_3(CO)_{15}(\mu_3\text{-}O)]^-$, respectively. The molecular structures of these clusters were established by X-ray methods [272]. The anionic cluster $[Au_3Fe_2(CO)_8(dppm)]^-$, whose ORTEP diagram is shown below in Fig. 20, has been isolated from the reaction of $Au_2(dppm)Cl_2$ with either $[AuFe_2(CO)_8]^{3-}$ or Collman's reagent. The synthesis and X-ray structure of the cationic cluster $[Au_5Fe_2(CO)_8(dppm)_2]^+$ are also discussed [273].

3.4. Hexanuclear clusters

Activation of the carbido cluster $Ru_5(\mu_5\text{-}C)(CO)_{15}$ by Me_3NO, followed by treatment with $CpW(CO)_3(CCPh)$ (where Cp = Cp, Cp*), gives the clusters $CpWRu_5(\mu_5\text{-}C)(CO)_{15}(CCPh)$ and $CpWRu_5(\mu_5\text{-}C)(CO)_{13}(CCPh)$. Thermolysis of the former cluster results in the irreversible formation of the latter cluster, whose reactivity with H_2 and CO has also been investigated. The carbide ligand is stable and serves as an anchor to hold the cluster together, unlike other clusters where the

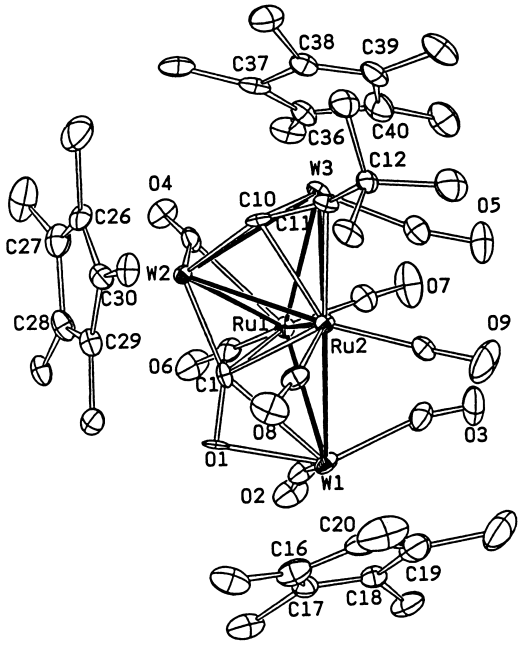

Fig. 19. X-ray structure of $Cp^*_3W_3Ru_2(\mu_3\text{-}CC^tBu)(CO)_9$. Reprinted with permission from Organometallics. Copyright 1997 American Chemical Society.

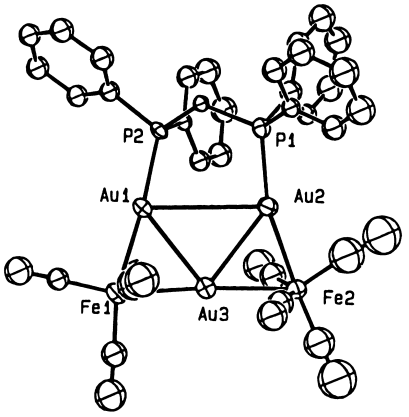

Fig. 20. X-ray structure of $[Au_3Fe_2(CO)_8(dppm)]^-$. Reprinted with permission from Organometallics. Copyright 1997 American Chemical Society.

carbido ligand enters into C–C bond-forming reactions with ancillary acetylide fragments. The solution NMR (^1H and ^{13}C) data and the X-ray structures of four clusters are discussed [274]. The reactivity of $Fe_2[\mu_4\text{-}Ge\{Co_2(CO)_7\}]_2(CO)_7$ with $GeMe_2H_2$ has been investigated. Of the several products isolated and characterized in solution, the molecular structures of $Fe_2[\mu_4\text{-}GeCo_2(CO)_6(\mu\text{-}GeMe_2)_2]_2(CO)_7$ and $Fe_3[\mu_3\text{-}GeCo(CO)_4]_2(CO)_9$ have been determined by X-ray crystallography [275]. The cluster $Ru_5Rh(CO)_{12}(\mu\text{-}CO)(\mu_4\text{-}\eta^2\text{-}CO)_2Cp^*$ has been synthesized from $[Ru_6(CO)_{18}]^{2-}$ and $[Cp^*Rh(MeCN)_3]^{2+}$. The solid-state structure consists of a bi-edge bridged tetrahedral core, with the Cp* moiety at the apex of the tetrahedron [276]. The X-ray structures of $Ru_3(\mu_3\text{-}CMeCHCMe)(CO)_8[Au(PPh_3)]_3$ and $Ru_3(\mu_3\text{-}C_2Ph)(CO)_8[Au(PPh_3)]_3$ have been determined. The polyhedral geometries of these clusters are compared with the parent Ru_3 cluster and other aurated derivatives [277]. The reaction of $[Fe_4C(CO)_{12}]^{2-}$ with electrophiles has been examined, and depending upon the nature of the electrophile, different sites of attachment to the cluster have been observed. The mercury compounds ClHgM [where M = Cp-$W(CO)_3$, $CpMo(CO)_3$, $Mn(CO)_5$, $CpFe(CO)_2$, $Co(CO)_4$] undergo reaction with $[Fe_4C(CO)_{12}]^{2-}$ to give $[Fe_4C(CO)_{12}(\mu\text{-}HgM)]^-$. The X-ray structure of the Mo derivative (Fig. 21) shows an Fe_4C butterfly core, with a Hg atom which bridges one of the two edges defined by the wingtip and hinge iron atoms [278].

3.5. Higher nuclearity clusters

The reaction of $[Os_3(CO)_{11}(\mu\text{-}H)]^-$ with $[Rh(nbd)Cl_2]_2$ in the presence of $AgPF_6$ gives the heptanuclear cluster $Os_4Rh_3(\mu_3\text{-}H)(CO)_{14}(\mu_3\text{-}CO)(\eta^4\text{-}C_7H_8)_2$ and the heneicosanuclear cluster $Os_{12}Rh_9(CO)_{44}(\mu_3\text{-}Cl)$ in moderate yield. The solid-state structures have been determined by X-ray crystallography [279]. The tetrahedrane cluster $(\mu_3\text{-}CBr)Co_3(CO)_9$ reacts with $[CpRu(CO)_2]^-$, which was prepared by sodium amalgam reduction of $Cp_2Ru_2(CO)_4$, to give $Cp_2Ru_2Co_4Hg(\mu_5\text{-}C)(CO)_{13}$ in

low yield. The carbide ligand is encapsulated in the pentanuclear $RuCo_4$ butterfly polyhedron, as verified by X-ray diffraction analysis. The related cluster (μ_3-CCl)$Co_3(CO)_6$(tdpm) reacts with $[CpRu(CO)_2]^-$ to afford $CpRu(CO)_2(\mu_4$-C)$Co_3(CO)_6$(tdpm) and (μ_3-CH)$Co_3(CO)_6$(tdpm). The formation of the μ_3-CH capping ligand in the latter cluster presumably arises from an electron transfer scheme involving the transient radical (μ_3-C˙)$Co_3(CO)_6$(tdpm) [280]. The Os/Pd clusters $Os_6Pd(\mu$-H)$_8(CO)_{18}$, $Os_4Pd(\mu$-H)$_4(CO)_{12}(\mu$-I)$_2$, and $Os_4Pd(\mu$-H)$_3(CO)_{12}(\mu$-I)$_3$ have been isolated from the reaction between $Os_3(\mu$-H)$_2(CO)_{10}$ and *trans*-$Pd(NH_3)_2I_2$. The X-ray structures of the first two clusters exhibit vertex-shared condensed polyhedra with Pd atoms at the vertex-sharing sites [281]. The synthesis and X-ray structures of $[Fe_6C(AuPPh_3)(CO)_{16}]^-$ and $Fe_4C(AuPPh_3)(CO)_{11}(NO)$ are reported. The results of extended Hückel MO calculations on $[Fe_4C(CO)_{12}]^{2-}$ are compared with data from $[Fe_4C(AuPPh_3)(CO)_{12}]^-$ and $[HFe_4C(CO)_{12}]^-$ in an effort to understand the structural differences between these clusters [282]. Low yields of $[Os_3(CO)_{10}(\mu$-Cl)$]_2(\mu_4$-Hg) and $[Os_3(CO)_{10}(\mu$-Cl)$]_2[\mu$-HgOs$(CO)_4]_2$ are observed in the reaction of RHgCl (where R = Me, Et, Ph, Fc) with $Os_3(CO)_{10}(MeCN)_2$. The latter product cluster reveals an unprecedented Os_8–Hg framework having a central linear Hg–$[Os(CO)_4]_2$–Hg molecular backbone with ligated Os_3 units [283]. Thermolysis of $Ru_3(CO)_{12}$ with $[\eta^5$-$C_5H_3(TMS)_2]W(CO)_3H$ gives the new WRu_6 cluster $[\eta^5$-$C_5H_3(TMS)_2]WRu_6(\mu_3$-H)$(CO)_{18}$. X-ray diffraction analysis confirms the presence of a tetrahedral WRu_3 core (Fig. 22). This cluster reacts with H_2 to afford $[\eta^5$-$C_5H_3(TMS)_2]WRu_6(\mu_3$-H$)_3(CO)_{17}$, whose structure was established by ^{1}H-NMR spectroscopy and X-ray crystallography [284].

The synthesis and X-ray characterization of the double cubane-like clusters $[(Cp^*WS_3)_2Cu_6(NCS)_6]^{2-}$ and $[(Cp^*WS_3)_2Cu_6Br_6]^{2-}$ have been published [285]. Stereochemical and electronic evidence of icosahedricity and polyicosahedricity has been presented. Some of the cluster systems examined include $[Ni_8Te_4(CO)_{12}]^{2-}$,

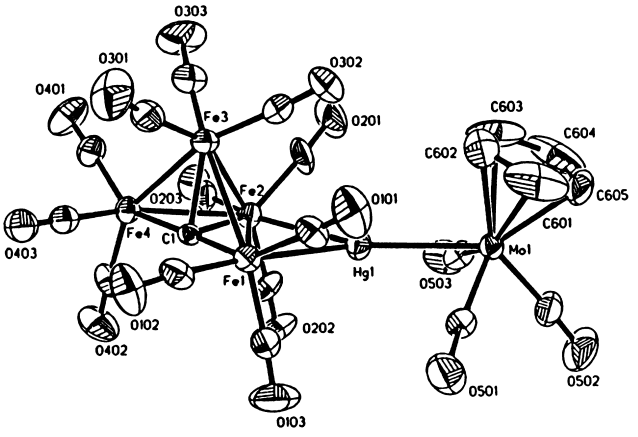

Fig. 21. X-ray structure of $[Fe_4C(CO)_{12}\{\mu$-HgMoCp$(CO)_3\}]^-$. Reprinted with permission from Organometallics. Copyright 1997 American Chemical Society.

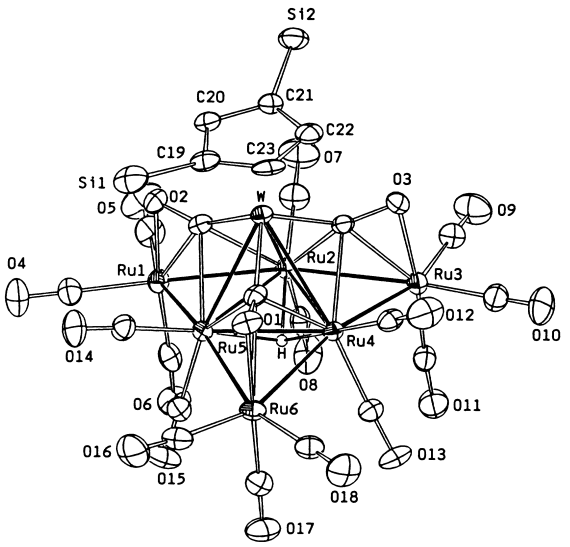

Fig. 22. X-ray structure of $[\eta^5\text{-}C_5H_3(TMS)_2]WRu_6(\mu_3\text{-}H)(CO)_{18}$. Reprinted with permission from Journal of American Chemical Society. Copyright 1997 American Chemical Society.

$[Ni_9(AsMe)_3(CO)_{15}]^{2-}$, and $[Ni_{10}Te_3(CO)_{15}]^{2-}$ [286]. The first cluster with an Os_4Au_4 core has been prepared. The cluster $Os_4H_2(CO)_{11}[Au_2(dppm)]_2$, prepared from $[Os_4H_3(CO)_{12}]^{2-}$ and $Au_2(dppm)Cl_2$, possesses a tetrahedral Os_4 core, with one face being capped by three Au atoms [287]. The amphiphilic cluster complex (p-cymene)$_4Ru_4Mo_4O_{16}$ has been synthesized from sodium molybdate and [(p-cymene)$RuCl_2]_2$. The solid-state structure was solved by X-ray analysis [288]. The synthesis, solid-state structure, and framework transformations exhibited by $[(Cp^*Rh)_2Mo_6O_{20}(OMe)_2]^{2-}$ have been published. The multi-valley sites in this cluster may be used as building blocks for the construction of larger clusters [289]. A report on the synthesis and X-ray structures of $[Re_7C(CO)_{21}HgOH]^{2-}$ and $[Re_7C(CO)_{21}HgSC_6H_4Br\text{-}4]^{2-}$ has appeared. The 1,4-bicapped octahedral structure exhibited by the former cluster (Fig. 23) was confirmed by X-ray crystallography. The use of these clusters as electron-dense markers is discussed [290].

The reactivity of $Pt_3Ru_6(CO)_{21}(\mu\text{-}H)_3(\mu_3\text{-}H)$ with PPh_3 and PMe_3 has been investigated. Both ligands react with the cluster at room temperature to give the ionic clusters $[Pt(PR_3)_3H][Pt_3Ru_6(CO)_{21}(\mu\text{-}H)_2(\mu_3\text{-}H)]$ in low yield. Cluster activation by Me_3NO with added PPh_3 affords $Pt_3Ru_6(CO)_{20}(PPh_3)(\mu\text{-}H)_3(\mu_3\text{-}H)$ in low yield. Two X-ray structures are reported [291]. The use of $(ClAu)_3$(triphos) as a building block for the construction of heterometallic clusters is described. The reaction of the anionic complexes $[Fe_2(\mu\text{-}CO)(CO)_6(\mu\text{-}L)]^{n-}$ (where L = PPh_2, CO, CH=CHPh, PhC=CHPh) with the gold reagent affords the polynuclear derivatives $[Fe_2(\mu\text{-}CO)(CO)_6(\mu\text{-}L)Au]_3$(triphos). The X-ray structure of the CH=CHPh complex consists of three Fe_2Au units linked by the three-legged propeller-like structure of the triphos ligand [292].

Thermolysis of $Os_5PdC(CO)_{14}(\mu\text{-dppf})$ yields $[Os_5PdC(CO)_{14}]_2(\mu\text{-dppf})$. The dppf ligand serves to bridge the two Os_5Pd units [293]. Linear columns and zigzag chains of multiple phenyl embraces in the gegencation $[Ph_4P]^+$ lead to concerted structural motifs. One such system examined in this study was $[(\mu_6\text{-C})Os_{10}(CO)_{24}HgCF_3][Ph_4P]$ [294]. The synthesis and host–guest chemistry of $[Ir(1,5\text{-COD})]_6W_4O_{16}$ are reported. This complex represents a hybrid inorganic–organometallic host complex, which binds MeCN via the methyl group rather than the nitrile group. The data from ^{1}H-NMR binding studies have allowed the MeCN binding constant to be calculated [295].

Low yields of $Os_5Pd_6(CO)_{13}(\mu\text{-CO})_5(\mu\text{-H})_2(\mu\text{-dppm})_2$ and $Os_5Pd_6(CO)_{13}(\mu\text{-CO})_6(\mu\text{-dppm})_2$ have been obtained from the reaction between $Os_3(CO)_{10}(\mu\text{-H})_2$ and $Pd_2(\mu\text{-dppm})_2Cl_2$. X-ray analysis reveals that both clusters consist of an inner Pd_6 bicapped tetrahedron with several triangular faces capped by the remaining Os and Pd atoms. Both clusters possess 146 CVE and do not obey conventional electron-counting rules [296]. Treatment of $Cp^*_2Mo_2Fe_2S_4Cl_2$ with Li_2S gave the unprecedented tricubane cluster $[Cp^*_2Mo_2Fe_2S_4]_3(\mu\text{-}S_4)_3$, whose X-ray structure has been solved. The redox chemistry has been studied, and the results from the positive electrospray ionization mass spectrum are discussed [297]. The use of clusters as ligands has been presented. The reaction of $(OC)_9Co_3(\mu_3\text{-}CCO_2H)$ as a cluster building block for new titanium and zirconium complexes is discussed [298]. The reaction between $[Ru_6H(CO)_{18}]^-$ and excess $[Cu(MeCN)_4]^+$ in CH_2Cl_2 gives $[Ru_8H_2Cu_7Cl_3(CO)_{24}]^{2-}$ in good yield. The solid-state structure of the dianion consists of two Ru_4 clusters which sandwich a Cu_7 metal core. Repeating the reaction with MeCN as the solvent furnishes the cluster $[Ru_{12}H_2Cu_6Cl_2(CO)_{34}]^{2-}$. The solution ^{1}H-NMR data and the X-ray structure of this cluster are reported

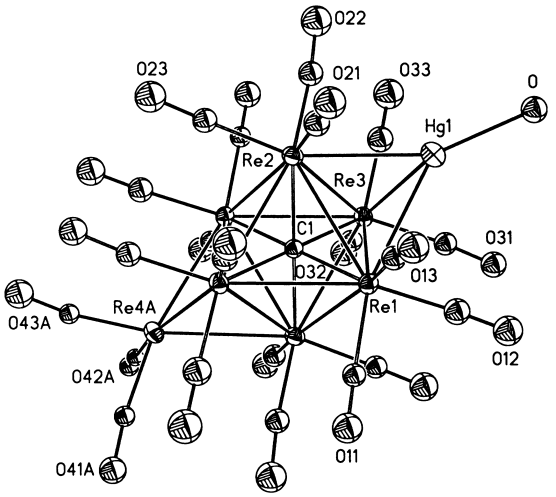

Fig. 23. X-ray structure of $[Re_7C(CO)_{21}HgOH]^{2-}$. Reprinted with permission from Inorganic Chemistry. Copyright 1997 American Chemical Society.

[299]. The cluster $[Ru_{10}H_2(CO)_{25}]^{2-}$ reacts with excess $[Cu(MeCN)_4]^+$ in CH_2Cl_2 and $[Bu_4N][OH]$ to give $[Ru_{20}H_4Cu_6Cl_2(CO)_{48}]^{4-}$. Included in this report are the X-ray structure and the ^{1}H-NMR data [300]. The synthesis and structural characterization of the ladder polymer $[Cp^*WS_3Ag_2Br]_n$ have been published [301].

Appendix A. Nomenclature

ampy	2-amino-6-methylpyridinate
binap	2,2′-bis(diphenylphosphino)-1,1′-binaphthyl
bma	2,3-bis(diphenylphosphino)maleic anhydride
bpcd	4,5-bis(diphenylphosphino)-4-cyclopenten-1,3-dione
bpy	2,2′-bipyridine
COD	1,5-cyclooctadiene
Cp	cyclopentadienyl
Cp*	pentamethylcyclopentadienyl
Cy	cyclohexyl
dmpm	bis(dimethylphosphino)methane
dpam	$Ph_2AsCH_2AsPh_2$
dpmp	$(Ph_2PCH_2)_2PPh$
dppa	1,2-bis(diphenylphosphino)acetylene
dppb	1,4-bis(diphenylphosphino)butane
dppe	1,2-bis(diphenylphosphino)ethane
dppf	1,1′-bis(diphenylphosphino)ferrocene
dpph	1,6-bis(diphenylphosphino)hexane
dppm	bis(diphenylphosphino)methane
dppp	1,3-bis(diphenylphosphino)propane
etpb	$P(OCH_2)_3CCH_2CH_3$
Fc	ferrocenyl
ind	indenyl
MAS	magic angle spinning
mes	mesityl
MeCp	methylcyclopentadienyl
PPN	bis(triphenylphosphine)iminium
py	pyridine
tdpm	$(Ph_2P)_3CH$
Tol	tolyl
Xyl	2,6-xylyl

References

[1] W.W. Zhuang, Diss. Abstr. B 58 (1997) 1286 [DA9728742].
[2] M.S. Morton, Diss. Abstr. B 58 (1997) 694 [DA9722147].
[3] J.W. van Hal, Diss. Abstr. B 58 (1997) 1285 [DA9727620].

[4] W.K. Leong, Diss. Abstr. B 58 (1997) 2419 [DANN16972].
[5] G.W. Drake, Diss. Abstr. B 57 (1997) 5044 [DA9703386].
[6] R.A. Burrow, Diss. Abstr. B 57 (1997) 5043 [DANN11683].
[7] J. Zhou, Diss. Abstr. B 57 (1997) 6257 [DA9710490].
[8] D.M. Norton, Diss. Abstr. B 57 (1997) 6925 [DA9714655].
[9] S.-H. Chun, Diss. Abstr. B 57 (1997) 6251 [DA9710549].
[10] T.R. Johnston, Diss. Abstr. B 57 (1997) 6921 [DA9711314].
[11] F.M. Asseid, Diss. Abstr. B 58 (1997) 2416 [DANN17921].
[12] A. Venturelli, Diss. Abstr. B 57 (1997) 5049 [DA9702702].
[13] W.D. King, Diss. Abstr. B 57 (1997) 6253 [DA9709034].
[14] F.H. Försterling, Diss. Abstr. B 57 (1997) 6252 [DA9709019].
[15] M.C. Comstock, Diss. Abstr. B 57 (1997) 6918 [DA9712238].
[16] X. Lei, Diss. Abstr. B 58 (1997) 1282 [DA9727405].
[17] J. Liu, Diss. Abstr. B 58 (1997) 694 [DA9721131].
[18] G.M. Ferrence, Diss. Abstr. B 57 (1997) 4382 [DA9638160].
[19] P.D. Mlynek, Diss. Abstr. B 57 (1997) 6255 [DA9706714].
[20] J.M. Bemis, Diss. Abstr. B 57 (1997) 7519 [DA9710018].
[21] M. Björgvinsson, S. Halldorsson, I. Arnason, J. Magull, D. Fenske, J. Organomet. Chem. 544 (1997) 207.
[22] R. Andrés, P. Gómez-Sal, E. de Jesús, A. Martin, M. Mena, C. Yélamos, Angew. Chem., Int. Ed. Engl. 36 (1997) 115.
[23] P. Yu, H.W. Roesky, A. Demsar, T. Albers, H.-G. Schmidt, M. Noltemeyer, Angew. Chem., Int. Ed. Engl. 36 (1997) 1766.
[24] O.M. Kekia, A.L. Rheingold, J. Organomet. Chem. 545–546 (1997) 277.
[25] C.D. Abernethy, F. Bottomley, A. Decken, R.C. Thompson, Organometallics 16 (1997) 1865.
[26] C. Ting, M.S. Hammer, N.C. Baenziger, L. Messerle, J. Deak, S. Li, M. McElfresh, Organometallics 16 (1997) 1816.
[27] H. Kawaguchi, K. Tatsumi, Organometallics 16 (1997) 307.
[28] J.E. Davies, M.C. Klunduk, M.J. Mays, P.R. Raithby, G.P. Shields, P.K. Tompkin, J. Chem. Soc., Dalton Trans. (1997) 715.
[29] J.E. Davies, M.J. Mays, E.J. Pook, P.R. Raithby, P.K. Tompkin, J. Chem. Soc., Dalton Trans. (1997) 3283.
[30] J.E. Davies, M.J. Mays, E.J. Pook, P.R. Raithby, P.K. Tompkin, J. Chem. Soc., Chem. Commun. (1997) 1997.
[31] M.H. Chisholm, K. Folting, K.S. Kramer, W.E. Streib, J. Am. Chem. Soc. 119 (1997) 5528.
[32] Y.V. Mironov, J.A. Cody, T.E. Albrecht-Schmitt, J.A. Ibers, J. Am. Chem. Soc. 119 (1997) 493.
[33] K.-C. Huang, Y.-C. Tsai, G.-H. Lee, S.-M. Peng, M. Shieh, Inorg. Chem. 36 (1997) 4421.
[34] S.D. Huang, C.P. Lai, C.L. Barnes, Angew. Chem., Int. Ed. Engl. 36 (1997) 1854.
[35] T. Beringhelli, G. D'Alfonso, M. Panigati, J. Organomet. Chem. 527 (1997) 215.
[36] B.-C. Jiang, H.-C. Horng, F.-L. Liao, C.P. Cheng, Organometallics 16 (1997) 4668.
[37] M. Bergamo, T. Beringhelli, G. D'Alfonso, P. Mercandelli, M. Moret, A. Sironi, Organometallics 16 (1997) 4129.
[38] T. Beringhelli, G. D'Alfonso, M. Freni, M. Panigati, Organometallics 16 (1997) 2719.
[39] W.-W. Zhuang, D.M. Hoffman, J. Chem. Soc., Chem. Commun. (1997) 295.
[40] D.M. Hoffman, D. Lappas, D.A. Wierda, Organometallics 16 (1997) 972.
[41] W.-W. Zhuang, D.M. Hoffman, Organometallics 16 (1997) 3102.
[42] U. Brand, J.R. Shapley, Inorg. Chem. 36 (1997) 253.
[43] B.E. Mann, J. Chem. Soc., Dalton Trans. (1997) 1457.
[44] B.F.G. Johnson, J. Chem. Soc., Dalton Trans. (1997) 1473.
[45] L.J. Farrugia, J. Chem. Soc., Dalton Trans. (1997) 1783.
[46] N. Chatani, Y. Ie, F. Kakiuchi, S. Murai, J. Org. Chem. 62 (1997) 2604.
[47] T. Morimoto, N. Chatani, Y. Fukumoto, S. Murai, J. Org. Chem. 62 (1997) 3762.

[48] T. Fukuyama, N. Chatani, F. Kakiuchi, S. Murai, J. Org. Chem. 62 (1997) 5647.
[49] Y. Ishii, K. Miyashita, K. Kamita, M. Hidai, J. Am. Chem. Soc. 119 (1997) 6448.
[50] L.A. Bruce, M. Hoang, A.E. Hughes, T.W. Turney, Inorg. Chim. Acta 254 (1997) 37.
[51] S.-H. Chun, T.B. Shay, S.E. Tomaszewski, P.H. Laswick, J.-M. Basset, S.G. Shore, Organometallics 16 (1997) 2627.
[52] D. Roberto, E. Cariati, E. Lucenti, M. Respini, R. Ugo, Organometallics 16 (1997) 4531.
[53] D. Roberto, E. Lucenti, C. Roveda, R. Ugo, Organometallics 16 (1997) 5974.
[54] J.T. Park, J.-J. Cho, H. Song, C.-S. Jun, Y. Son, J. Kwak, Inorg. Chem. 36 (1997) 2698.
[55] H.-F. Hsu, S.R. Wilson, J.R. Shapley, J. Chem. Soc., Chem. Commun. (1997) 1125.
[56] B.K. Das, M.G. Kanatzidis, Polyhedron 16 (1997) 3061.
[57] A.J. Arce, A. Karam, Y. De Sanctis, R. Machado, M.V. Capparelli, J. Manzur, Inorg. Chim. Acta 254 (1997) 119.
[58] K. Badyal, W.R. McWhinnie, T.A. Hamor, H. Chen, Organometallics 16 (1997) 3194.
[59] P.E. Gaede, S. Parsons, B.F.G. Johnson, J. Chem. Soc., Dalton Trans. (1997) 3833.
[60] D. Braga, F. Grepioni, D.B. Brown, B.F.G. Johnson, M.J. Calhorda, L.F. Veiros, J. Chem. Soc., Dalton Trans. (1997) 547.
[61] G. Gervasio, D. Marabello, E. Sappa, J. Chem. Soc., Dalton Trans. (1997) 1851.
[62] Y. Zhang, S. Xu, X. Zhou, Organometallics 16 (1997) 6017.
[63] D. Braga, P.J. Dyson, F. Grepioni, B.F.G. Johnson, C.M. Martin, L. Scaccianoce, A. Steiner, J. Chem. Soc., Chem. Commun. (1997) 1259.
[64] V.N. Lebedev, D.F. Mullica, E.L. Sappenfield, F.G.A. Stone, J. Organomet. Chem. 536–537 (1997) 537.
[65] B. Wrackmeyer, H.-J. Schanz, W. Milius, Angew. Chem., Int. Ed. Engl. 36 (1997) 1117.
[66] P. Braunstein, J.R. Galsworthy, W. Massa, J. Chem. Soc., Dalton Trans. (1997) 4677.
[67] H. Shen, S.G. Bott, M.G. Richmond, J. Chem. Crystallogr. 27 (1997) 25.
[68] A.Z. Voskoboynikov, M.A. Osina, A.K. Shestakova, M.A. Kazankova, I.G. Trostyanskaya, I.P. Beletskaya, F.M. Dolgushin, A.I. Yanovsky, Y.T. Struchkov, J. Organomet. Chem. 545–546 (1997) 71.
[69] X.-W. Dong, Y.-Z. Lun, K.-B. Yu, Polyhedron 16 (1997) 593.
[70] S.P. Tunik, E.V. Grachova, V.R. Denisov, G.L. Starova, A.B. Nikol'skii, F.M. Dolgushin, A.I. Yanovsky, Y.T. Struchkov, J. Organomet. Chem. 536–537 (1997) 339.
[71] M.I. Rybinskaya, L.V. Rybin, S.V. Osintseva, F.M. Dolgushin, A.I. Yanovsky, Y.T. Struchkov, P.V. Petrovskii, J. Organomet. Chem. 536–537 (1997) 345.
[72] A.A. Koridze, A.M. Sheloumov, F.M. Dolgushin, A.I. Yanovsky, Y.T. Struchkov, P.V. Petrovskii, J. Organomet. Chem. 536–537 (1997) 381.
[73] A.J. Deeming, D.M. Speel, Organometallics 16 (1997) 289.
[74] S. Aime, W. Dastrú, R. Gobetto, L. Milone, A. Viale, J. Chem. Soc., Chem. Commun. (1997) 267.
[75] J.U. Köhler, J. Lewis, P.R. Raithby, M.A. Rennie, Organometallics 16 (1997) 3851.
[76] A.K. Hughes, K.L. Peat, K. Wade, J. Chem. Soc., Dalton Trans. (1997) 2139.
[77] J.W. van Hal, L.B. Alemany, K.H. Whitmire, Inorg. Chem. 36 (1997) 3152.
[78] A. Inagaki, Y. Takaya, T. Takemori, H. Suzuki, J. Am. Chem. Soc. 119 (1997) 625.
[79] B.F.G. Johnson, J.M. Matters, P.E. Gaede, S.L. Ingham, N. Choi, M. McPartlin, M.-A. Pearsall, J. Chem. Soc., Dalton Trans. (1997) 3251.
[80] M.I. Bruce, R.J. Surynt, B.W. Skelton, A.H. White, Aust. J. Chem. 50 (1997) 701.
[81] K.R. Hash, R.J. Field, E. Rosenberg, Inorg. Chim. Acta 259 (1997) 329.
[82] K.R. Hash, E. Rosenberg, Organometallics 16 (1997) 3593.
[83] J.-Y. Huang, K.-J. Lin, K.-M. Chi, K.-L. Lu, J. Chem. Soc., Dalton Trans. (1997) 15.
[84] V.A. Maksakov, V.A. Ershova, V.P. Kirin, A.V. Golovin, J. Organomet. Chem. 532 (1997) 11.
[85] J.-H. Chung, E.P. Boyd, J. Liu, S.G. Shore, Inorg. Chem. 36 (1997) 4778.
[86] R.H.E. Hudson, A.J. Pöe, Inorg. Chim. Acta 259 (1997) 257.
[87] M.I. Bruce, B.W. Skelton, A.H. White, N.N. Zaitseva, Aust. J. Chem. 50 (1997) 163.
[88] X. Chen, B.E. Mann, J. Chem. Soc., Chem. Commun. (1997) 2233.
[89] R. Giordano, E. Sappa, G. Predieri, A. Tiripicchio, J. Organomet. Chem. 547 (1997) 49.

[90] B.F.G. Johnson, J. Lewis, E. Nordlander, P.R. Raithby, J. Chem. Soc., Dalton Trans. (1997) 3825.
[91] M.V. Capparelli, Y. De Sanctis, A.J. Arce, E. Spodine, Acta Crystallogr. C53 (1997) 302.
[92] H.-G. Ang, S.-G. Ang, Q. Zhang, J. Chem. Soc., Dalton Trans. (1997) 3843.
[93] E.N.-M. Ho, W.-T. Wong, J. Chem. Soc., Dalton Trans. (1997) 915.
[94] A.M.Z. Slawin, M.B. Smith, J.D. Wollins, J. Chem. Soc., Dalton Trans. (1997) 1877.
[95] B.F.G. Johnson, J. Lewis, E. Nordlander, P.R. Raithby, C.E. Housecroft, Inorg. Chim. Acta 259 (1997) 345.
[96] L.T. Byrne, J.A. Johnson, G.A. Koutsantonis, B.W. Skelton, A.H. White, J. Chem. Soc., Chem. Commun. (1997) 391.
[97] G.M. Ferrence, P.E. Fanwick, C.P. Kubiak, R.J. Haines, Polyhedron 16 (1997) 1453.
[98] D. Cauzzi, C. Graiff, M. Lanfranchi, G. Predieri, A. Tiripicchio, J. Organomet. Chem. 536–537 (1997) 497.
[99] H.-C. Böttcher, M. Graf, K. Merzweiler, C. Bruhn, Polyhedron 16 (1997) 3253.
[100] H. Shen, J.C. Wang, S.G. Bott, M.G. Richmond, J. Chem. Crystallogr. 27 (1997) 649.
[101] A.J. Deeming, D.M. Speel, M. Stchedroff, Organometallics 16 (1997) 6004.
[102] M. Shimizu, Y. Nakamura, M. Tadokoro, Polyhedron 16 (1997) 577.
[103] V. Ferrand, C. Gambs, N. Derrien, C. Bolm, H. Stoeckli-Evans, G. Süss-Fink, J. Organomet. Chem. 549 (1997) 275.
[104] S.E. Kabir, H. Vahrenkamp, M.B. Hursthouse, K.M.A. Malik, J. Organomet. Chem. 536–537 (1997) 509.
[105] S. Kumaresan, K.-L. Lu, J.-T. Hung, F.-Y. Lee, Y.-S. Wen, J.R. Hwu, J. Organomet. Chem. 549 (1997) 155.
[106] L.P. Clarke, P.R. Raithby, G.P. Shields, Polyhedron 16 (1997) 3775.
[107] N.E. Leadbeater, J. Lewis, P.R. Raithby, G.N. Ward, J. Chem. Soc., Dalton Trans. (1997) 2511.
[108] F.-S. Kong, W.-T. Wong, J. Chem. Soc., Dalton Trans. (1997) 1237.
[109] S. Aime, R. Gobetto, E. Valls, Organometallics 16 (1997) 5140.
[110] E. Rosenberg, L. Milone, R. Gobetto, D. Osella, K. Hardcastle, S. Hajela, K. Moizeau, M. Day, E. Wolf, D. Espitia, Organometallics 16 (1997) 2665.
[111] S.E. Kabir, E. Rosenberg, L. Milone, R. Gobetto, D. Osella, M. Ravera, T. McPhillips, M.W. Day, D. Carlot, S. Hajela, E. Wolf, K. Hardcastle, Organometallics 16 (1997) 2674.
[112] A.J. Arce, R. Machado, Y. De Sanctis, M.V. Capparelli, R. Atencio, J. Manzur, A.J. Deeming, Organometallics 16 (1997) 1735.
[113] J.A. Cabeza, I. del Río, R.J. Franco, F. Grepioni, V. Riera, Organometallics 16 (1997) 2763.
[114] J.A. Cabeza, I. del Río, V. Riera, S. García-Granda, S.B. Sanni, Organometallics 16 (1997) 1743.
[115] J.A. Cabeza, I. del Río, V. Riera, F. Grepioni, Organometallics 16 (1997) 812.
[116] J.A. Cabeza, I. del Río, V. Riera, J. Organomet. Chem. 548 (1997) 255.
[117] J.A. Cabeza, I. del Río, V. Riera, S. García-Granda, S.B. Sanni, Organometallics 16 (1997) 3914.
[118] V. Ferrand, K. Merzweiler, G. Rheinwald, H. Stoeckli-Evans, G. Süss-Fink, J. Organomet. Chem. 549 (1997) 263.
[119] L.-C. Song, C.-G. Yan, Q.-M. Hu, H.-T. Fan, T.C.W. Mak, B.-M. Wu, Polyhedron 16 (1997) 3475.
[120] W.-Y. Yeh, C.L. Stern, D.F. Shriver, Inorg. Chem. 36 (1997) 4408.
[121] S. Inomata, K. Hitomi, H. Ogino, Chem. Lett. (1997) 1169.
[122] K.W. Muir, L. Manojlović-Muir, F. Morrice, K. Guennou, F. Pétillon, R. Rumin, Acta Crystallogr. C53 (1997) 219.
[123] P. Mathur, S. Ghose, M.M. Hossain, C.V.V. Satyanarayana, S. Banerjee, G.R. Kumar, P.B. Hitchcock, J.F. Nixon, Organometallics 16 (1997) 3815.
[124] W. van der Berg, L. Boot, H. Joosen, J.G.M. van der Linden, W.P. Bosman, J.M.M. Smits, R. de Gelder, P.T. Beurskens, J. Heck, A.W. Gal, Inorg. Chem. 36 (1997) 1821.
[125] M.I. Bruce, M. Schulz, E.R.T. Tiekink, Aust. J. Chem. 50 (1997) 879.
[126] W.K. Leong, F.W.B. Einstein, R.K. Pomeroy, Acta Crystallogr. C53 (1997) 24.

[127] J.E. Davies, M.J. Mays, P.R. Raithby, K. Sarveswaran, Angew. Chem., Int. Ed. Engl. 36 (1997) 2668.
[128] J.S. Bradley, S. Harris, E.W. Hill, J. Chem. Soc., Dalton Trans. (1997) 3139.
[129] A.J. Carty, G. Hogarth, G. Enright, G. Frapper, J. Chem. Soc., Chem. Commun. (1997) 1883.
[130] A.A. Koridze, V.I. Zdanovich, A.M. Sheloumov, V.Y. Lagunova, P.V. Petrovskii, A.S. Peregudov, F.M. Dolgushin, A.I. Yanovsky, Organometallics 16 (1997) 2285.
[131] C.E. Housecroft, J.S. Humphrey, A.L. Rheingold, Inorg. Chim. Acta 259 (1997) 85.
[132] K.O. Kallinen, T.T. Pakkanen, T.A. Pakkanen, J. Organomet. Chem. 547 (1997) 319.
[133] J.R. Eveland, J.-Y. Saillard, K.H. Whitmire, Inorg. Chem. 36 (1997) 330.
[134] J.R. Eveland, J.-Y. Saillard, K.H. Whitmire, Inorg. Chem. 36 (1997) 4387.
[135] W. Wang, G.D. Enright, A.J. Carty, J. Am. Chem. Soc. 119 (1997) 12370.
[136] M. Scheer, J. Krug, P. Kramkowski, J.F. Corrigan, Organometallics 16 (1997) 5917.
[137] M. Shieh, Y.-C. Tsai, J.-J. Cherng, M.-H. Shieh, S.-M. Peng, G.-H. Lee, Organometallics 16 (1997) 456.
[138] D.H. Farrar, J. Hao, O. Mourad, A.J. Pöe, Organometallics 16 (1997) 5015.
[139] G. Frapper, J.-F. Halet, M.I. Bruce, Organometallics 16 (1997) 2590.
[140] G. Freeman, S.L. Ingham, B.F.G. Johnson, M. McPartlin, I.J. Scowen, J. Chem. Soc., Dalton Trans. (1997) 2705.
[141] C.J. Adams, M.I. Bruce, B.W. Skelton, A.H. White, J. Chem. Soc., Dalton Trans. (1997) 2937.
[142] J. Lewis, C.A. Morewood, P.R. Raithby, M.C.R. de Arellano, J. Chem. Soc., Dalton Trans. (1997) 3335.
[143] N.E. Leadbeater, J. Lewis, P.R. Raithby, A.J. Edwards, J. Organomet. Chem. 545–546 (1997) 567.
[144] R.A.A.-M. Muna, J. Lewis, P.R. Raithby, J. Organomet. Chem. 530 (1997) 247.
[145] K. Lee, H.-F. Hsu, J.R. Shapley, Organometallics 16 (1997) 3876.
[146] R. Bau, S.A. Mason, L. Li, W.-T. Wong, J. Am. Chem. Soc. 119 (1997) 11992.
[147] M.I. Bruce, P.A. Humphrey, B.W. Skelton, A.H. White, Aust. J. Chem. 50 (1997) 535.
[148] D.B. Brown, P.J. Dyson, B.F.G. Johnson, C.M. Martin, D.G. Parker, S. Parsons, J. Chem. Soc., Dalton Trans. (1997) 1909.
[149] M.I. Bruce, P.A. Humphrey, B.W. Skelton, A.H. White, J. Chem. Soc., Dalton Trans. (1997) 1485.
[150] K.S.-Y. Leung, W.-T. Wong, J. Chem. Soc., Dalton Trans. (1997) 4357.
[151] R.L. Mallors, A.J. Blake, S. Parsons, B.F.G. Johnson, P.J. Dyson, D. Braga, F. Grepioni, E. Parisini, J. Organomet. Chem. 532 (1997) 133.
[152] B.F.G. Johnson, D.S. Shephard, D. Braga, F. Grepioni, S. Parsons, J. Chem. Soc., Dalton Trans. (1997) 3563.
[153] T. Adatia, G. Conole, S.R. Drake, B.F.G. Johnson, M. Kessler, J. Lewis, M. McPartin, J. Chem. Soc., Dalton Trans. (1997) 669.
[154] T. Chihara, A. Jesorka, H. Ikezawa, Y. Wakatsuki, J. Chem. Soc., Dalton Trans. (1997) 443.
[155] A.J. Blake, J.L. Haggitt, B.F.G. Johnson, S. Parsons, J. Chem. Soc., Dalton Trans. (1997) 991.
[156] A.J. Edwards, B.F.G. Johnson, S. Parsons, D.S. Shephard, J. Chem. Soc., Dalton Trans. (1997) 3837.
[157] H.-F. Hsu, S.R. Wilson, J.R. Shapley, Organometallics 16 (1997) 4937.
[158] R.L. Mallors, A.J. Blake, P.J. Dyson, B.F.G. Johnson, S. Parsons, Organometallics 16 (1997) 1668.
[159] T. Chihara, H. Kubota, M. Fukumoto, H. Ogawa, Y. Yamamoto, Y. Wakatsuki, Inorg. Chem. 36 (1997) 5488.
[160] J.W. Benson, T. Ishida, K. Lee, S.R. Wilson, J.R. Shapley, Organometallics 16 (1997) 4929.
[161] M.P. Cifuentes, M.G. Humphrey, G.A. Heath, Inorg. Chim. Acta 259 (1997) 273.
[162] M.P. Cifuentes, M.G. Humphrey, J.E. McGrady, P.J. Smith, R. Stranger, K.S. Murray, B. Moubaraki, J. Am. Chem. Soc. 119 (1997) 2647.
[163] D. Braga, F. Grepioni, E. Tedesco, H. Wadepohl, S. Gebert, J. Chem. Soc., Dalton Trans. (1997) 1727.
[164] N.C. Alexander, B.H. Robinson, J. Simpson, Acta Crystallogr. C53 (1997) 425.
[165] T. Räsänen, S. Jääskeläinen, T.A. Pakkanen, J. Organomet. Chem. 548 (1997) 263.
[166] X. Lei, M. Shang, T.P. Fehlner, Polyhedron 16 (1997) 1803.

[167] G.A. Acum, M.J. Mays, P.R. Raithby, H.R. Powell, G.A. Solan, J. Chem. Soc., Dalton Trans. (1997) 3427.
[168] H.-F. Klein, M. Mager, A. Schmidt, M. Hüber, W. Haase, U. Flörke, H.-J. Haupt, R. Boca, Inorg. Chem. 36 (1997) 4303.
[169] H. Wadepohl, T. Borchert, H. Pritzkow, Chem. Ber. 130 (1997) 593.
[170] M.C. Comstock, T. Prussak-Wieckowska, S.R. Wilson, J.R. Shapley, Organometallics 16 (1997) 4033.
[171] F.H. Försterling, C.E. Barnes, J. Am. Chem. Soc. 119 (1997) 7585.
[172] W.E. Geiger, M.J. Shaw, M. Wünsch, C.E. Barnes, F.H. Foersterling, J. Am. Chem. Soc. 119 (1997) 2804.
[173] F.H. Försterling, C.E. Barnes, W.D. King, Inorg. Chem. 36 (1997) 3532.
[174] W.D. King, C.E. Barnes, J.A. Orvis, Organometallics 16 (1997) 2152.
[175] R. Ros, A. Tassan, Inorg. Chim. Acta 260 (1997) 89.
[176] L. Huang, A. Liu, Y. Xu, J. Mol. Catal. A 124 (1997) 57.
[177] Z. Tang, Y. Nomura, Y. Ishii, Y. Mizobe, M. Hidai, Organometallics 16 (1997) 151.
[178] Y. Ishii, N. Chatani, F. Kakiuchi, S. Murai, Organometallics 16 (1997) 3615.
[179] R.M.S. Pereira, F.Y. Fujiwara, M.D. Vargas, D. Braga, F. Grepioni, Organometallics 16 (1997) 4833.
[180] A. Caiazzo, R. Settambolo, G. Uccello-Barretta, R. Lazzaroni, J. Organomet. Chem. 548 (1997) 279.
[181] P. Macchi, D.M. Proserpio, A. Sironi, Organometallics 16 (1997) 2101.
[182] B. Zhuang, P. Yu, L. Huang, L. He, G. Pan, Polyhedron 16 (1997) 1425.
[183] S.F.A. Kettle, E. Diana, R. Rossetti, P.L. Stanghellini, J. Am. Chem. Soc. 119 (1997) 8228.
[184] R.D. Pergola, L. Garlaschelli, S. Martinengo, A. Repossi, J. Mol. Catal. A 115 (1997) 265.
[185] A. Fumagalli, S. Martinengo, G. Bernasconi, G. Ciani, D.M. Proserpio, A. Sironi, J. Am. Chem. Soc. 119 (1997) 1450.
[186] S. Pasynkiewicz, W. Buchowicz, A. Pietrzykowski, J. Organomet. Chem. 531 (1997) 121.
[187] J.J. Schneider, U. Denninger, J. Hagen, C. Krüger, D. Bläser, R. Boese, Chem. Ber. 130 (1997) 1433.
[188] I. Ara, L.R. Falvello, S. Fernández, J. Forniés, E. Lalinde, A. Martín, M.T. Moreno, Organometallics 16 (1997) 5923.
[189] L.R. Falvello, J. Forniés, C. Fortuño, A. Martín, A.P. Martínez-Sariñena, Organometallics 16 (1997) 5849.
[190] T. Tanase, H. Takahata, M. Hasegawa, Y. Yamamoto, J. Organomet. Chem. 545–546 (1997) 531.
[191] I. Gauthron, Y. Mugnier, K. Hierso, P.D. Harvey, Can. J. Chem. 75 (1997) 1182.
[192] D.G. Holah, A.N. Hughes, E. Krysa, G.J. Spivak, M.D. Havighurst, V.R. Magnuson, Polyhedron 16 (1997) 2353.
[193] D.G. Holah, A.N. Hughes, E. Krysa, R.T. Markewich, M.D. Havighurst, V.R. Magnuson, Polyhedron 16 (1997) 2789.
[194] L. Hao, L. Manojlovic-Muir, K.W. Muir, R.J. Puddephatt, G.J. Spivak, J.J. Vittal, D. Yufit, Inorg. Chim. Acta 265 (1997) 65.
[195] G.J. Spivak, R.J. Puddephatt, Inorg. Chim. Acta 264 (1997) 1.
[196] P.D. Mlynek, L.F. Dahl, Organometallics 16 (1997) 1641.
[197] P.D. Mlynek, L.F. Dahl, Organometallics 16 (1997) 1655.
[198] J.M. Bemis, L.F. Dahl, J. Am. Chem. Soc. 119 (1997) 4545.
[199] V.W.-W. Yam, W.K.-M. Fung, K.-K. Cheung, J. Chem. Soc., Chem. Commun. (1997) 963.
[200] M.J. Irwin, L. Manojlović-Muir, K.W. Muir, R.J. Puddephatt, D.S. Yufit, J. Chem. Soc., Chem. Commun. (1997) 219.
[201] J. Vicente, M.-T. Chicote, M.-C. Lagunas, P.G. Jones, B. Ahrens, Inorg. Chem. 36 (1997) 4938.
[202] J. Vicente, M.-T. Chicote, P. González-Herrero, C. Grünwald, P.G. Jones, Organometallics 16 (1997) 3381.
[203] V.W.-W. Yam, W.K.-M. Fung, M.-T. Wong, Organometallics 16 (1997) 1772.
[204] V.W.-W. Yam, W.K.-M. Fung, K.-K. Cheung, Organometallics 16 (1997) 2032.

[205] M. Contel, J. Garrido, M.C. Gimeno, J. Jiménez, P.G. Jones, A. Laguna, M. Laguna, Inorg. Chim. Acta 254 (1997) 157.
[206] M.A. Bennett, L.L. Welling, A.C. Willis, Inorg. Chem. 36 (1997) 5670.
[207] F. Bottomley, J.E. McKenzie-Boone, J. Organomet. Chem. 534 (1997) 23.
[208] H. Adams, N.A. Bailey, L.J. Gill, M.J. Morris, N.D. Sadler, J. Chem. Soc., Dalton Trans. (1997) 3041.
[209] P. Mathur, P. Sekar, A.L. Rheingold, L.M. Liable-Sands, Organometallics 16 (1997) 142.
[210] P. Mathur, S. Ghosh, A. Sarkar, C.V.V. Satyanarayana, J.E. Drake, J. Yang, Organometallics 16 (1997) 6028.
[211] L.-C. Song, Y.-B. Dong, Q.-M. Hu, X.-Y. Huang, J. Sun, Organometallics 16 (1997) 4540.
[212] E.-R. Ding, S.-M. Liu, Y.-Q. Yin, J. Sun, Polyhedron 16 (1997) 3273.
[213] L.-C. Song, J.-Q. Wang, Q.-M. Hu, X.-Y. Huang, Polyhedron 16 (1997) 2249.
[214] E.-R. Ding, S.-M. Liu, Z.-Y. Zhao, Y.-Q. Yin, J. Shun, Polyhedron 16 (1997) 2387.
[215] E.-R. Ding, Y.-Q. Yin, J. Sun, Polyhedron 16 (1997) 3067.
[216] S.N. Konchenko, A.V. Virovets, S.V. Tkachev, N.V. Podberezskaya, Polyhedron 16 (1997) 1549.
[217] S.N. Konchenko, A.V. Virovets, S.V. Tkachev, N.V. Podberezskaya, Polyhedron 16 (1997) 707.
[218] L.-C. Song, L.-Y. Zhang, Z.-F. Tao, Q.-M. Hu, X.-Y. Huang, Polyhedron 16 (1997) 403.
[219] Y. Chi, H.-L. Wu, C.-C. Chen, C.-J. Su, S.-M. Peng, G.-H. Lee, Organometallics 16 (1997) 2434.
[220] H. Shimomura, X. Lei, M. Shang, T.P. Fehlner, Organometallics 16 (1997) 5302.
[221] H.-P. Wu, Y.-Q. Yin, X.-Y. Huang, Inorg. Chim. Acta 255 (1997) 167.
[222] O.J. Scherer, C. Vondung, G. Wolmershäuser, Angew. Chem., Int. Ed. Engl. 36 (1997) 1303.
[223] R. Galassi, R. Poli, E.A. Quadrelli, J.C. Fettinger, Inorg. Chem. 36 (1997) 3001.
[224] H.-J. Haupt, M. Schwefer, H. Egold, U. Flörke, Inorg. Chem. 36 (1997) 184.
[225] W.-F. Liaw, W.-Z. Lee, C.-Y. Wang, G.-H. Lee, S.-M. Peng, Inorg. Chem. 36 (1997) 1253.
[226] M.C. Comstock, T. Prussak-Wieckowska, S.R. Wilson, J.R. Shapley, Inorg. Chem. 36 (1997) 4397.
[227] M. Bergamo, T. Beringhelli, G. Ciani, G. D'Alfonso, M. Moret, A. Sironi, Inorg. Chim. Acta 259 (1997) 291.
[228] A.S. Fung, M.J. Kelly, D.C. Koningsberger, B.C. Gates, J. Am. Chem. Soc. 119 (1997) 5877.
[229] A. Venturelli, T.B. Rauchfuss, A.K. Verma, Inorg. Chem. 36 (1997) 1360.
[230] P. Blenkiron, G.D. Enright, A.J. Carty, J. Chem. Soc., Chem. Commun. (1997) 483.
[231] S. Banerjee, G.R. Kumar, P. Mathur, P. Sekar, J. Chem. Soc., Chem. Commun. (1997) 299.
[232] B. Manzano, F. Jalon, J. Matthes, S. Sabo-Etienne, B. Chaudret, S. Ulrich, H.-H. Limbach, J. Chem. Soc., Dalton Trans. (1997) 3153.
[233] P. Mathur, P. Sekar, J. Organomet. Chem. 527 (1997) 29.
[234] I. Ara, J.R. Berenguer, J. Forniés, E. Lalinde, Organometallics 16 (1997) 3921.
[235] I. Ara, J.R. Berenguer, J. Forniés, E. Lalinde, Inorg. Chim. Acta 264 (1997) 199.
[236] H. Liu, A.L. Tan, K.F. Mok, T.C.W. Mak, A.S. Batsanov, J.A.K. Howard, T.S.A. Hor, J. Am. Chem. Soc. 119 (1997) 11006.
[237] P. Mathur, P. Sekar, A.L. Rheingold, L.M. Liable-Sands, J. Chem. Soc., Dalton Trans. (1997) 2949.
[238] J.W. Raebiger, C.A. Crawford, J. Zhou, R.H. Holm, Inorg. Chem. 36 (1997) 994.
[239] M.A. Tyson, D. Coucouvanis, Inorg. Chem. 36 (1997) 3808.
[240] S.N. Konchenko, A.V. Virovets, N.V. Podberezskaya, Polyhedron 16 (1997) 1689.
[241] L.-C. Song, J.-Q. Wang, Q.-M. Hu, W.-Q. Gao, B.-S. Han, Polyhedron 16 (1997) 481.
[242] P. Mathur, A.K. Dash, M.M. Hossain, C.V.V. Satyanarayana, A.L. Rheingold, L.M. Liable-Sands, G.P.A. Yap, J. Organomet. Chem. 532 (1997) 189.
[243] Y. Chi, C. Chung, Y.-C. Chou, P.-C. Su, S.-J. Chiang, S.-M. Peng, G.-H. Lee, Organometallics 16 (1997) 1702.
[244] C.-W. Shiu, Y. Chi, A.J. Carty, S.-M. Peng, G.-H. Lee, Organometallics 16 (1997) 5368.
[245] M.D. Curtis, S.H. Druker, J. Am. Chem. Soc. 119 (1997) 1027.
[246] M.A. Mansour, M.D. Curtis, J.W. Kampf, Organometallics 16 (1997) 275.
[247] M.D. Curtis, S.H. Druker, L. Goossen, J.W. Kampf, Organometallics 16 (1997) 231.
[248] M.A. Mansour, M.D. Curtis, J.W. Kampf, Organometallics 16 (1997) 3363.

[249] O.J. Curnow, M.D. Curtis, J.W. Kampf, Organometallics 16 (1997) 2523.
[250] N.T. Lucas, M.G. Humphrey, D.C.R. Hockless, J. Organomet. Chem. 535 (1997) 175.
[251] N.T. Lucas, M.G. Humphrey, P.C. Healy, M.L. Williams, J. Organomet. Chem. 545–546 (1997) 519.
[252] A.A. Pasynskii, Y.V. Torubaev, S.E. Nedefov, I.L. Eremenko, O.G. Ellert, V.K. Belsky, A.I. Stastch, J. Organomet. Chem. 536–537 (1997) 433.
[253] S.B. Falloon, W. Weng, A.M. Arif, J.A. Gladysz, Organometallics 16 (1997) 2008.
[254] L. Hao, J. Xiao, J.J. Vittal, R.J. Puddephatt, Organometallics 16 (1997) 2165.
[255] M. Reinikainen, J. Kiviaho, M. Kröger, M. Niemelä, S. Jääskeläinen, J. Mol. Catal. A 118 (1997) 137.
[256] G. Süss-Fink, S. Haak, V. Ferrand, H. Stoeckli-Evans, J. Chem. Soc., Dalton Trans. (1997) 3861.
[257] A.U. Härkönen, M. Ahlgrén, T. Pakkanen, J. Pursiainen, Organometallics 16 (1997) 689.
[258] M.J. Calhorda, F. Canales, M.C. Gimeno, J. Jiménez, P.G. Jones, A. Laguna, L.F. Veiros, Organometallics 16 (1997) 3837.
[259] D. Braga, F. Grepioni, G.R. Desiraju, J. Organomet. Chem. 548 (1997) 33.
[260] A. Härkönen, M. Ahlgrén, T.A. Pakkanen, J. Pursiainen, J. Organomet. Chem. 530 (1997) 191.
[261] H.-C. Böttcher, M. Graf, K. Merzweiler, J. Organomet. Chem. 531 (1997) 107.
[262] H.-C. Böttcher, M. Graf, K. Merzweiler, J. Organomet. Chem. 534 (1997) 43.
[263] R. Vilar, S.E. Lawrence, S. Menzer, D.M.P. Mingos, D.J. Williams, J. Chem. Soc., Dalton Trans. (1997) 3305.
[264] S. Yamazaki, A.J. Deeming, D.M. Speel, D.E. Hibbs, M.B. Hursthouse, K.M.A. Malik, J. Chem. Soc., Chem. Commun. (1997) 177.
[265] H. Adams, L.J. Gill, M.J. Morris, J. Organomet. Chem. 533 (1997) 117.
[266] B.E. Collins, Y. Koide, C.K. Schauer, P.S. White, Inorg. Chem. 36 (1997) 6172.
[267] P. Blenkiron, A.J. Carty, S.-M. Peng, G.-H. Lee, C.-J. Su, C.-W. Shiu, Y. Chi, Organometallics 16 (1997) 519.
[268] P.-C. Su, Y. Chi, C.-J. Su, S.-M. Peng, G.-H. Lee, Organometallics 16 (1997) 1870.
[269] S.P. Gubin, T.V. Galuzina, I.F. Golovaneva, A.P. Klyagina, L.A. Polyakova, O.A. Belyakova, Y.V. Zubavichus, Y.L. Slovokhotov, J. Organomet. Chem. 549 (1997) 55.
[270] M.I. Bruce, J.M. Gulbis, P.A. Humphrey, R.J. Surynt, E.R.T. Tiekink, Aust. J. Chem. 50 (1997) 875.
[271] C.-H. Ueng, S.-M. Lu, Inorg. Chim. Acta 262 (1997) 113.
[272] L.A. Poliakova, S.P. Gubin, O.A. Belyakova, Y.V. Zubavichus, Y.L. Slovokhotov, Organometallics 16 (1997) 4527.
[273] V.G. Albano, M.C. Iapalucci, G. Longoni, L. Manzi, M. Monari, Organometallics 16 (1997) 497.
[274] W.-J. Chao, Y. Chi, C.-J. Way, I.J. Mavunkal, S.-L. Wang, F.-L. Liao, L.J. Farrugia, Organometallics 16 (1997) 3523.
[275] S.G. Anema, K.M. Mackay, B.K. Nicholson, J. Chem. Soc., Dalton Trans. (1997) 3853.
[276] J.E. Davies, S. Nahar, P.R. Raithby, G.P. Shields, J. Chem. Soc., Dalton Trans. (1997) 13.
[277] M.I. Bruce, P.A. Humphrey, B.W. Skelton, A.H. White, J. Organomet. Chem. 545–546 (1997) 207.
[278] R. Reina, O. Riba, O. Rossell, M. Seco, P. Gómez-Sal, A. Martin, Organometallics 16 (1997) 5113.
[279] S.Y.-W. Hung, W.-T. Wong, J. Chem. Soc., Chem. Commun. (1997) 2099.
[280] Y. Takahashi, M. Akita, Y. Moro-oka, J. Chem. Soc., Chem. Commun. (1997) 1557.
[281] J.W.-S. Hui, W.-T. Wong, J. Chem. Soc., Dalton Trans. (1997) 1515.
[282] O. Rossell, M. Seco, G. Segalés, S. Alvarez, M.A. Pellinghelli, A. Tiripicchio, D. de Montauzon, Organometallics 16 (1997) 236.
[283] Y.-K. Au, W.-T. Wong, Inorg. Chem. 36 (1997) 2092.
[284] Y. Chi, C.-J. Su, S.-M. Peng, G.-H. Lee, J. Am. Chem. Soc. 119 (1997) 11114.
[285] J. Lang, H. Kawaguchi, S. Ohnishi, K. Tatsumi, J. Chem. Soc., Chem. Commun. (1997) 405.
[286] H. Zhang, B.K. Teo, Inorg. Chim. Acta 265 (1997) 213.
[287] M.R.A. Al-Mandhary, J. Lewis, P.R. Raithby, J. Organomet. Chem. 536–537 (1997) 549.

[288] G. Süss-Fink, L. Plasseraud, V. Ferrand, H. Stoeckli-Evans, J. Chem. Soc., Chem. Commun. (1997) 1657.
[289] S. Takara, T. Nishioka, I. Kinoshita, K. Isobe, J. Chem. Soc., Chem. Commun. (1997) 891.
[290] U. Brand, J.L. Coffer, T.J. Henly, S.R. Wilson, J.R. Shapley, Inorg. Chem. 36 (1997) 3386.
[291] R.D. Adams, T.S. Barnard, Z. Li, L. Zhang, Chem. Ber. 130 (1997) 729.
[292] M. Ferrer, A. Juliá, O. Rossell, M. Seco, M.A. Pellinghelli, A. Tiripicchio, Organometallics 16 (1997) 3715.
[293] J.W.-S. Hui, W.-T. Wong, J. Chem. Soc., Dalton Trans. (1997) 2445.
[294] I. Dance, M. Scudder, J. Chem. Soc., Dalton Trans. (1997) 3755.
[295] Y. Hayashi, F. Müller, Y. Lin, S.M. Miller, O.P. Anderson, R.G. Finke, J. Am. Chem. Soc. 119 (1997) 11401.
[296] J.W.-S. Hui, W.-T. Wong, J. Chem. Soc., Chem. Commun. (1997) 2009.
[297] H. Kawaguchi, K. Yamada, S. Ohnishi, K. Tatsumi, J. Am. Chem. Soc. 119 (1997) 10871.
[298] X. Lei, M. Shang, T.P. Fehlner, Organometallics 16 (1997) 5289.
[299] M.A. Beswick, J. Lewis, P.R. Raithby, M.C.R. de Arellano, Angew. Chem., Int. Ed. Engl. 36 (1997) 291.
[300] M.A. Beswick, J. Lewis, P.R. Raithby, M.C.R. de Arellano, Angew. Chem., Int. Ed. Engl. 36 (1997) 2227.
[301] J.-P. Lang, H. Kawaguchi, K. Tatsumi, Inorg. Chem. 36 (1997) 6447.